POLITECNICO DI TORINO

Collegio di Ingegneria Energetica

Master of Science in
Nuclear and Energy Engineering

Master's Thesis

Urban energy planning and economic–environmental impacts assessment through spatiotemporal modeling of residential energy consumptions

Tara Maya Trafton

September 20, 2018

POLITECNICO DI TORINO

Collegio di Ingegneria Energetica

Master of Science in
Nuclear and Energy Engineering

Master's Thesis

Urban energy planning and economic–environmental impacts assessment through spatiotemporal modeling of residential energy consumption

Supervisors

signature of supervisor
Prof. Stefano Paolo Corgnati

signature of candidate
Tara Maya Trafton

InnoEnergy MSc SELECT:
Environomical Pathways for
Sustainable Energy Systems

signature of co-supervisor
Asst. Prof. Cristina Becchio

Double Degree:
KTH Royal Institute of Technology

signature of co-supervisor
Chiara Delmastro, PhD.

signature of co-supervisor
Giulia Vergerio, PhD. Candidate

September 20, 2018

Abstract

There is growing need to understand the ways in which we are using energy in our day to day lives. As urbanization is increasing, there is particular interest in urban and district level energy consumption. In this thesis, current research in the field of district level energy modeling is reviewed. While many models focus on either an analytical or statistical model, the model presented in this thesis is a hybrid spatiotemporal one looking specifically at residential energy demand. The model was applied in a case study of the 3rd district of Turin, Italy. The aim of the thesis was to develop a Geographic Information System (GIS) based hybrid urban buildings energy model as a supportive tool for energy planning and economic-environmental impacts assessment of explorative building retrofit scenarios. The final energy model is focused both on thermal and electrical consumptions.

Concerning thermal energy, making use of GIS georeferenced critical data regarding building geometry and construction period, 36 building archetypes are identified and a reference building (RB, associating TABULA thermophysical properties) is defined for each. The analytical model developed is a powerful tool which allows for the calculation of thermal energy demand for reference buildings. An initial calibration of the analytical model was carried out through the use of measured data in parallel with statistical information. The calibrated model was then applied at a district level via application of the specific consumption values to each building in the district. This method provides the opportunity to see exactly where the energy is being consumed.

Varied energy efficiency interventions related to the building energy systems and envelope were considered for the generation of retrofit scenarios. Expansion of district heating systems were not considered. It is known that Turin has a well-established plan to expand the district heating system, but the objective of this thesis is to be broadly applicable and to consider a scenario where the interventions are focused on electrification. Electricity consumptions at district level were calculated through a statistical model based on inhabitants' socio-economic characteristics. With the models established, different penetration rates for the building retrofits were considered and the forecast changes in both thermal and electric demand were applied thus establishing trends through the year 2050. Based on these demands, the greenhouse gas (GHG) emissions and local air pollution reductions were calculated as well as the corresponding savings related to healthcare of local residents. The costs associated with implementing these changes were also determined. Finally, the results were reintegrated in the QGIS model to allow for district level scenarios to be observed. Indeed, spatial visualization of results could be a supportive tool for decision makers.

Turin is consistently ranked among the worst European cities in terms of air quality. In 2017, the city exceeded the World Health Organization's (WHO) guideline value for concentration 66 days out of the year. This inspired the consideration of the link between retrofit interventions and local air pollution. Appropriate energy efficiency interventions alone can lead to significant reductions in energy demand. These interventions, along with increases in renewable energy shares of the power generation mix demonstrate that in the residential sector, the greenhouse gas reductions required to mitigate climate change can be obtained at competitive costs.

Key words:
Urban building energy modelling, hybrid model, retrofit, GIS, economic impacts, environmental impacts, electrification.

Nomenclature

General

Symbol	Variable name	Unit
A	area	m2
a	numerical parameter in utilization factor	1
B	correction factor for an unconditioned adjacent space	1
C	effective heat capacity of a conditioned space	J/K
c	specific heat capacity	J/(kg·K)
d	layer thickness	m
E	energy	MJ
El	electricity	
F	factor	1
g	total solar energy transmittance of a building element	1
H	heat transfer coefficient	W/K
h	surface coefficient of heat transfer	W/(m^{2}·K)
I_{sol}	solar irradiance	W/m^{2}
L	length	m
N	number	1
Q	quantity of heat	MJ
q	heat flow density	W/m^{2}
q_{v}	(volumetric) airflow rate	m^{3}/s
R	thermal resistance	m^{2}·K/W
S/V	shape factor	1/m
T	thermodynamic temperature	K
t	time, period of time	Ms^{a}
U	thermal transmittance	W/(m^{2}·K)
V	volume of air in a conditioned zone	m^{3}
X	any of the geometrical parameters of RB	N/A
Z	heat transfer parameter for solar walls	W/(m^{2}·K)
α	absorption coefficient of a surface for solar radiation	1
γ	heat-balance ratio	1
ε	emissivity of a surface for long-wave thermal radiation	1
η	efficiency, utilization factor	1
θ	centigrade temperature	°C
κ	heat capacity per area	J/(m^{2}·K)
ρ	density	kg/m^{3}
σ	Stefan-Boltzmann constant (σ = 5,67 × 10^{-8})	W/(m^{2}·K^{4})
τ	time constant	h
Φ	heat flow rate, thermal power	W
χ	point thermal transmittance	W/K
Ψ	linear thermal transmittance	W/(m·K)

Subscripts

15	first fifteen-minute time step
30	second fifteen-minute time step
45	third fifteen-minute time step
60	fourth fifteen-minute time step
a	air
A	appliances
adj	adjusted
avg	time average
C	cooling, capacity
e	external, exterior, envelope
el	electricity
em	emission
F	frame
f	floor
g	ground

gl	glazing, glazed element
gn	gains
ht	heat transfer
H	heating
H,nd	heating need, or building need for heating
HC,nd	heating and/or cooling need; building need for heating and/or cooling
hr	hourly
i	index value for buildings of a sample
ls	loss
mean	mean value of parameter
nd	need
Oc	occupants
ren	renewable
set	set-point
sh	shading
sol	solar (heat gains)
Tot	Total (system)
tot	total
tr	transmission (heat transfer)
V	ventilation (system)
v	volume
ve	ventilation (heat transfer)
W	hot water (system or need)

Table of Contents

List of Figures

List of Tables

1 Introduction

1.1 Problem Statement

According to the International Energy Agency (IEA) [1], in order to meet the 2DS, the scenario which limits global warming by two degrees above pre-industrial levels, approximately 90% of the residential buildings in OECD countries require energy efficiency retrofits to reduce their specific consumption and achieve lower energy standards. This means that approximately 400 million residential dwellings must be refurbished. This case study aims to assess the impact of different levels of building retrofit interventions, implemented starting from a baseline in 2014 through 2050, in order to gauge their impact relative to the goals identified by the IEA in regard to specific consumption and reductions on greenhouse gas emissions. In order to have a more comprehensive understanding of the impacts, the targets outlined by the Italian government in their National Energy Strategy [2] for increased renewable energy penetration in the electricity supply mix are applied.

This case study also looks at another problem plaguing the city of Turin: air pollution. Approximately 6.5 million worldwide deaths each year are attributed to pollution [3] making it the fourth biggest threat to human health. Turin is consistently ranked among the worst European cities in terms of air quality. In 2017, the city exceeded the World Health Organization's (WHO) guideline value for concentration 66 days out of the year. [4] Through the energy retrofits, the quantity and type of energy consumed changes. The demand decreases and, in this study, fossil-fuel burning boilers are replaced heat pumps, therefore eliminating sources of local air pollution within the district. The impacts on particulate matter (PM) and other air pollutant emissions will be quantified along with greenhouse gas (GHG) emissions.

This study elaborates on the current research on district scale energy consumption and energy efficiency measures with a focus on the impact of increased electrification and changes in the electricity supply mix as an alternative to fossil fuels boilers to understand the benefits of these measures in terms of energy, air pollution and greenhouse gas emission reductions. A GIS-based hybrid urban buildings energy model was developed as a supportive tool for energy planning and spatial comprehension of the impacts of the explorative retrofit scenarios. The use of building archetypes and reference buildings[1] (RBs) are employed in analytical and statistical contexts to define the demands of the district.

1.2 Case Study: 3rd District of Turin, Italy

Turin, Italy is located in the northwest of Italy at the base of the alps (45°04′24.60″ N, 7°40′32.52″ E) [5] in climate zone E [6] and had a population of 906,874 in 2011 [7]. There are approximately 40,000 residential buildings in the city [8].

Figure 1: "Circoscrizioni" (districts) of Turin

Turin is divided into 10 “circoscrizioni,” or districts, and the case analyzed in this thesis is that of the 3rd district (central-east of Turin). In this study 5301 residential buildings in the district with a total volume of 24,676,450 m^3 and surface area of 1,172,317 m^2 were evaluated. Real space heating data in the form of district heating consumption was provided by IREN for 247 buildings. The population of the buildings analyzed was 117,075 which represents 65,936 households.

1.3 Literature Review

Current trends suggest that the importance of urban energy planning is increasing as the share of the world’s population living in urban areas is expected to increase from 54% in 2014, to 66% by 2050

---

[1] In this study, “archetype” is used as the general expression of a building class based on its shape factor and construction period. These archetypes have well known geometric and thermophysical characteristics. “Reference building” in this study refers to the theoretical building belonging to an archetype and its associated specific geometry which is used as input values in the elaboration of the models.

[9]. Due to this, the idea of energy-driven urban planning will become a new métier [10] and the practitioners of this developing field will need tools to aid in their efforts.

1.3.1 European Context

Europe has been at the forefront of legislation, policy, and research in regard to climate change. As a result, many of the most well-developed strategies have come from the European Union. The first of these is the 2020 Strategy [11] adopted by the European Commission (EC) in 2010. The objective of the 2020 Strategy was outline a plan for smart, sustainable, and inclusive growth. In the field of urban energy planning, “smart” implies innovation and “sustainable” relates to decoupling economic growth from GHG emissions through smarter use of resources and energy efficiency, thus combatting the trends that have existed since the industrial revolution. It outlines the European strategy to meet the goals outlined by the IEA in the 2DS, specifically to reduce GHG emissions by 20%, increase the renewable share final energy consumption by 20% and increase energy efficiency by 20% relative to 1990 levels. The next important directive issued was the Energy Performance Building Directive (EPBD) [12] issued by the European Parliament which directed Member States (MS) that they must establish minimum requirements for the energy performance of buildings and building elements in order to meet the objectives detailed in the 2020 Strategy. MS were directed to establish guidelines for determining the energy performance of buildings and methods for determining cost-optimal strategies for renovations as well. The 2020 Strategy was meant to spark public awareness and investment in research towards combatting climate change, and therefore presented short-term objectives. The Energy Roadmap 2050 [13] released by the EC in 2012 states the requirement to cut GHG emissions by 80% - 95%. In that document, the EC acknowledges the fact that future energy demand will likely increase and that it, therefore, needs to be almost completely emission free. This is a huge challenge. It is not only the energy production that needs to change, the transmission and distribution infrastructure needs to be prepared for this additional demand. The decentralization of energy and the electrification of transportation will require advances in technology and innovation on all fronts. The scenarios detailed to achieve the decarbonization objectives suggest that renewables will account for 97% of the electricity share by 2050 with prices increasing until 2030, and then declining. Despite the supply size challenges, the 2050 Roadmap emphasizes that energy efficiency is the most critical pathway to our sustainable future.

1.3.2 District Level Energy Models

Urban planning usually occurs at the the district level [14], rather than the city or individual building level, therefore it is critical that the models developed reflect this.

1.3.2.1 Modeling Techniques

There are many different modeling techniques which can be used to provide insights into the energy demands of a district. Swan, et al. [15] suggested they can first be characterized as top-down or bottom-up. A top-down approach relates the energy consumption of buildings to macro-economic variables ignoring the built environment and its characteristics and performances. A bottom-up approach uses analysis of single buildings to examine performance of building systems and thermophysical properties.

Another differentiation can be made between statistical and analytical models. Statistical models forecast the energy performance of buildings based on historical data based on variables such as typology, appliance ownership, etc. The pros of using statistical modes is that they require few inputs and are still able to predict energy consumption at the city level. Unfortunately, the cons are the lack of granularity relating to both the spatial and the temporal dimensions of analysis. Despite that, several studies [16], [17] [18] [19] of this type have been elaborated. Analytical models are based on the dynamic exchanges of energy and matter between a building, other buildings, and the ambient environment. These complex models have higher data requirements but provide a fair characterization of energy consumption patterns in the spatial and temporal dimensions. These studies can be elaborated using simplified models [20], or third party software [21].

The compromise between analytical and statistical modeling is hybrid modeling. This is achieved through the use of building archetypes. This has been demonstrated by a study performed by Loughborough University [22] examining the impact of energy efficiency improvements on the English building stock. This study was carried out by creating nominal averages of building physical parameters, heretofore referred to as reference buildings (RBs), for each building archetype and aggregating the predicted consumptions of each building stock to understand the overall housing stock consumption. Similar research has been carried out for in the Japanese [23] and Swiss [24] urban settings. Fonseca, et al. [25] uses a GIS framework to overlay building architypes and geometry with consumption to arrive at a model which accurately characterizes the energy consumption patterns in Zug, Switzerland.

Many of these models do not consider the electrical energy consumption due to domestic appliances. With increasing urbanization, typically incomes also increase relative and this leads to an increase in appliance electricity consumption, as noted in a study by the Institute of Future Energy Consumer Needs and Behavior (FCN) [26]. Therefore, policy-makers in developed countries have imposed energy efficiency improvements for goods sold in their countries. Unfortunately, some say [27] that this leads to a so-called “rebound effect” further increasing demand by between 0% and 15%.

Therefore, it is something which should be considered and one study by Mikkola and Lund [16] produced the spatiotemporal electrical load profiles to develop a more complete picture in regard to the total energy demand for the district.

1.3.3 Turin

Turin is home to Politecnico di Torino, one of the leading technical universities in Europe. As such, many case studies regarding the energy consumption, production, building characteristics, etcetera have been developed relating the case of the building stock and urban development of Turin. A previously elaborated study on the third district in Turin [8] also used GIS along with data related to the space heating (SH) demand to present a cost-optimal methodology which also prioritized buildings in need of retrofit action. In Ballarini and Corrado, [28] three scenarios of building retrofits in the Piedmont region are presented along with objectives outlined in the Italian National Energy Strategy (SEN) for 2030. IN [29] [30], the district heating system of Turin was analyzed. In several other studies [6], [28], [31], [32], the use of reference buildings and the findings of the TABULA project are also elaborated in Italian/Piedmont/Turin case studies.

1.3.4 District Heating

When considering the measures to adopt for energy systems in this case, as district heating is already widely studied ([29] [30]), only heat pumps were considered in order to explore alternative solutions for applications where expansion of district heat may not be possible. The intention was not to study Turin, which has a strong planning activity based on district heating and cooling, but rather to use Turin as a case study for analyzing potential electrification scenarios of the final uses in buildings, considering the potential benefits and costs at district level. For example, a case study on Portland, Oregon, USA performed by MIT CoLab [33] found there are also sometimes hurdles to expansion of district level energy systems. These can be in the form of protected zones, disturbances to transportation as road are excavated, insufficient heat generation plants, or financial concerns for a project of this scale.

Therefore, the work carried out in this project, aims to fix a methodology to explore electrification scenarios at district level though the spreading of electrical heat pumps using a portion of the building stock of Turin as a case study. Research at the IEA [34] suggests that heat pumps offer quick and save solutions to conserve energy and they have ongoing projects dedicated to exploring their applications in existing and new buildings on a wide scale. Another initiative supported by the European Union called Energiesprong [35] has developed systems which are currently being implemented on social housing projects across Europe which apply insulation and advanced energy systems present a "quick and easy"

1.3.5 Emissions

GHG emissions are a common consideration in many of the afore mentioned studies. While GHG emissions pose a serious threat to human development, air quality is also an important concern. Many studies document the cost to society of pollution [36]–[41]. Most of these studies focus on the impacts related to transportation emissions such as [40] and [42]. Using the results from a study carried out by Copenhagen Economics, [43], this work will present the avoided healthcare costs due to the implementation of the various retrofit scenarios.

1.3.6 Novelty

After performing this literature review and to summarize the novelty of the approach detailed in this work, Figure 2 highlights the unique aspects of this research. The most significant novelty stems from the energy system modelling. The hybrid approach is hybrid, spatiotemporal, and includes domestic appliance electricity consumption to create a comprehensive characterization of the district consumption. Another novel aspect is in the consideration of the impacts. Many studies address greenhouse gas emissions, but few also touch on air quality and the related healthcare costs. While many of the previously mentioned studies touch on one or more of the key characteristics of the energy model, measures, impacts, or case, none combine all of these elements to present new insights into the district level energy simulations.

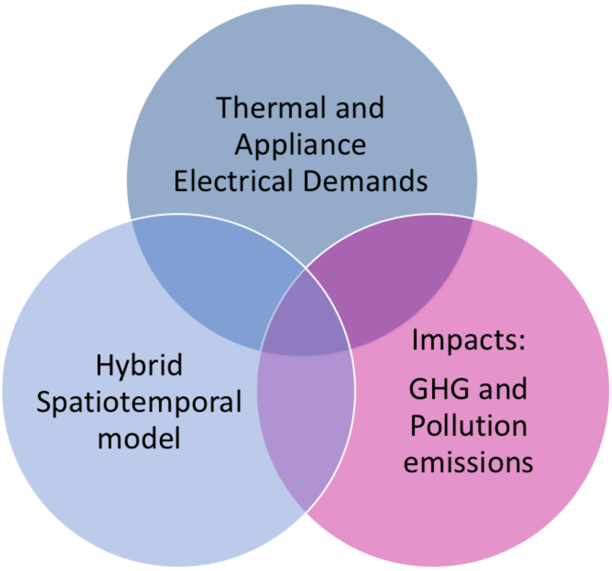

Figure 2: Thesis novelty

1.4 Structure of Thesis

1.4.1 Chapter 1: Introduction

The first chapter introduces the problem addressed in the thesis research and the case which is used to elaborate the work. A literature review on the topics of district level energy modelling methodologies, interventions, and energy related emissions research is presented and allows for the identification of the novelties of this research.

1.4.2 Chapter 2: Materials and Methods

In this chapter, the input data required to elaborate the research is presented along with the methodology and equations employed to create the model which was used for this study. The subchapters are broken down by step in the methodology; QGIS initialization, model development and calibration, district calculations, scenario analysis, financial analysis and finally QGIS visualization.

1.4.3 Chapter 3: Results

The third chapter presents the results of each of the afore mentioned steps in terms of qualitative values as well as QGIS visualizations.

1.4.4 Chapter 4: Discussion

In chapter four, the importance and accuracy of the results and assumptions are discussed. Opportunities to build upon this work and use the flexible model developed to elaborate new research on other cases is also presented.

1.4.5 Chapter 5: Conclusion

The results discussed in light of established targets set by the European Union and final thoughts are presented.

2 Materials and Methods

As shown in Figure 3, there are 6 steps in the process to develop this thesis; model development and calibration, measures implementation, cost calculations, scenario application, results, and finally integrating the results into QGIS to detect neighborhood patterns. In the first step, the QGIS project is created from shapefiles provided by the Municipality of Turin. From these files, residential buildings of interest are identified, and their shape factor is calculated to enable building classification into 36 building archetypes by pairing the shape factor ranges and construction periods. In the second step, the resulting georeferenced building geometry data is used in both the statistical and analytical models for the thermal energy demand evaluation. The models were developed using inputs from the databases indicated and the analytical model. The analytical model was calibrated against the statistical results and the measured data available (247 buildings, 13 archetypes) using the reference buildings (RBs) developed for each of the 13 archetypes for which measured data was available. On the basis of these RBs and knowing the calibrated thermal demand for each RB type, the building energy consumption for space heating (SH), space cooling (SC), and domestic hot water production at district level has been assessed. In lieu of selecting the most common of the archetypes present, the calculations were elaborated on all 36 of the reference buildings in order to create a result that more closely resembles the energy balance of the district. In parallel, the electrical appliance demand for the district was calculated based on census information and statistical data from the master's thesis of Daniele Schiera [44] regarding consumption of Italian households based on social groups. Having characterized the current state of the district from the energy point of view, different retrofit options have been defined and assessed though the analytical models. With the total consumption information determined for the RBs with varied levels of energy efficiency retrofit measures and the district level appliance consumption calculated, the fourth step introduces different rates of retrofit penetration and appliance electricity demand changes. This information along with the necessary coefficients allos for the emissions of each scenario to be calculated. The fifth step draws on the results from the scenario analysis and uses local pricelists regarding retrofit costs as well as data from literature regarding savings in healthcare costs from avoided emissions to assess the economic impacts. Finally, in the sixth step, the results are re-imported in to QGIS to allow for visualization of the trends.

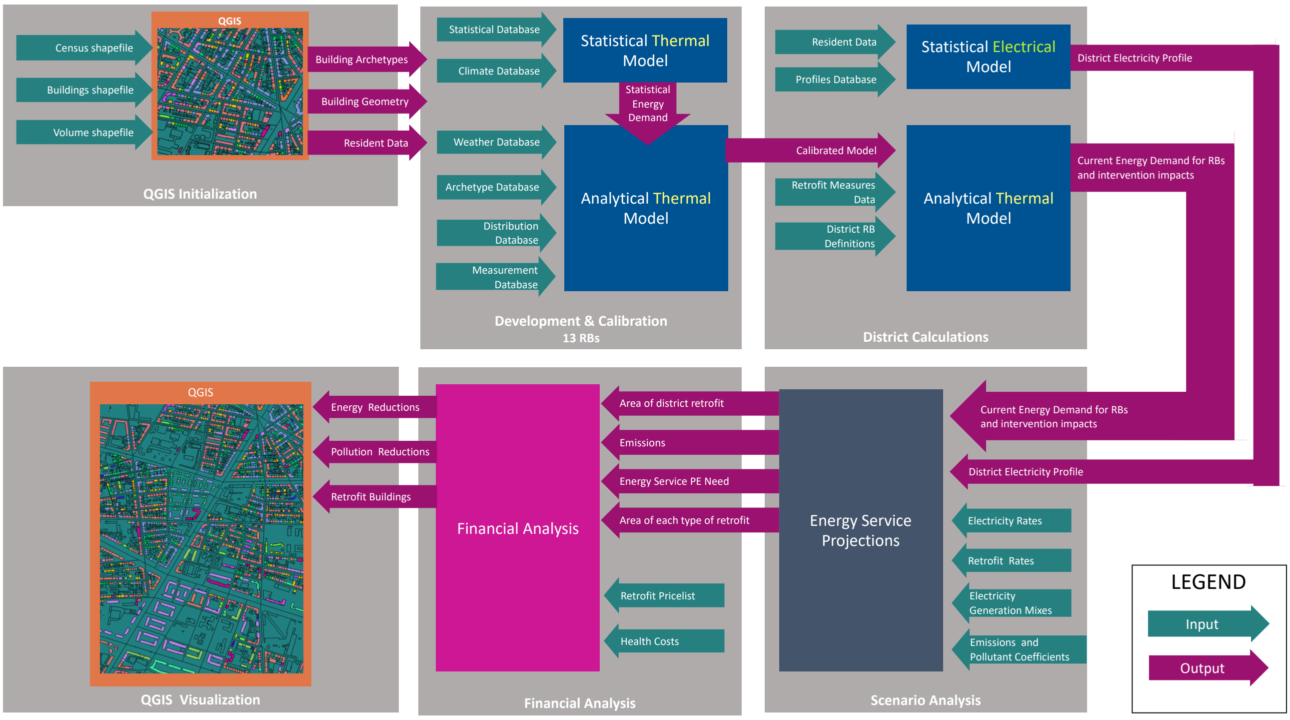

Figure 3: Methodology flowchart

2.1 Assumptions

Some assumptions made in the calculations are as follows:

- The buildings are treated as one large volume (single zone);
- Utility costs are fixed;
- District heating (DH) is fixed;
- The primary energy conversion factor for DH is fixed.

2.2 Step 1: QGIS Initialization

The objective of step 1 was to characterize the district in terms of the building typologies present as well as the demographic make-up of the district. This information provided the foundation for the subsequent steps. Figure 4 provides a reminder of the inputs and outputs associated to this step.

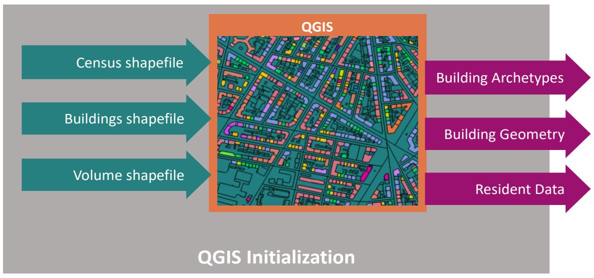

Figure 4: Step 1 flowchart

2.2.1 Input Materials

Shapefile, .shp extension, is a file format used by geographic imaging software (GIS) to read geospatial vector data. This file format allows for attributes to be associated to vector features. The shapefile files used in this research were provided by the Municipality of Turin, and the vector features represented were the buildings and boundaries associated to the 3rd district.

2.2.1.1 “Buildings” shapefile

The “buildings” shapefile contained vector features associated to the buildings and attributes for the construction period and type of building (residential, commercial, etc.) which were used for analysis.

2.2.1.2 “Census Sections” shapefile

The “census sections” shapefile contained vector features associated to the district boundaries and attributes providing the statistical zone and demographic information about residents (number of families, men, women, and ages of residents).

2.2.1.3 “Volumetric Unit” shapefile

The “volumetric unit” shapefile contained vector features associated to the buildings and attributes pertaining to building geometry such as height, number of floors, and surface area.

2.2.2 Analysis

Each shapefile was imported into QGIS, an opensource GIS software program, creating a layer. The layers were then superimposed using the “union” tool in QGIS in order to create a single layer with all of the important information needed to proceed with the calculations.

With a single layer created, the data was filtered by attributes in order to identify only the buildings of interest for this case. The following parameters were used to identify and remove buildings from the layer:

- Buildings not associated to the 3rd district.
- Buildings whose type was not residential.
- Buildings whose height was a single floor.
- Buildings whose footprint surface area was less than 10 m^2.

The assumptions made when eliminating single floor buildings and buildings with a low footprint surface area were that they represented garages and elevators, respectively. Once this was done, the process of determining the shape factor began.

The shape factor (S/V) is defined as the surface to volume ratio [29] and is calculated using Equation 2.1. This parameter is commonly used along with construction period in order to classify buildings by archetypes [6].

$$S/V = \frac{Surface_{ext}}{Volume_{building}} \quad \text{Equation 2.1}$$

The envelope surface exposed to external transmission ($Surface_{ext}$) was determined using QGIS by identifying shared walls, as shown in Figure 5, and the shorter building height and applying Equation 2.2. Wall thickness was omitted, and the building is considered to be an empty shell.

$$Surface_{ext} = (Perimeter \times Height) - Surface_{shared} + 2 \times Surface_{horiz} \quad \text{Equation 2.2}$$

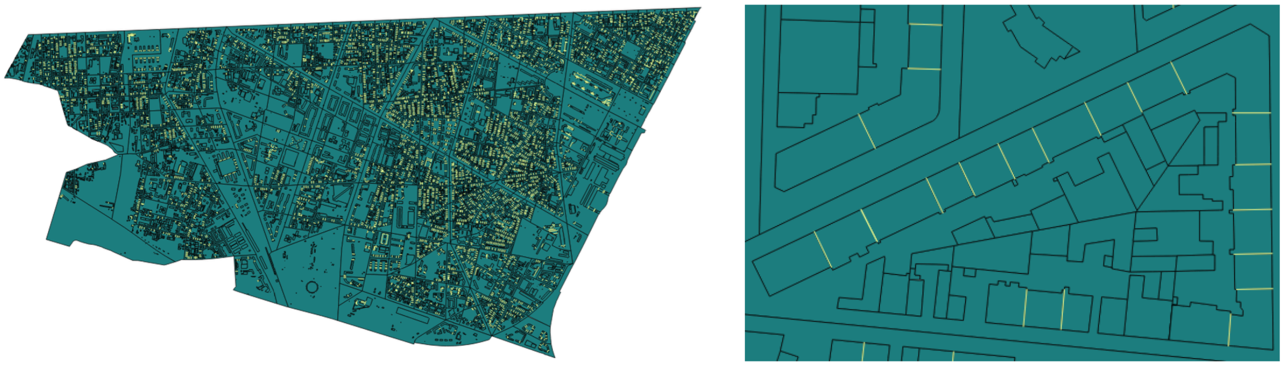

Figure 5: QGIS identification of shared walls between residential buildings. Left: 3rd district. Right: Zoom.

Once $Surface_{ext}$ was determined, the volume was calculated (Equation 2.3) allowing for the final determination of the shape factor.

$$Volume_{building} = Area \cdot Height \quad \text{Equation 2.3}$$

The type of residence was determined based upon the resulting shape factors as presented in Table 1. In order to create the archetype classes, buildings are also grouped based on their construction period as shown in Table 2. Use of shape factors and building construction class for building characterization is a common practice [6] and has been applied to the 3rd district of Turin in previous studies [8]. The combination of 4 building types and 9 construction periods means there are 36 different building archetypes which could be present in the district.

Table 1: Residence type based on shape factor

Type of Building	S/V value	Identifier
Single Family	> 0.8	SF
Terrace House	0.6 - .08	TH
Multi-family Home	0.4 - 0.6	MF
Apartment Block	< 0.4	AB

Table 2: Building construction classes

Construction Period	Class Identifier
Pre 1918	C1
1919 - 1945	C2
1946 - 1960	C3
1961 - 1970	C4
1971 - 1980	C5
1981 - 1990	C6
1991 - 2000	C7
2001 - 2005	C8
2006 - Present	C9

2.3 Step 2: Development and Calibration

During the second step in the process, the analytical thermal model is developed and calibrated. The flow for this process is shown in Figure 6.

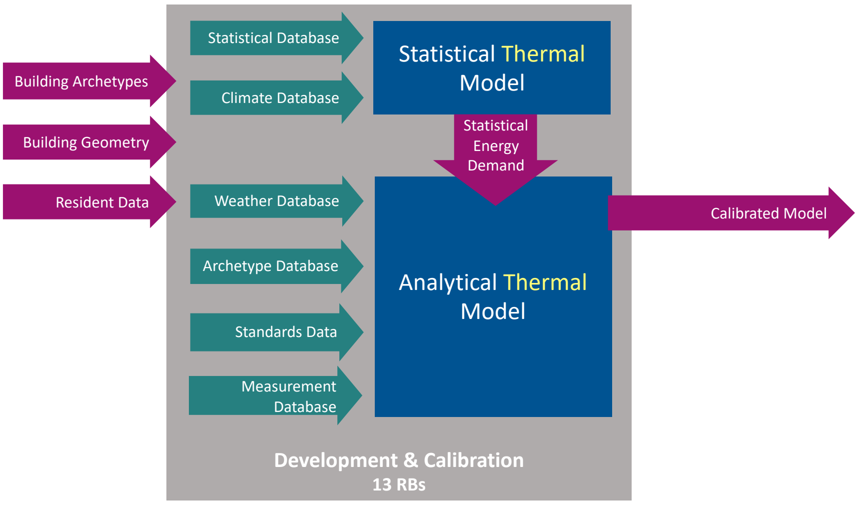

Figure 6: Step 2 flowchart

2.3.1 Input Materials

2.3.1.1 Statistical Database

The statistical values regarding energy consumption for heating and domestic use came from the Italian statistical database, ISTAT [45]. The value used was presented in terms of cubic meters of methane per capita for residents of Turin for 2011.

2.3.1.2 Climate Database

The climate database contains information regarding the heating degree days (HDD) for several years. The years required for this study were 2011, the year from which the statistical data was available, and 2014, the reference year from which the DH consumption data from IREN is available. The HDD data came from ARPA Piemonte [46].

2.3.1.3 Weather Database

The weather database contains information related monthly values for ambient temperatures, solar irradiation [47] from 2014.

2.3.1.4 Archetypes Database

The archetypes database used was from TABULA ([6]), a project providing typology based information for building stock energy assessments. The project was developed as part of the European program “Intelligent Energy Europe” (IEE). The Italian TABULA database contained information describing the standard properties of the Italian building stock. The archetypes are categorized by occupancy type and construction period. One minor inconvenience is that the periods of construction for this database is not completely synchronized with the census construction periods. The TABULA database currently only contains information regarding the residential building stock [32].

2.3.1.5 Standards Data for Hot Water Demand

For the method applied in this thesis, the domestic hot water consumption must also be considered. An Italian standard [48] contained information regarding the domestic hot water requirements based on floor area and temperature set points.

2.3.1.6 Thermal energy measurements database

The measurements database contains information regarding the monthly district heat consumption for 247 buildings in the area of interest. This information has been provided by the district heating service provider, IREN.

2.3.1.7 Thermal Analytical Model

The thermal analytical model developed is based on physical characteristics as defined in the TABULA Italian building typology study [6] and describes the dynamic exchanges of energy between the building and its environment on a monthly basis (quasi-steady state). The required thermal energy services of space heating, space cooling and domestic hot water can then be determined for each building. In order to create the model, the simple monthly dynamic method of the European Committee of Standardization [48]–[56] was applied to a reference building for each of the 36 archetypes.

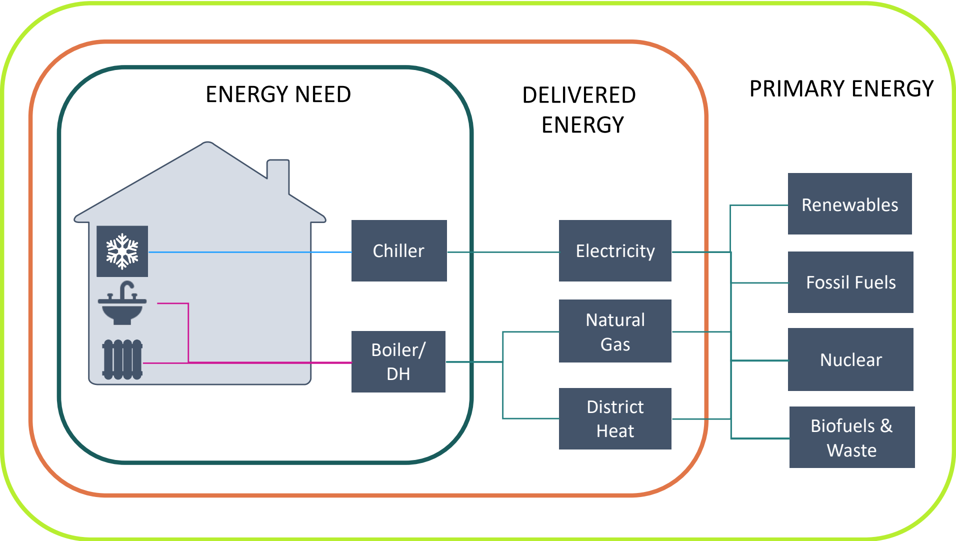

Figure 7: Energy system boundaries schematic

In order to elaborate these thermodynamic calculations for each of the 36 building typologies considered in this thesis, an excel-based tool was developed which allows the user to predefine building geometry and construction material thermophysical characteristics and then to calculate the energy need, delivered energy, and primary energy of a configuration by simply choosing from drop-down menus. The file created allows an engineer to quickly recalculate the consumption of reference buildings with limited data. Figure 7 shows the energy system boundaries. It is important to remember each line on the figure, representing distribution, has losses and that the efficiency of equipment such as boilers, chillers, power generation units is less than 100%. For this reason, buildings with traditional systems for thermal comfort will have higher values of delivered energy than energy need.

2.3.1.8 Definition of Reference Buildings

The use of reference buildings associated to specific building archetypes is a well-established process in modeling of building energy consumption. Making use of the statistical information contained within the archetype database related to thermophysical and building construction typologies, along with the building geometry determined from QGIS, the RBs can be defined. In this study, two sets of reference buildings (RBs) were defined. The first set of RBs was based on buildings for which measured data was available allowing for accurate calibration of the model before implementation on reference buildings defined by a larger sample of the district. Equation 2.4 was used to determine the critical parameters of the RBs.

$$X_{mean,RB} = \frac{\sum_{i=0}^{N} X_{i,RB}}{N_{RB}} \qquad \text{Equation 2.4}$$

Where:

$X_{mean,RB}$ *is a the mean value of a building geometrical feature for the RB;*

$X_{i,RB}$ *is the value for the building geometrical feature of i, RB;*

N_{RB} *is the number of buildings of the same archetype for which the RB is being defined.*

The geometrical feature X could represent the building height, surface area exposed to ambient, wall area shared between buildings, volume, number of floors, or percentage of walls covered by glazing.

The make-up of the 247-building initial sample is presented in Table 3. This sample contains buildings of the apartment block (AB) type from each of the construction periods with the exception of C8 (2001-2005) along with multi-family (MF) homes and terraced homes (TH). No single-family (SF) homes were identified as part of the sample and for some archetypes there was only a single sample. The construction periods are predominately post-war (World War 2), identified as periods C3 and later, which is logical given it was heavily bombed during the war.

The second set of RBs represents the entire residential building stock of the 3rd district and are presented in Table 4. There are 5301 buildings and each of the 36 possible building archetypes. The composition indicating a predominance of multi-family dwellings and post-war construction are maintained in this sample as well.

Table 3: Initial RB sample

Class	Count
C1AB	2
C2AB	32
C2MF	6
C3AB	48
C3MF	4
C4AB	94
C4MF	3
C5AB	39
C5MF	4
C5TH	1
C6AB	12
C7AB	1
C9AB	1

Table 4: District level RB sample

Class	Count	Class	Count	Class	Count
C1AB	78	C4AB	986	C7AB	102
C1MF	25	C4MF	292	C7MF	54
C1SF	2	C4SF	17	C7SF	7
C1TH	18	C4TH	58	C7TH	14
C2AB	735	C5AB	376	C8AB	78
C2MF	408	C5MF	95	C8MF	40
C2SF	14	C5SF	6	C8SF	18
C2TH	67	C5TH	25	C8TH	13
C3AB	860	C6AB	93	C9AB	72
C3MF	489	C6MF	52	C9MF	55
C3SF	15	C6SF	7	C9SF	9
C3TH	99	C6TH	8	C9TH	14

For each set of RBs, the space heating (SH), space cooling (SC), and domestic hot water (DHW) consumption were calculated following the methodology presented in the subsequent sections.

2.3.1.9 Space Heating Requirement

The space heating requirement was determined by performing an energy balance, Equation 2.5, over the course of the heating period in Turin which is from October 15th - April 15th. The RB is treated as a single zone in this analysis and recovered energy is not considered.

$$Q_{H,need} = Q_{H,ht} - Q_{H,gn} \cdot \mu_{gn} \\ = \left(Q_{H,tr} + Q_{H,ve}\right) - \mu_{H,gn} \cdot \left(Q_{int} + Q_{sol}\right) \qquad \text{Equation 2.5}$$

Where:

$Q_{H,need}$	*is the building energy need for space heating;*
$Q_{H,ht}$	*is the heat loss;*
$Q_{H,gn}$	*is the heat gain;*
μ_{gn}	*is the utilization factor;*
$Q_{H,tr}$	*is the heat loss by transmission;*
$Q_{H,ve}$	*is the heat loss by ventilation;*
Q_{int}	*is the internal gain;*
Q_{sol}	*is the solar gain.*

Looking at the losses first, Equation 2.6 and Equation 2.7 represent the equations used to determine the heat losses due to transmission and ventilation, respectively. These values are calculated on a monthly basis as the set temperatures vary seasonally and the mean external temperature and number of days vary monthly.

$$Q_{tr} = H_{tr,adj} \cdot \left(\theta_{i,set} + \theta_e\right) \cdot t \qquad \text{Equation 2.6}$$

$$Q_{ve} = H_{ve,adj} \cdot \left(\theta_{i,set} + \theta_e\right) \cdot t \qquad \text{Equation 2.7}$$

The coefficients of heat loss, $H_{tr,adj}$ and $H_{ve,adj}$ must be calculated using Equation 2.8 and Equation 2.10, respectively. The coefficient of heat loss via transmission, $H_{tr,adj}$, is the sum of the direct heat transfer coefficients; transmission to the ground (H_g), unconditioned spaces (H_u), directly to external environment (H_d), and adjacent buildings (H_a).

$$H_{tr,adj} = H_g + H_u + H_d + H_a \qquad \text{Equation 2.8}$$

Each of the direct heat transfer coefficients is made up of three parts representing transmissions over a surface area, linear, and point transmissions. Equation 2.9 allows for these variables to be calculated. In this model, the contributions from linear and point transmissions were omitted and $b_{tr,x}$ values were taken from literature [55].

$$H_x = b_{tr,x} \cdot (\Sigma_i A_i \cdot U_i + \Sigma_k \psi_k \cdot l_k + \Sigma_j x_j) \qquad \text{Equation 2.9}$$

The transmission losses due to ventilation are based on the volume of the building that can be occupied by air (V_{net}), the number of air changes (n) [57] measured in m^3/hour, the specific heat capacity of air per volume ($\rho_a C_a$) measured in J/m^{3}K and 3600 represents the number of seconds in an hour. Equation 2.10 is used to determine the proper value.

$$H_{ve,adj} = \frac{\rho_a C_a}{3600} \cdot n \cdot V_{net} \qquad \text{Equation 2.10}$$

With the losses evaluated, the gains must be calculated. There are two main sources of gains, solar and internal. The solar gains are due to solar irradiation interacting with the building. The internal gains are based on inhabitants, their quantity and behaviors, as well as heat from any equipment (computers, etc) which may be in the volume of interest.

Solar gains are calculated using Equation 2.11 where $F_{sh,ob}$ is a dimensionless obstruction correction factor, A_{sol} is the area of irradiated elements, opaque and transparent, I_{sol} is the solar irradiation, and t represents the time step of the calculation.

$$Q_{sol} = F_{sh,ob} \cdot A_{sol} \cdot I_{sol} \cdot t = F_{sh,ob} \cdot (A_{sol,tr} + A_{sol,op}) \cdot I_{sol} \cdot t \qquad \text{Equation 2.11}$$

Traditionally, the obstruction correction factor would be calculated with Equation 2.12, factoring in obstructions from other buildings (F_{hor}), overhangs (F_{ov}), or vertical fins (F_{fin}). In this model, $F_{sh,ob}$ was used as a calibration variable.

$$F_{sh,ob} = F_{hor} \cdot F_{ov} \cdot F_{fin} \qquad \text{Equation 2.12}$$

The opaque area, $A_{sol,op}$, was determined based on Equation 2.13. An assumption was made for the opaque surface area, A_c, only two of the building walls were considered exposed to the sunlight as most of the buildings in the district share two walls with neighboring buildings. The values for the color correction factor, α_{sc}, and the external surface resistance, R_{se}, were taken from literature [55] and U_c is determined from TABULA based on the RB archetype. In this study, α_{sc} was used as a calibration variable.

$$A_{sol,op} = \alpha_{sc} \cdot R_{se} \cdot A_c \cdot U_c \qquad \text{Equation 2.13}$$

The equivalent transparent area, $A_{sol,tr}$, is calculated with Equation 2.14 The window area, A_w, is determined based on the RB archetype data in TABULA as a percentage of the wall area. The and frame factor, F_F, value are determined based on literature [55].

$$A_{sol,tr} = F_{sh,gl} \cdot g_{gl} \cdot (1 - F_F) \cdot A_w \qquad \text{Equation 2.14}$$

The total solar transmittance, g_{gl}, is determined using Equation 2.15 based on a correction factor for non-scattering glazing, F_w, and the time-average total solar energy transmittance, $g_{gl,n}$, related to the type of window.

$$g_{gl} = g_{gl,n} \cdot F_w \qquad \text{Equation 2.15}$$

The shading reduction factor, $F_{sh,gl}$, allows for the consideration of the use of shutters and other shading devices through the application of Equation 2.16. The total solar energy transmittance of the window, g_{gl}, is the value when no shading device is in use. However, $g_{gl,sh}$ represents the value when a shading device is being used.

$$F_{sh,gl} = \left(1 - f_{sh,with}\right) + (f_{sh,with} \cdot \frac{g_{gl,sh}}{g_{gl}}) \qquad \text{Equation 2.16}$$

Once the solar gains are determined, the internal gains, Q_{int}, must be determined. Equation 2.17 provides the means to do so. The time-average heat flow rate from internal heat source, $\phi_{int,min}$, is based on the net floor area, A_{NF}, of the building and calculated in accordance with Equation 2.18.

$$Q_{int} = \phi_{int,min} \cdot t \qquad \text{Equation 2.17}$$

$$\phi_{int} = \begin{cases} 450, & A_{NF} > 120m^2 \\ 7.98 \cdot A_{NF} - 0.035 \cdot A_{NF}^2, & A_{NF} \leq 120m^2 \end{cases} \qquad \text{Equation 2.18}$$

Lastly, the utilization factor must be determined. The utilization factor in Equation 2.5 is a dimensionless factor to balance the gains in the case of possible overheating due to solar gains and must be calculated for each month. The utilization factor is determined based on the value of another variable, γ_H, which is the heat balance ratio, calculated with Equation 2.19, for the heating mode and the utilization factor is then calculated with the appropriate equation.

$$\gamma_H = \frac{Q_{H,gn}}{Q_{H,ht}} \qquad \text{Equation 2.19}$$

Equation 2.20 is applied to determine the utilization factor according to the previously obtained heat balance ratio value.

$$\mu_{gn} = \begin{cases} \dfrac{1-\gamma_H^{\alpha_H}}{1+\gamma_H^{\alpha_H+1}}, & \gamma_H > 0, \gamma_H \neq 1 \\ \dfrac{\alpha_H}{\alpha_H+1}, & \gamma_H = 1 \\ \dfrac{1}{\gamma_H}, & \gamma_H < 0 \end{cases} \qquad \text{Equation 2.20}$$

Where the dimensionless parameter, α_H, is calculated with Equation 2.21 and the values for and the values for the numerical parameter, α_{H0}, the reference time constant, τ_{H0}, are found in literature [49]. For this model, the values were α_{H0} = 1 and τ_{H0} = 15 (hours).

$$\alpha_H = \alpha_{H0} + \frac{\tau}{\tau_{H0}} ; \qquad \text{Equation 2.21}$$

The thermal inertia of the building, τ, is calculated per Equation 2.22 and the thermal capacity, C_m, can be found in literature [55] (115 kJ/m^{2}K).

$$\tau = \frac{C_m/3600}{H_{tr,adj} + H_{ve,adj}} \qquad \text{Equation 2.22}$$

With the afore mentioned calculations, $Q_{H,need}$ is determined, but that value does not take into consideration that there are inefficiencies in the system. These must be determined in order to calculate the final energy consumption, $Q_{H,use}$, which corresponds to the delivered energy in Figure 7. In order to calculate the overall system efficiency, $\eta_{H,sys}$, Equation 2.23 is use and values for the regulation system efficiency, η_{rg}, the distribution system efficiency, η_d, and the generation system efficiency, η_g,can all be found in literature [55]. The emission system efficiency must be determined with Equation 2.24 and Equation 2.25.

$$\eta_{H,sys} = \eta_e \cdot \eta_{rg} \cdot \eta_d \cdot \eta_g \qquad \text{Equation 2.23}$$

For the medium value of the heating requirement, $Q_{H,medium}$, the total annual heating requirement is determined by summing the monthly values for the heating requirement, $Q_{H,medium,ANNUAL}$, and this value is then divided by the hours in which the heating system is used, 14 hours/day, and the length of the heating season, 183 days, along with the gross heated volume, V_{gr}. Depending on the value of $Q_{H,medium}$ the appropriate system efficiency is selected.

$$Q_{H,medium} = \frac{Q_{H,need,ANNUAL}}{14 \cdot 183 \cdot V_{gr}} ; \qquad \text{Equation 2.24}$$

$$\eta_e = \begin{cases} 0.98, & Q_{H,medium} < 4 \\ 0.97, & 4 < Q_{H,medium} < 10 \\ 0.95\,, & 10 < Q_{H,medium} \end{cases} \qquad \text{Equation 2.25}$$

2.3.1.10 Space Cooling Requirement

The required cooling, $Q_{C,need}$, is calculated by following the same process as $Q_{H,need}$, but changing the set temperature to 26^{oC} and using the meteorological data from May-September. If $Q_{C,need}$is found to be less than 15 kWh/m^{2}y, then standard practice dictates no cooling system is required.

2.3.1.11 Domestic Hot Water

The amount of domestic hot water (DHW) required is determined based on Equation 2.26 where the total energy need for hot water, $Q_{w,need}$, is calculated using Equation 2.27 and the generation system efficiency, η_g, comes from literature. Water density, ρ_w, and specific heat, c_w, are well known constants. The desired water temperature, θ_{er}, and water supply temperature, θ_o, from the aqueduct in Turin were provided by Politecnico di Torino. The number of working days the hot water must be available, G, is set as 365 days.

$$Q_{w,use} = \frac{Q_{w,need}}{\eta_g} \qquad \text{Equation 2.26}$$

$$Q_{w,need} = \rho_w \cdot c_w \cdot V_w \cdot (\theta_{er} - \theta_o) \cdot G \qquad \text{Equation 2.27}$$

In order to determine the appropriate volume of water needed, V_w, the net conditioned floor area, S_w, is used along with two factors, a and b which come from literature [55].

$$V_w = a \cdot S_w \cdot b \qquad \text{Equation 2.28}$$

At this point the values for need and final energy consumption for SH, SC and DHW have been determined and this process was carried out for each of the RBs.

2.3.2 Statistical Thermal Model

The statistical model is adapted from the simple heating degree days (HDD) method presented in literature [58]. The statistical information available in terms of heating need for Turin was available in terms of methane required per capita, $V_{CH4,use,2011}$. Therefore, Equation 2.29 was created to make use of the information that was available. This value, 599.62 m^3/person/year [45], was from the year 2011 and included cooking and production of domestic hot water. The heating degree days, HDD_{2014} and HDD_{2011}, were obtained from ARPA [46]. As the information regarding the methane consumption pertained to the region of Torino and not the city of Turin, the HDD value is that of the region in 2011. In order to be applicable for our district, the 2014 HDD value was obtained from the nearest weather station, Alenia. The gross volume used was that of the RB for each archetype and the census data was used to determine the mean number of residents in each building, P.

$$q_{use,stat} = \frac{\mathrm{V}_{CH4,use,2011}}{person} \cdot \frac{38113\ kJ}{1\ std\ m^3\ CH_4} \cdot \frac{277.778\ kWh}{1e^6 kJ} \cdot V_{gr} \cdot P \cdot \frac{HDD_{2014}}{HDD_{2011}} \quad \text{Equation 2.29}$$

Where:

$q_{use,stat}$	*is the final specific heat consumption with cooking & DHW [kWh/m²];*
$V_{CH4,use,2011}$	*is of heating need for Turin province [m³ CH₄];*
HDD_{2014}	*is the heating degree days in the 3rd district in 2014 [days];*
HDD_{2011}	*is the heating degree days for the province of Turin in 2011 [days];*
V_{gr}	*is the gross volume of the RB [m³];*
P	*is the population of the RB [people];*
$\frac{1\ std\ m^3\ CH_4}{38113\ kJ}$	*is the conversion from m³ CH₄ to kJ* [59];
$\frac{1e^6 kJ}{277.778\ kWh}$	*is the conversion from kJ to kWh;*

Once the value was defined, an adjustment had to be made in order to address the fact that the statistical value included cooking and DHW production. Based on literature, [60] the share of final consumption for cooking and DHW production have remained relatively steady and their values were 5.5% and 8.5%, respectively in 2013 and were therefore assumed to be the same in 2014. Therefore, the values found through Equation 2.29 were adjusted using Equation 2.30.

$$q_{use,stat,adj} = q_{use,stat} \cdot (100 - S_{DHW} - S_{CK}) \quad \text{Equation 2.30}$$

Where:

$q_{use,stat,adj}$	*is the adjusted value for specific final heat consumption [kWh/m²]*
S_{DHW}	*is the share of final consumption of DHW [%];*
S_{CK}	*is the share of final consumption of cooking [%];*

2.3.3 Calibration with Measurement Database

The measurement database comes from the district heat provider, IREN. The file provided contained information such as the building address, an ID from a previous QGIS project in the district, and the consumption in MCalh. Figure 8 shows some examples of the DH heating data which was present in the database.

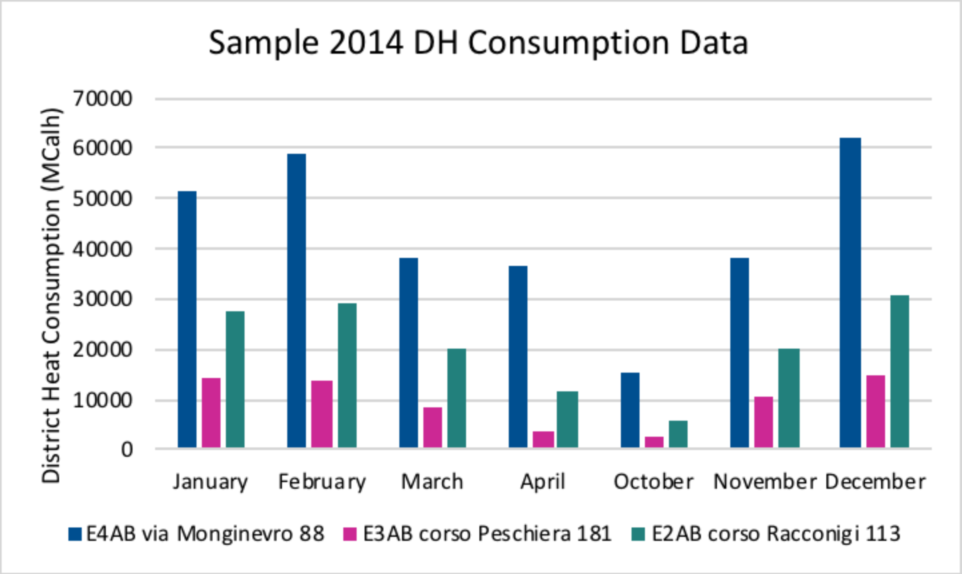

Figure 8: Sample DH data for 3rd district, 2014

The QGIS union tool was used again in order to reconcile the new project building IDs with the old ones and associate the consumption to the appropriate building. There were a few instances where the old building ID corresponded to several new ones, indicating higher granularity in the building shapefile used in this study. These issues (10 instances) were investigated and resolved manually by combining some buildings in order to associate their consumption data which was not as granular. The specific heating need was then calculated for each building. With the specific consumption determined and associated to the appropriate archetype, the RB mean measured consumptions could be determined.

For each archetype there were a different number of buildings in the sample as shown in Table 3. For those with higher number of samples, it would be expected that the RB may be more representative for the district and it is therefore more critical that the calibration reduces the error as it pertains to the higher frequency RBs. In order to determine the error for both the analytical and statistical models, Equation 2.31 was used.

$$\%\, error = \frac{approximate - measured}{measured} \qquad \text{Equation 2.31}$$

2.3.3.1 Calibration Variables

The variables which were changed in order to facilitate the calibration were the building orientation, the color correction factor, and the obstruction correction factor. These variables impact the solar gains of the building. In an urban environment, it is logical that the obstruction correction factor should be less than one as it is probable that buildings would cast shadows on each other. In regard to the orientation, most of the buildings in this study were best calibrated with an east-west orientation and the . All other variables had been determined based on building geometry or values from literature which are fixed.

Again, in this step, the development of a tool which rapidly recalculates the energy need and use for SH, SC, and DHW was imperative in order to perform the calculations and iterate for each of the RBs.

Once satisfied with the range of error across the initial RBs, the model was considered calibrated.

2.4 Step 3: District Calculation and Introduction of Measures

As shown in Figure 9, the calibrated analytical thermal model is applied to newly calculated RBs representing the entire district and all 36 archetypes. Several retrofit measures are considered, and their impacts on consumption are determined. In parallel, the statistical electrical consumption for the district is determined based on the profiles database and information regarding the district residents. The outputs are the district level electrical profile and the energy consumption for each RB with each retrofit.

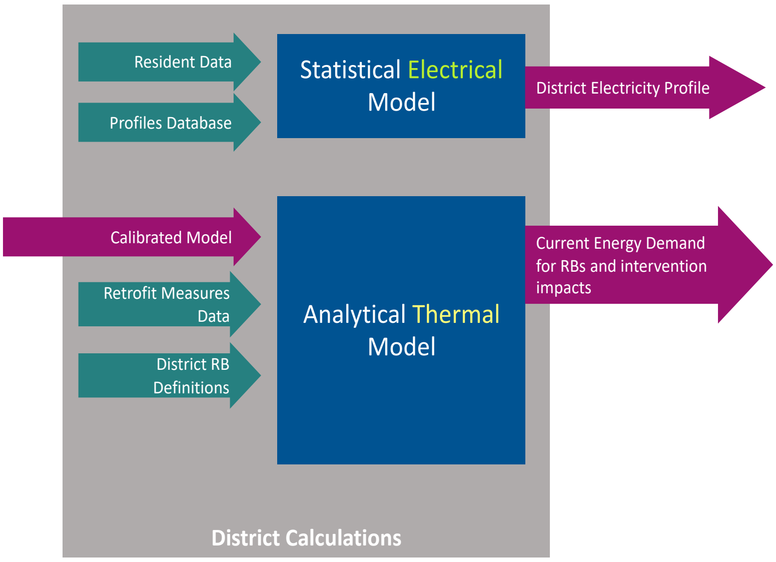

Figure 9: Step 3 flowchart

2.4.1 Input Materials

2.4.1.1 Retrofit Measures Data

The retrofit measures were initially defined based on TABULA data and were specific to each RB. As some TABULA values no longer meet the current standards, those values replaced and values related to the envelope retrofit were taken from the IEA [1] or academia [61] and values for energy system retrofits came from the IEA “Transitions to Sustainable Buildings” as well [1].

2.4.1.2 District RB Definitions

For the definition of the district level reference buildings, the process was the same as that which was elaborated in 2.3.1.8, but the sample encompassed the whole district (5301 buildings). The results of the breakdown by archetype can be seen in Table 4.

2.4.1.3 Resident Data

Additional census information, not found in the census GIS shapefile, related to level of education and citizenship which are defining parameters used in the classification of the groups were provided in the form of an excel file containing census information for all of Turin.

2.4.1.4 Profiles Database

The electricity consumption profiles database was provided by previous master's thesis research [44]. The data is provided as consumption in Wh at fifteen-minute intervals for an entire year. Each profile was specific to a social group as they are identified by ISTAT [62].

2.4.2 Processing District Level RBs and Tuilding thermophysical Properties

With the critical inputs gathered, the consumption data was recalculated using the analytical thermal model. For both the systems and the envelope, two levels of intervention were considered, and they are detailed in Table 5 and Table 6. The "Basic" envelope intervention was comprised of adding insulation to the roof and ground level and replacing the windows with more efficient, low-e, double-glazed models with vinyl frames. In the "Advanced" building envelope intervention, insulation is added to the walls as well and the windows are double low-e, triple glazed with vinyl frames. For the systems, the boilers are replaced with heat pumps for both heating and cooling. The difference between the "Basic" and the "Advanced" is simply the coefficient of performance (COP) of each. In "Basic" it is 2.9 and in "Advanced" it is 4.0 [1].

Table 5: Envelope retrofit measures

	WALL (to ambient)		**ATTIC**		**FLOOR (to basement)**		**JOINERY - Windows**		
Classification	Additional Insulation thickness (m)	U [W/(m^{2}K)]	Additional Insulation thickness (m)	U [W/(m^{2}K)]	Additional Insulation thickness (m)	U [W/(m2K)]	Description	U [W/(m^{2}K)]	$g_{gl,n}$
Envelope: Advanced	0.14	0.15	0.15	0.13	0.15	0.23	Triple glaze, double low-e, vinyl frame	1.1	0.27
Envelope: Basic	0	0	0.11	0.27	0.1	0.3	Double low-e, vinyl frame	1.7	0.5

Table 6: System retrofit measures

	Heat Generation		**Cooling Generation**	
	Description	Efficiency ($\eta_{H,gn}$) or COP	Description	Efficiency ($\eta_{H,gn}$) or COP
Systems: Advanced	ground heat pump with COP = 4	4	ground heat pump with COP = 4	4
Systems: Basic	air heat pump with COP = 2.9	2.9	air heat pump with COP = 2.9	2.9

These interventions were combined to create four unique possibilities as demonstrated in Table 7.

Table 7: Retrofit measure combinations

Systems Envelope	Advanced	Basic
Advanced	EASA	EASB
Basic	EBSA	EBSB

Throughout the remainder of the analysis when referring to building interventions pertaining to SH, SC and DHW, the codes indicated in Table 7 will be used. Ex: 1% EASA implemented per year. In these interventions, endogenous energy production, energy storage and changes in emission, distribution and regulation system efficiency were not considered.

2.4.3 Electrical Profiles

2.4.3.1 Determining Social Group Representation in 3rd district

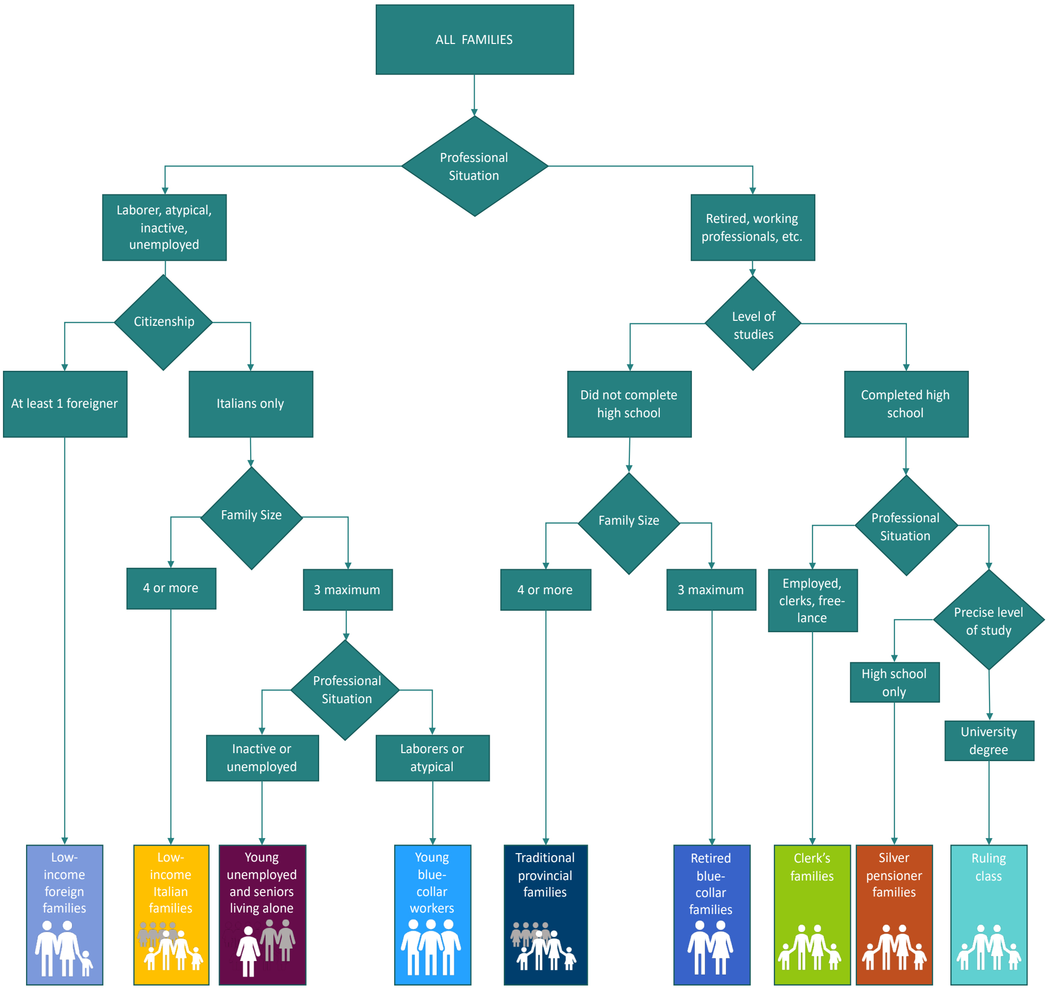

Figure 10: Classification of Social Groups in Italy

Electricity profiles based on household social groups were made available by previous research [44] along with some more census information related to various zones in the city. The new census information, not in the form of a GIS shapefile, contained information related to level of education and citizenship. These are defining parameters used in the classification of the groups, as shown in Figure 10, which is based on information provided by ISTAT [62]. The new census information was filtered for the zones which are only applicable to the 3rd district; zones 31, 32, 33, 34, 51, and 52. For each census zone, the sorting indicated in Figure 10 was carried out, and the number of households of each type was determined at a zone level.

2.4.3.2 Creation of District Level Electrical Load Profile

Unfortunately, measured data is not available regarding the appliance electricity consumption in the district. Therefore, previous research which uses a socio-techno-economic analysis based on census data to identify the penetration of certain devices and technologies to construct electrical load profiles based on so-called "social groups" as they will differ based on each household's circumstances. The objective for this process was to arrive at monthly values for electricity consumption based on domestic appliances which was representative of the district. In order to do this, the individual social group electricity consumption profiles with fifteen-minute increments were converted into hourly, then daily, then monthly values by taking the average of the fifteen-minute time steps as shown in Equation 2.32. Once this was complete, the profile for the district was calculated by applying the values found in Section 2.4.3.1 regarding how many of each type of social group household were present in the district. This allowed for the determination of the monthly and annual electricity consumption values.

$$El_{hr} = \frac{El_{15} + El_{30} + El_{45} + El_{60}}{4}$$ Equation 2.32

Where:

El_{hr} *is the hourly consumption [kWh];*

El_x *where x is 15, 30, 45, or 60 represents the consumption at each minute mark [kWh];*

2.5 Step 4: Scenarios

The fourth step is the establishment of the scenarios which introduce changes to the building stock and electrical consumption patterns on an annual basis. These changes allow for projections of the impacts on key parameters such as energy consumption, greenhouse gas emissions, and local air pollution as a result of the changing energy service demands. The inputs and outputs of this step are presented in Figure 11.

A more detailed process is presented in Figure 12. The first step in the process was prioritizing the application of the retrofit interventions. Next, the scenarios with different intervention rates are applied to each of the area of the district corresponding to the RBs respecting the prioritization.

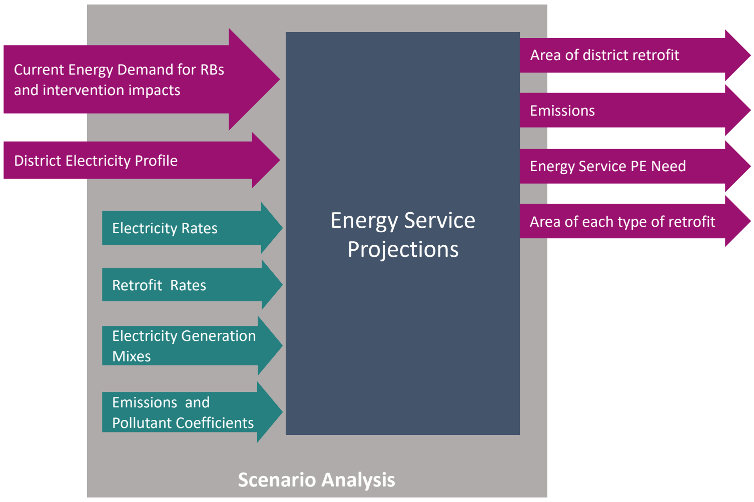

Figure 11: Step 4 flowchart

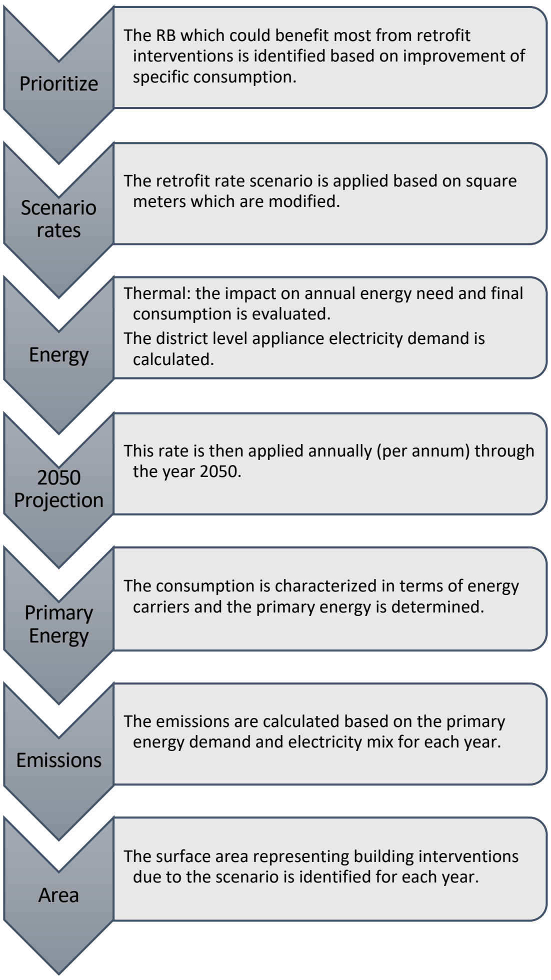

Figure 12: Detailed scenario analysis flowchart

This is done for each year through 2050, where each year more buildings are impacted. The energy need, which is reduced thanks to envelope interventions, is subsequently determined. The previous steps had not yet taken into consideration the increased electrical demand due to the addition of heat pumps or the domestic appliance electricity use and that is addressed in the energy consumption assessment, and these consumptions are also characterized by their energy carriers. Based on the different energy carriers, the primary energy demand is determined at a district level each year. With the demands and the energy carriers used to generate the energy required to meet the demand clear, the emissions, greenhouse gas as well as other pollutants, can be determined for each year. As an input for the following step of the process, the financial calculations, the area impacted by the interventions is also identified.

2.5.1 Input Materials

2.5.1.1 Electricity Consumption Rates

According to a study performed by researchers at Arizona State University [63], it is expected that with the increased rates of electrification in our homes, electricity demand will increase at a rate of 1% per year, this is considered the business as usual (BAU) case. There will, of course, be improvements in the efficiency of the devices in question and the same study suggests that these could offset the growth in demand by 0.5% (optimistic) or 0.25% (conservative).

2.5.1.2 Retrofit Rates

According to BPIE [64], it is estimated that building stock renovation rates range between 0.5% and 2.5% per year, with the most common rate across Europe being 1%. Therefore, no scenario was considered where retrofit rates were outside of those bounds.

2.5.1.3 Electricity Generation Mix Evolution

The current electricity generation mix for Italy [65] is presented in Table 8 along with possible combinations which are aligned national and international objectives. The National Energy Strategy defines the target for renewable share of final electricity consumption in 2030 as 55% [2] and the trend was expected to continue in a similar fashion until 2050.

Table 8: Electricity supply mix - current and future

Year	2014	2030	2050
Natural Gas	38.3%	32%	1.4%
Coal	16.6%	11%	0.6%
Oil	4.8%	0%	0.17%
Biofuels and Waste	7.8%	2%	0.6%
Wind	5.2%	11%	15.6%
Hydropower	15.6%	21%	45.7%
Geothermal	2.2%	8%	8%
Solar	9.3%	15%	27.9%
Non- RE Share	67.7%	45%	2.7%
Renewable Share	32.3%	55%	97.3%

2.5.1.4 Greenhouse Gas and Pollutant Coefficients

The emission and pollutant coefficients came from multiple sources. For greenhouse gasses methane (CH_4), nitrous oxide (N_2O), and the combined particulate matter PM from the combustion of natural gas values were obtained from the Environmental Protection Agency (EPA) [66][67]. The values for carbon dioxide (CO_2), other nitric oxides (NO_x), sulfur dioxide (SO_2) and $PM_{2.5}$ values were obtained from research carried out by Copenhagen Economics using the GAINS model [43]. The values for global warming potential (GWP) for each of the greenhouse gasses were obtained from the

Greenhouse Gas Protocol outlined by the Intergovernmental Panel on Climate Change [68]. All values are presented concisely in Table 9.

Table 9: Emissions coefficients and global warming potential (GWP)

Fuel type	Greenhouse Gasses						
	kg CO_2/GWh	kg CH_4/GWh	kg N_2O/GWh	kg NO_x/GWh	kg SO_2/GWh	kg $PM_{2.5}$/GWh	kg PM_{tot}/ GWh
Natural Gas	204879.6	3.4	0.341	133.2	270.0		56.0
Coal	339109.2	37.5	5.5	234.0	298.8	14.4	
Biofuels and Waste	360015.1	109.2	14.3	216.0	100.8	3.6	
Oil	254341.0	10.2	2.05	1846.8	795.6	68.4	
GWP	1	258	298				

For the electricity mix which varies with time in this study, the emissions factors of each individual fuel were considered in the proportion which it is consumed.

2.5.2 Prioritization

The implementation of the energy efficiency retrofits was prioritized starting with the RBs which demonstrated the greatest improvements in final energy consumption based on the results of the analytical thermal model. The determination of greatest improvement was an absolute assessment in terms of kWh/m^2 of final consumption, not based on the percentage of reduction.

2.5.3 Scenario Rates

The scenario rates were assumed in accordance with the BPIE study and are as presented in Table 10.

Table 10: Building retrofit yearly rates (p.a.)

	EASA	EBSA	EASB	EBSB	Total Change
Slow Rate	0.00%	0.00%	0.10%	0.50%	0.60%
Moderate Rate	0.10%	0.00%	0.50%	1.00%	1.60%
Fast Rate	0.50%	0.00%	1.50%	0.00%	2.00%

This nomenclature, “Slow,” “Moderate,” and “Fast” will be used throughout the text and refers back to these combinations of envelope and system interventions as detailed in Table 7.

2.5.4 District energy need and final consumption

For each year, Equation 2.33 is used to calculate the district energy thermal need and use for SH, SC, and DHW.

$$Q_{dist,y} = \sum_i (E_{RBi,or} \cdot A_{RBi} \cdot R_{RBi,or} \cdot y + E_{RBi,EASA} \cdot A_{RBi} \cdot R_{RBi,EASA} \cdot y + E_{RBi,EBSA} \cdot A_{RBi} \cdot R_{RBi,EBSA} \cdot y + E_{RBi,EASB} \cdot A_{RBi} \cdot R_{RBi,EASB} \cdot y + E_{RBi,EBSB} \cdot A_{RBi} \cdot R_{RBi,EBSB} \cdot y) \quad \text{Equation 2.33}$$

Where:

$Q_{dist,y}$	*is the district level energy need [kWh/y] or use related to SH, SC and DHW;*
i	*is the index corresponding to the 36 RBs;*
y	*is the year value (1, 2, 3, etc.) corresponding to 2015, 2016, 2017, etc.;*
A_{RBi}	*is the area [m2] of the district comprised of buildings of RB_i type;*
$E_{RBi,or}$	*is the original/pre-retrofit energy (need or use) [kWh/m²y] for RB_i;*
$R_{RBi,or}$	*is the rate (% p.a.) of the RB_i building stock in its original state;*
$E_{RBi,EASA}$	*is the EASA energy (need or use) [kWh/m²y] for RB_i;*
$R_{RBi,EASA}$	*is the rate (% p.a.) of the RB_i building stock with EASA interventions;*
$E_{RBi,EBSA}$	*is the EBSA energy (need or use) [kWh/m²y] for RB_i;*
$R_{RBi,EBSA}$	*is the rate (% p.a.) of the RB_i building stock with EBSA interventions;*
$E_{RBi,EASB}$	*is the EASB energy (need or use) [kWh/m²y] for RB_i;*
$R_{RBi,EASB}$	*is the rate (% p.a.) of the RB_i building stock with EASB interventions;*
$E_{RBi,EBSB}$	*is the EBSB energy (need or use) [kWh/m²y] for RB_i;*
$R_{RBi,EBSB}$	*is the rate (% p.a.) of the RB_i building stock with EBSB interventions;*

2.5.5 2050 Projections

For each of the scenarios, slow, moderate, and fast, Equation 2.33 gives the total annual energy need and use. These projections are carried out through 2050 by incrementing the year value, Y. This provides the trend for each scenario.

Additionally, the district level electrical profiles are added and the future values were extrapolated according to the rates defined in Table 11 which come from literature [63].

Table 11: Domestic appliance energy demand scenarios

Domestic Appliance Energy Demand Scenarios	%
Business as usual (BAU)	1.00%
Appliance Efficiency Improvements Conservative (EC)	0.75%
Appliance Efficiency Improvements Optimistic (EO)	0.50%

The value for the contribution of the domestic appliance electricity use (GWh), $El_{dist,y}$, can be determined for any given year, y, based on the original value for the district in 2014 (GWh), $El_{dist,2014}$, and the rate related to the electricity demand scenario (%) selected, R_{el}, as shown in Equation 2.37.

$$El_{dist,y} = El_{dist,2014} \cdot (1 + R_{el})^{y}$$

Equation 2.34

The addition of the building retrofit, and domestic appliances scenarios lead to a total of 9 scenarios related to energy demand which are outlined in Table 12.

Table 12: Demand scenarios

Building Appliance	Slow	Moderate	Fast
BAU	Slow - BAU	Moderate - BAU	Fast - BAU
EC	Slow - EC	Moderate - EC	Fast - EC
EO	Slow - EO	Moderate - EO	Fast - EO

The total energy demand for the district, $E_{dist,y}$, for a given year is therefore given by Equation 2.35.

$$E_{dist,y} = El_{dist,y} + Q_{dist,y}$$

Equation 2.35

In addition to these 9 demand side scenarios, there are two additional supply side scenarios to consider. With the increasing electrification of the demand, it is wise to also quantify the impact of increasing the renewable share in the electricity generation mix. Table 8 shows the current and future energy mixes. The resulting scenarios are presented in Table 13.

Table 13: Final scenarios

Supply Demand	Current	Identifier Current	Future	Identifier Future
Slow - BAU	Slow - BAU - Current	SBC	Slow - BAU - Future	SBF
Slow - EC	Slow - EC - Current	SCC	Slow - EC - Future	SCF
Slow - EO	Slow - EO - Current	SOC	Slow - EO - Future	SOF
Moderate - BAU	Moderate - BAU - Current	MBC	Moderate - BAU - Future	MBF
Moderate - EC	Moderate - EC - Current	MCC	Moderate - EC - Future	MCF
Moderate - EO	Moderate - EO - Current	MOC	Moderate - EO - Future	MOF
Fast - BAU	Fast - BAU - Current	FBC	Fast - BAU - Future	FBF
Fast - EC	Fast - EC - Current	FCC	Fast - EC - Future	FCF
Fast - EO	Fast - EO - Current	FOC	Fast - EO - Future	FOF

2.5.6 District Primary Energy

The calculation primary energy consumption is critical because aggregation of energy from multiple energy carriers cannot be completed otherwise and buildings typically use energy from more than one carrier (gas, electricity, district heat, etc.).

Primary energy conversion factors (PEC) are used to represent the energy lost in conversion processes. For renewables, the PEC is typically set as 1, meaning 100% conversion efficiency [69]. As the electricity mix is typically composed of both renewable and fossil fuel-based energy, this value is sometimes difficult to quantify. There are two types of PEC to consider; total and non-renewable. For this study, the non-renewable PEC was considered for electricity. With the introduction of the theoretical future energy mixes for electricity, the PEC will evolve over time. Initial values for the PECs were found in literature [25] for natural gas and district heating. The value for electricity came from Italian Standards [70]. The initial values are presented in Table 14.

Table 14: Primary energy conversion (PEC) factors, 2014

Primary Energy Conversion Factors	Value
Natural Gas	1.403
District Heating	1.500
Electricity	1.950

The future PEC values for electricity considering the increasing renewable share are presented in Table 15 and were calculated using proportional decrease relative to the decreasing fossil fuel share in the electricity generation mix as show in Figure 13. These values were assumed based on the NES and 2050 Energy Roadmap.

Table 15: Electricity PEC evolution

PEC	2014	2030	2050
Electricity	1.950	1.475	0.148

The PEC values for all other energy carriers were maintained at their 2014 value in order to isolate the impacts of electrification in the scenarios. It is understood that research suggests the district heating PEC will also decrease in the future, but that was considered to be out of scope for this case.

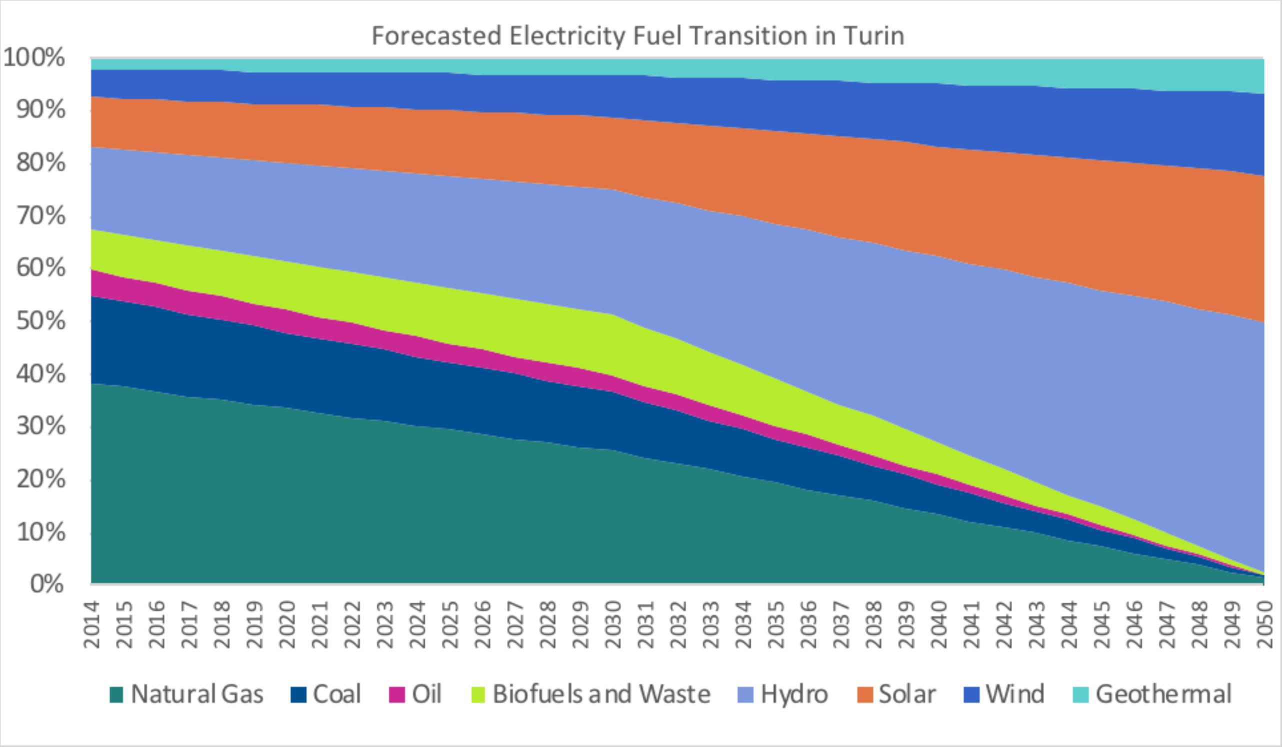

Figure 13:Assumed electricity fuel transition in Turin

In the analytical thermal model, it was assumed that pre-retrofit heat and hot water come from boilers burning natural gas except for the buildings which had district heat. Post retrofit, these services are provided by heat pumps, thus changing the energy carrier to electricity and the primary energy demand is calculated with Equation 2.36.

$$PE = \Sigma PEC_{c,y} \cdot E_{use,c,y} \quad \text{Equation 2.36}$$

Where:

PE *is the primary energy demand [GWh$_{PE}$/y] for year,* y*;*

c *is the energy carrier (electricity, district heat, or natural gas);*

$PEC_{c,y}$ *is the PEC for carrier,* c*, for year,* y*;*

$E_{use,c,y}$ *is the finale energy consumption [GWh/y] by carrier,* c*, for year,* y*;*

This value was calculated for every scenario and every year.

2.5.7 Emissions

There are two main types of emissions considered in this study; greenhouse gas emissions and air pollutants. Volatile organic compounds (VOCs) were not considered.

2.5.7.1 Greenhouse Gas Emissions

Greenhouse gas emissions were determined using the coefficients identified in Table 9 and applied to Equation 2.37 as suggested in literature [71]. The greenhouse gasses evaluated are carbon dioxide (CO_2), methane (CH_4), and nitrous oxide (N_2O).

$$Emission_x = \Sigma EF_c \cdot E_c \quad \text{Equation 2.37}$$

Where:

$Emission_x$ *is the emissions [kg/y] of pollutant* x*;*

EF_c *is the emission factor [kg* x */GWh] of energy carrier,* c*;*

E_c *is the final energy consumption [GWh/y] of energy carrier,* c*;*

Once the emissions are determined, the greenhouse gasses emitted can be calculated with Equation 2.38.

$$GHG = \Sigma Emission_x \cdot GWP_x \quad \text{Equation 2.38}$$

Where:

GHG *is total GHG emitted [kg CO2 equivalent/y];*

$Emission_x$ *is the emissions [kg/y] of greenhouse gas* x*;*

GWP_x *is global warming potential of greenhouse gas* x*;*

2.5.7.2 Local Air Pollutant Emissions

Local air pollutant emissions follow a process very similar to that of GHG emissions. In this case, it is important to mention that the source of local pollution is the combustion of fossil fuels within the district, i.e. the boilers. Therefore, in this instance, the equation is simplified to that of Equation 2.39.

$$Emission_p = EF_p \cdot E_b \qquad \text{Equation 2.39}$$

Where:

$Emission_p$ *is the emissions [kg/y] of pollutant* p*;*

EF_p *is the emission factor [kg* p */GWh] of natural gas from boilers,* b*;*

E_b *is the final energy consumption [GWh/y] of natural gas by boilers,* b*.*

This equation is elaborated for all nitric oxides (NO_x), sulfur dioxide (SO_2), and particulate matter (PM).

2.5.8 Area

A simple result of the scenario analysis is the area of the district which receives the interventions in each of the building retrofit scenarios. This information is useful for the cost calculations in the following section and to ensure appropriate spatial modeling in GIS.

2.6 Step 5: Financial Analysis

Building retrofits on the scale of those presented in this paper would require a significant investment. In some countries, policies have been introduced which reduce costs to individuals and spark more widespread adoption of such measures. It is therefore important to quantify the financial impact of a retrofit effort at the district this scale; both the costs and the benefits. The costs considered will be the investment, maintenance, and operation costs. The benefits of can also be monetized in terms of reduced operating costs of buildings and reduced healthcare costs for district residents. The financial analysis

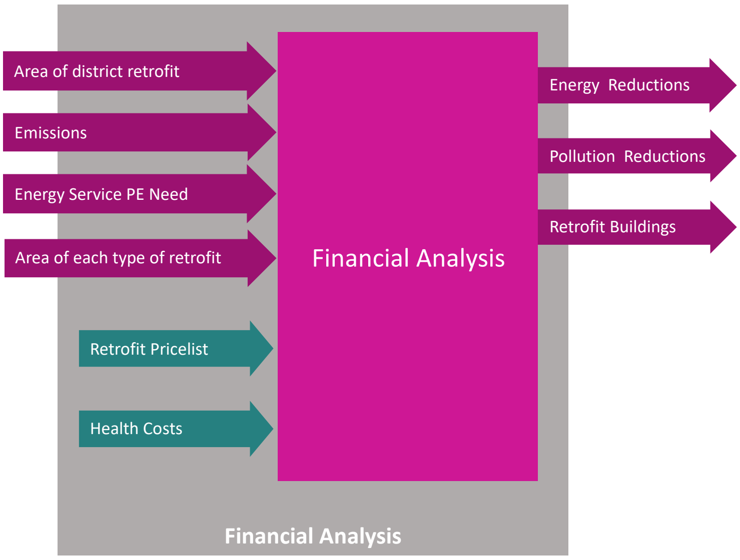

Figure 14: Step 5 flowchart

was elaborated in accordance with European Standard EN 15459 [72] and European Union Directives [73], [74]. The global investment and maintenance costs were determined for each of the original building retrofit scenarios; EASA, EASB, EBSA, and EBSB.

2.6.1 Input Materials

2.6.1.1 Piedmont Regional Pricelist

In the Piedmont region, the government produces a document called "Prezzario Regione Piemonte" which is the pricelist for all renovation work and includes prices for materials and labor. There are many chapters of this document, for this work the chapters pertaining to sustainable buildings [75] and general buildings works [76] provided the necessary inputs.

2.6.1.2 Healthcare Costs

One benefit is the offset healthcare costs as a result of the reduction of local pollution. The values associated were found in research from Copenhagen Economics [43].

2.6.1.3 Utility Costs

The utility costs were provided by Politecnico di Torino, Table 16, and were assumed to be constant for the duration of the study. This assumption is not ideal; however energy prices are extremely volatile and unpredictable. Therefore, they were fixed for this study.

Table 16: Utility costs

	Electricity	**District Heat**	**Natural Gas**
Price (€/MWh)	300.00	80.00	49.06

2.6.2 Global Cost Calculation

The objective of the global cost calculation is to determine value of future cashflows in terms of present-day currency values per square meter of a project. This actualization is done by employing net present value (NPV) and the discount rate to different contributors to the global cost. As can be seen in Figure 15, there are several contributors to the global cost of a project. In this study, the boxes indicated in gray were considered for the global cost, the boxes in pink represent elements which were omitted from the calculation, and the green box representing the energy costs were determined outside of the global cost calculation.

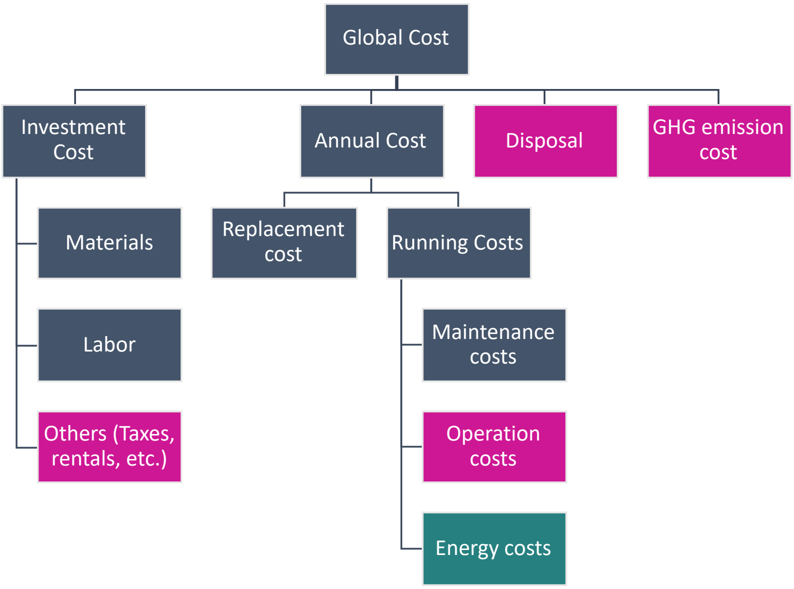

Figure 15: Global cost components

Equation 2.40 was then used for each of the building retrofit scenarios to determine their global cost based on the investment and annual costs indicated.

$$C_G(\tau) = C_I + \sum_j \left\{ \sum_{i=1}^{\tau} \left(C_{a,i}(j) \cdot R_d(i) \right) - V_{f,\tau}(j) \right\} \qquad \text{Equation 2.40}$$

Where:

$C_G(\tau)$	*is the global cost (referred back to starting year* τ_0*);*
C_I	*is the initial investment cost (euros);*
$C_{a,i}(j)$	*is the annual cost in year* i *for component* j*;*
$R_d(i)$	*is the discount rate in year* i*;*
$V_{f,\tau}(j)$	*is the final value (salvage) of component* j *(referred back to starting year* τ_0*);*

2.6.2.1 Calculation Period

The calculation period for this project was 36 years, from 2014-2050.

2.6.2.2 Discount Rate and Net Present Value (NPV)

The discount rate is used to determine the future value of components, either their residual value after depreciation or their replacement cost. The net present value is used to determine the present-day value of future annual cashflows, such as maintenance. The equations for the discount rate and NPV are Equation 2.41 and Equation 2.42, respectively.

$$R_d = \left(\frac{1}{1 + R_R} \right)^p \qquad \text{Equation 2.41}$$

$$f_{pv}(n) = \left(\frac{1-(1+R_R)}{R_R}\right)^{-n}$$ Equation 2.42

Where:

R_d *is the discount rate [%];*

R_R *is the interest rate [%/year];*

p *is the lifespan of the component [years].*

And:

$f_{pv}(n)$ *is the present value factor in year n;*

n *is the calculation period of the project [years].*

In this case, the interest rate of 4% was selected based on an EU directive and the resulting values for the discount rates and present value factors can be seen Table 17.

Table 17: Global cost calculation variables

Variable	Value
Life of Retrofit Scenario (yrs)	32
Interest Rate	4%
Present value factor	17.87
discount rate for 20 years	0.46
discount rate for 25 years	0.38
discount rate of remaining value	0.31

2.6.2.3 Investment Costs

The investment cost represents the initial cash injection required to bring the project to fruition. Investment costs typically consider materials, labor, disposal, and equipment rental. For this analysis, as previously mentioned, disposal and equipment rental were not considered, leaving the investment costs to be comprised of materials and labor.

2.6.2.4 Maintenance Costs

Maintenances costs are typically associated to repairs, cleaning, consumable items, etc. Maintenance costs were assumed to be fixed at 1% of the investment costs. Maintenance costs must be actualized (brought to present-day currency values) using NPV.

2.6.2.5 Replacement Costs and Residual Value

If any component purchased at the initial stages of the project has a lifetime inferior to that of the project, they will need to be replaced at a later date. As the lifetime of a heat pump was found to be either 20 or 25 years depending on the type [1], they would need to be replaced once during the project. The residual value of the second heat pump was determined using straight line depreciation, which is easily calculated with the excel function “SYD”. Both the replacement cost and the residual value need to be actualized using the discount rate.

2.6.2.6 Operating Costs

For the operating costs, only the energy costs were considered. To calculate each cost, the consumption values from the model were taken and the values for costs of the energy service are as presented in Table 16. These values were assumed to be constant throughout the duration of the study.

2.7 Step 6: QGIS Visualization

Once all of the calculations were performed, the indicators of interest regarding final consumption and electrification were re-integrated into the QGIS environment to allow for spatial understanding of the factors of interest at 2030 and 2050 for each of the scenarios.

3 Results

The baseline against which results are compared is the original energy performance of the district from 2014. Key indicators are assessed at 2030 and 2050 as those are strategic milestones in many European Union and Italian energy planning reports.

3.1 QGIS Initialization

The QGIS initialization provides some of the critical details related to the content of the baseline definition as it pertains to the district building stock. Following the QGIS Initialization step, the district was found to contain 5301 residential buildings meeting the parameters for this study. The distribution of the building classes identified can be shown in Figure 16. It is clear from this result that the district is mostly comprised of multi-family dwellings; either apartment blocks or multi-family homes.

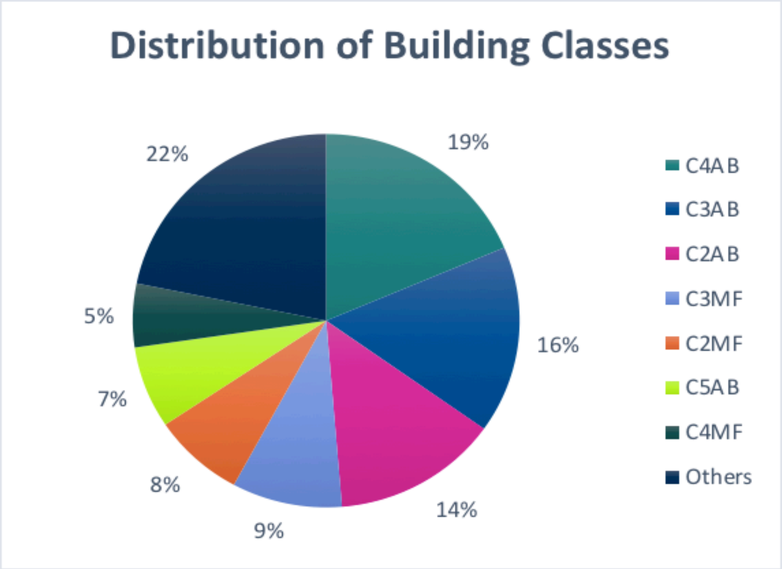

Figure 16: Distribution of building archetypes

In Figure 17, the buildings which were examined in this study are shown and that each of the 36 possible building archetypes are present in the district are identified with unique colors. In ANNEX 1: Supplementary QGIS Initialization Results, zoomed in visualizations can be found allowing for better differentiation of the building archetypes and their exact locations.

Figure 17: QGIS visualization of building characterization

Of the 5301 buildings, data for calibration purposes was available for 247 buildings. The calibration RB dimensions can be seen in Table 18.

Table 18: Calibration RB dimensions

Class	Qty.	Building Height (m)	Floors	Volume (m^3)	Perimeter (m)	Area to external environment (m^2)	Footprint Area (m^2)	Total Shared Wall Area (m^2)	Surface covered by windows (%)
C1AB	2	18.83	5.50	4640.50	65.57	65.57	250.18	225.50	16%
C2AB	32	21.81	6.03	6113.63	73.41	73.41	279.90	277.66	14%
C2MF	6	19.29	5.17	1855.67	47.88	47.88	99.44	235.99	9%
C3AB	48	25.00	7.08	8685.88	97.47	97.47	364.62	300.19	13%
C3MF	4	19.81	5.50	2923.50	50.62	50.62	148.70	86.00	19%
C4AB	94	27.56	7.87	9103.88	88.95	88.95	322.69	294.52	10%
C4MF	3	23.69	6.67	4393.00	97.46	97.46	201.56	0.00	8%
C5AB	39	29.25	8.21	12426.72	108.49	108.49	417.76	222.69	12%
C5MF	4	30.65	9.25	3982.50	97.69	97.69	133.51	0.00	11%
C5TH	1	35.88	11.00	3932.00	65.31	65.31	109.59	0.00	12%
C6AB	12	25.21	7.42	12648.08	120.96	120.96	480.52	163.00	12%
C7AB	1	23.58	7.00	12455.00	119.50	119.50	528.20	161.00	20%
C9AB	1	24.96	7.00	5079.00	59.25	59.25	203.50	291.00	11%

The District level RB definitions for each archetype based on the mean values of all buildings found in the district appear in Table 19. The values for the surface covered by windows came from the online TABULA tool [77].

Table 19: District RB dimensions

RB	Qty.	Building Height (m)	# Floors	Volume (m^3)	Perimeter (m)	Shared Wall Area (m^2)	Area to external environment (m^2)	Footprint Area (m^2)	Surface covered by windows (%)
C1AB	78	19.22	4.92	5485.67	71.64	282.17	1666.79	281.11	16%
C1MF	25	11.51	2.96	1685.12	52.20	86.60	800.16	151.02	11%
C1SF	2	4.59	2.00	501.00	47.00	22.00	417.00	115.75	8%
C1TH	18	8.43	2.39	747.22	43.44	39.44	502.67	92.58	10%
C2AB	735	18.24	4.89	4246.13	63.22	261.27	1363.16	228.18	14%
C2MF	408	13.17	3.44	1778.77	49.63	121.77	801.99	137.59	9%

RB	Qty.	Building Height (m)	# Floors	Volume (m^3)	Perimeter (m)	Shared Wall Area (m^2)	Area to external environment (m^2)	Footprint Area (m^2)	Surface covered by windows (%)
C2SF	14	7.75	2.07	274.71	25.64	29.71	238.07	38.88	9%
C2TH	67	8.43	2.25	767.75	43.58	39.67	508.49	95.95	9%
C3AB	860	19.83	5.45	4758.31	64.68	270.62	1501.98	233.00	13%
C3MF	489	12.45	3.34	1651.76	48.52	100.96	768.68	134.93	19%
C3SF	15	9.71	3.00	507.67	35.13	29.53	453.53	57.30	9%
C3TH	99	8.56	2.30	681.26	39.23	46.39	451.64	82.15	18%
C4AB	986	23.67	6.71	6522.46	70.90	296.35	1958.90	267.78	10%
C4MF	292	14.61	4.02	2049.91	50.68	103.53	919.03	144.29	8%
C4SF	17	7.47	2.53	549.47	45.65	25.53	489.24	85.23	12%
C4TH	58	9.18	2.45	787.53	40.84	30.79	513.50	93.85	6%
C5AB	376	26.23	7.44	12143.20	95.60	212.26	3307.44	423.44	12%
C5MF	95	15.58	4.39	2055.27	49.71	93.65	945.76	139.48	11%
C5SF	6	7.77	2.17	311.33	27.50	21.50	270.17	44.74	12%
C5TH	25	11.84	3.16	994.40	42.48	43.20	649.12	91.95	12%
C6AB	93	22.90	6.61	9417.04	88.57	212.03	2703.65	375.45	12%
C6MF	52	14.50	4.31	2277.33	55.92	99.96	1041.25	160.69	15%
C6SF	7	15.95	5.00	454.00	24.14	62.86	417.14	23.97	12%
C6TH	8	11.03	3.13	758.38	40.13	77.38	496.25	90.96	6%
C7AB	102	24.36	7.18	9868.59	93.58	244.36	2903.08	371.88	20%
C7MF	54	16.38	4.94	2557.52	56.24	118.61	1125.46	159.88	11%
C7SF	7	10.07	2.71	410.43	35.00	73.43	338.00	46.51	20%
C7TH	14	11.76	3.14	882.86	41.64	35.57	599.79	81.69	8%
C8AB	78	22.49	6.74	7305.88	84.63	178.83	2429.45	308.33	23%
C8MF	40	17.88	5.28	2431.53	52.25	153.00	1064.68	136.05	12%
C8SF	18	6.32	2.00	215.89	23.67	40.11	177.39	34.55	12%
C8TH	13	10.60	3.15	551.85	30.92	49.85	398.85	48.34	18%
C9AB	72	23.24	7.04	6172.81	74.90	252.18	2046.44	256.51	11%
C9MF	55	18.69	5.60	2591.53	54.84	153.67	1156.85	138.63	12%
C9SF	9	9.80	3.00	254.00	22.44	38.78	227.56	35.63	12%
C9TH	14	12.43	3.64	839.36	39.36	51.79	559.71	78.78	8%

The resulting values from the analytical model regarding the SH, SC, and DHW need and used for each RB and each intervention combination can be found in Table 29 and Table 30 in ANNEX 3: Results from Analytical Model for Original and Modified Buildings.

3.2 Model Development and Calibration Results

Once the statistical and analytical models were developed, the analytical model was calibrated against the average annual consumption data from the IREN district heating data. During the calibration phase, the variables which were modified pertained to solar gains. The building orientation, the shading factor, $F_{sh,ob}$, and the color correction factor, α_{sc}, were used in order to minimize the error and their values can be seen in Table 20. Priority was given to minimizing error on archetypes who had larger sample sizes and are therefore more reliable. As this was done manually, in the future, an optimization could be performed with a more powerful computing tool.

Table 20: Calibration values and model resulting error

Class	Qty	Average Annual Heat Consumption (kWh/m^{2}y)	Analytical Model Value (kWh/m^{2}y)	Statistical Model Value (kWh/m^{2}y)	Analytical Model ERROR	Statistical Model ERROR	Orientation	$F_{sh,ob}$	α_{sc}
C1AB	2	201.52	197.95	225.07	2%	12%	E/W	0.8	0.3
C2AB	32	193.03	199.00	196.76	3%	2%	N/S		
C2MF	6	262.03	272.01	372.07	4%	42%	N/S		
C3AB	48	132.71	130.93	119.54	1%	10%	N/S		
C3MF	4	376.37	369.17	324.64	2%	14%	E/W		
C4AB	94	123.58	117.67	113.13	5%	8%	N/S		
C4MF	3	72.95	136.73	95.51	87%	31%	N/S		
C5AB	39	90.00	88.31	90.31	2%	0%	N/S		
C5MF	4	172.29	137.56	100.78	20%	42%	E/W		
C5TH	1	322.76	239.38	143.52	26%	56%	E/W		
C6AB	12	69.42	86.34	102.74	24%	48%	N/S		
C7AB	1	107.57	97.75	37.16	9%	65%	E/W		
C9AB	1	701.94	78.58	236.93	89%	66%	E/W		

As can be seen, 8 of the analytical model RB energy consumption values have error less than 10% and the values against which they are compared seem reasonable. For C4MF, the measured value is lower than what might be expected when considered to other "MF" buildings or the other C4 building in the calibration RB set and this could be part of the reason for the 87% error, which is extremely high. In the cases of C5MF and C5TH where the errors were 20% and 26%, relatively, the small sample of measured data could mean that factors such as unusual resident behavior or lack of building maintenance, etc. have an impact on the average measured value and could therefore be contributing to higher measured values than expected. In the case of C6AB, the residents could conversely be more conscientious about their consumption thus having a lower than expected value. The measured value for C9AB, is much higher than is reasonable at ~702 kWh/m^{2}y. Given that it is the newest construction period the analytical model value seems reasonable.

The statistical model has higher percentage error values than those of the analytical model. This could be due to misreporting of building occupancy since the statistical data that was available regarding consumption for heating is in terms of the natural gas requirement per person per year. This data follows the same trend as the analytical data which is more accurate for the buildings where the measured average comes from a larger sample size.

If a larger sample of measured data were available, the analytical model could be further optimized with individual values for the shading and color correction values, which could virtually eliminate the error.

3.3 District Calculation and Introduction of Measures Results

3.3.1 Analytical Thermal Model

The orientation used during the calibration phase of the analytical was maintained for the district level calculation phase and the values are present in Table 21, along with the values for the remaining building archetype RBs. When assigning the orientation to the RBs for which there was no measured data, considerations were made regarding the majority orientation for buildings of the same type (AB, MF, SF, or TH).

Table 21: District RB orientation values

RB	Orientation	RB	Orientation	RB	Orientation
C1AB	E/W	**C4AB**	N/S	**C7AB**	E/W
C1MF	E/W	**C4MF**	N/S	**C7MF**	N/S
C1SF	E/W	**C4SF**	E/W	**C7SF**	E/W
C1TH	E/W	**C4TH**	E/W	**C7TH**	E/W
C2AB	N/S	**C5AB**	N/S	**C8AB**	E/W
C2MF	N/S	**C5MF**	E/W	**C8MF**	N/S
C2SF	E/W	**C5SF**	E/W	**C8SF**	E/W
C2TH	E/W	**C5TH**	E/W	**C8TH**	E/W
C3AB	N/S	**C6AB**	N/S	**C9AB**	E/W
C3MF	E/W	**C6MF**	E/W	**C9MF**	E/W
C3SF	E/W	**C6SF**	E/W	**C9SF**	E/W

RB	Orientation	RB	Orientation	RB	Orientation
C3TH	E/W	C6TH	E/W	C9TH	E/W

With the variables set, the monthly consumption, both need and final, for each energy service was calculated for each RB and for each of the possible building retrofit scenarios.

The values for the RBs without energy efficiency interventions (initial values) are presented in Figure 18, Figure 19, Figure 20, and Figure 21. In Turin, the heating season is from October 15th - April 15th. As October and April are only partial months, this, along with the more temperate weather, explains the significantly lower values for heating need in those months. From these figures, it can be seen that generally speaking, the building types AB and MF require less heating and cooling than those of SF and TH. There is also a key trend highlighting the improvements in building energy efficiency throughout the years. The C2 buildings, constructed between 1919 and 1945, have the worst winter performance and C4 buildings, 1961-1970, has the worst summer performance. Generally speaking, the building performances improve the more recently they were constructed with C9 buildings (2006-present) having the best performance.

One parameter which could narrow the performance gap between older and newer construction periods for buildings of the same type is occupant behavior. It is reasonable to assume that residents of older buildings are more conscientious energy consumers than those of newer buildings, however, that impact was out of the scope of this study.

For each RB and each intervention combination, the monthly values were aggregated in order to allow for comparison with the statistical data, which did not possess the same temporal granularity.

The aggregated annual results for every building class and every intervention can be seen in Table 29 and Table 30 in ANNEX 3: Results from Analytical Model for Original and Modified Buildings. The original RBs each had overall energy systems efficiency of less than one, meaning the energy used was always greater than the energy need. With the introduction of heat pumps, whose coefficients of performance (COP) were greater than one, the result is that the energy used is less than the energy need. Of course, the heat pumps require electricity in order to generate the heat. The additional electricity demand for the heat pumps was considered.

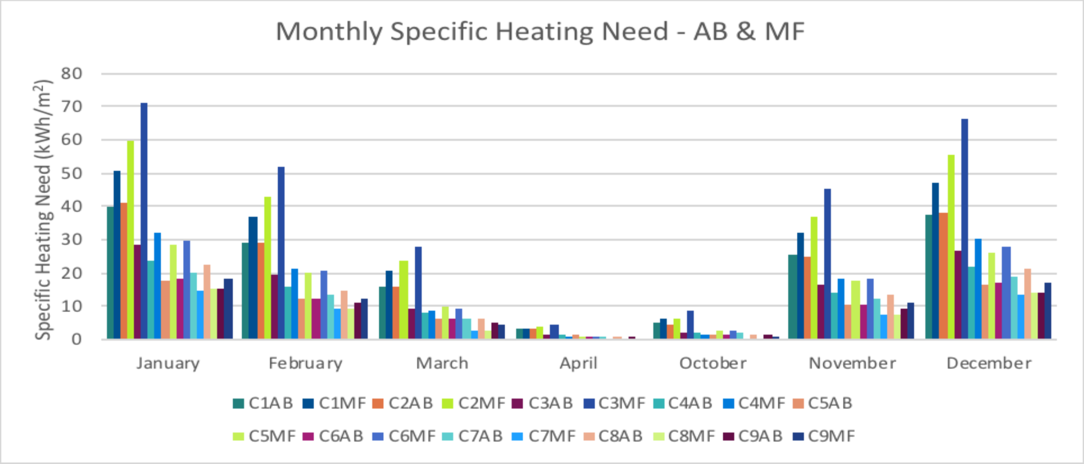

Figure 18: Monthly specific heating need - AB & MF

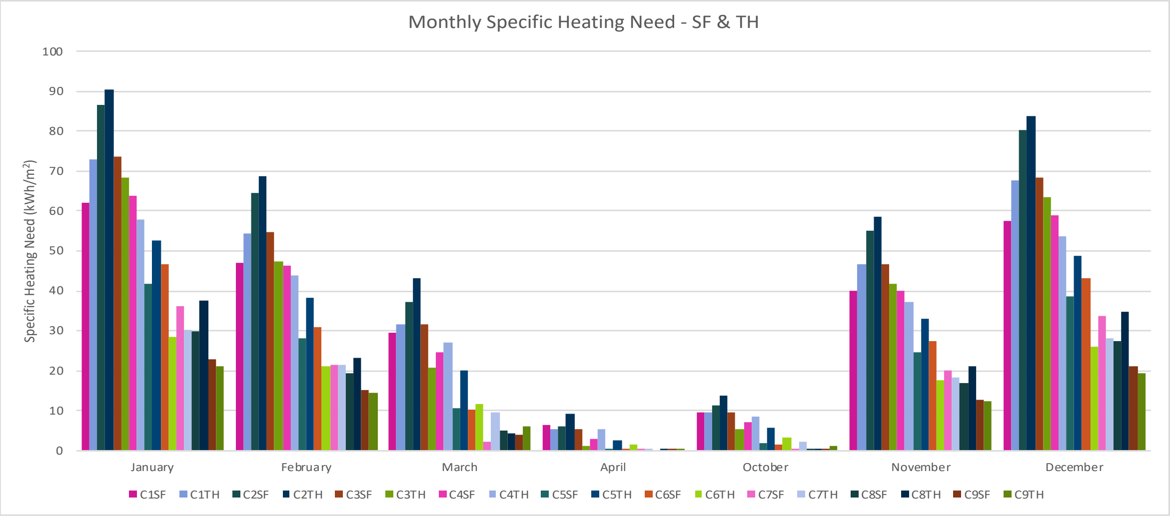

Figure 19: Monthly specific heating need - SF & TH

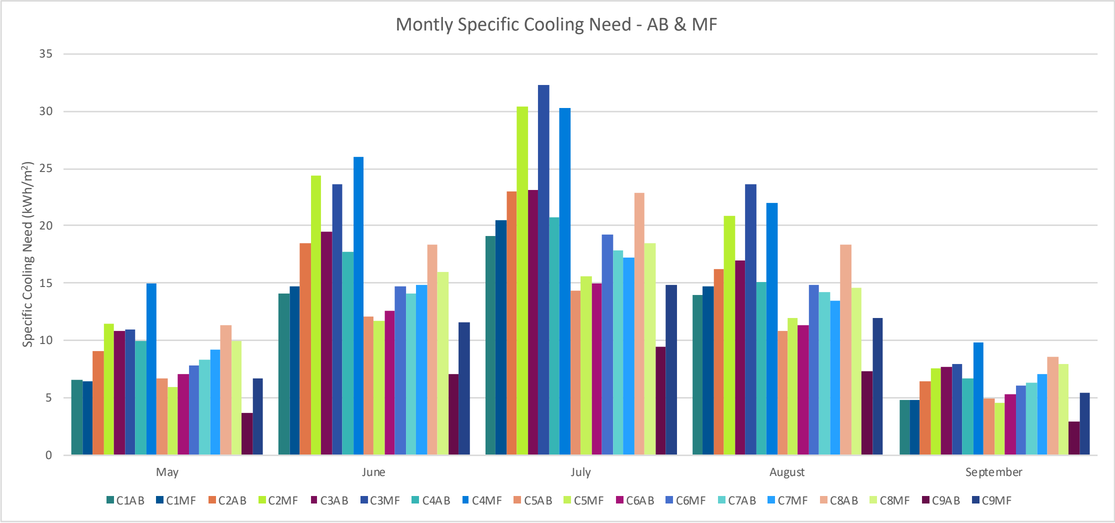

Figure 20: Monthly specific cooling need - AB & MF

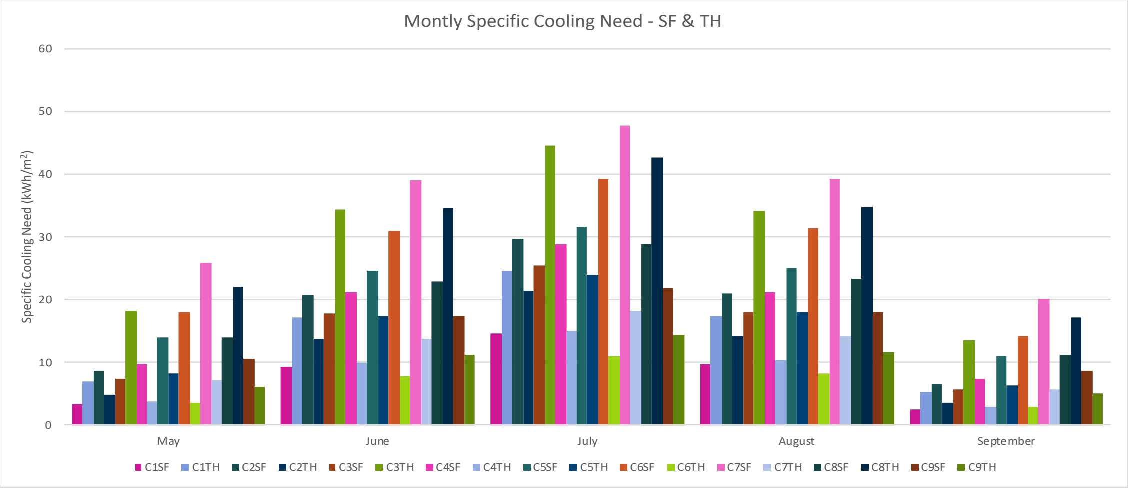

Figure 21: Monthly specific cooling need - SF & TH

Based on the reduction in energy need across all of the retrofit combinations, the RBs which are the priority for retrofit were identified and the results are presented in Table 22.

Table 22: Priority of building retrofits

RB	Priority	RB	Priority	RB	Priority
C1TH	1	**C5TH**	13	**C3AB**	25
C2TH	2	**C5SF**	14	**C4AB**	26
C3TH	3	**C2AB**	15	**C7MF**	27
C3MF	4	**C8TH**	16	**C8SF**	28
C3SF	5	**C4MF**	17	**C9MF**	29
C2SF	6	**C1AB**	18	**C9TH**	30
C1MF	7	**C7SF**	19	**C8AB**	31
C2MF	8	**C7TH**	20	**C9SF**	32
C4SF	9	**C6TH**	21	**C7AB**	33
C1SF	10	**C6MF**	22	**C6AB**	34

RB	Priority	RB	Priority	RB	Priority
C4TH	11	**C5MF**	23	**C5AB**	35
C6SF	12	**C8MF**	24	**C9AB**	36

As might be expected, early archetypes typically have the highest priority. It can also be seen that apartment blocks typically have better performance than the other building types and are therefore lower priorities for interventions. With the results of the different energy efficiency interventions and the priority established, it was possible to characterize the neighborhood energy demand regarding space heating (SH), space cooling (SC), and domestic hot water (DHW). It is important to also remember that each RB represents a different total surface area in the district. The floorspace by archetype is presented in Figure 22 with a logarithmic scale. The district has a total surface area of 1,172,317 m^2 and it can be seen that most of the surface area of the district is associated to AB type buildings.

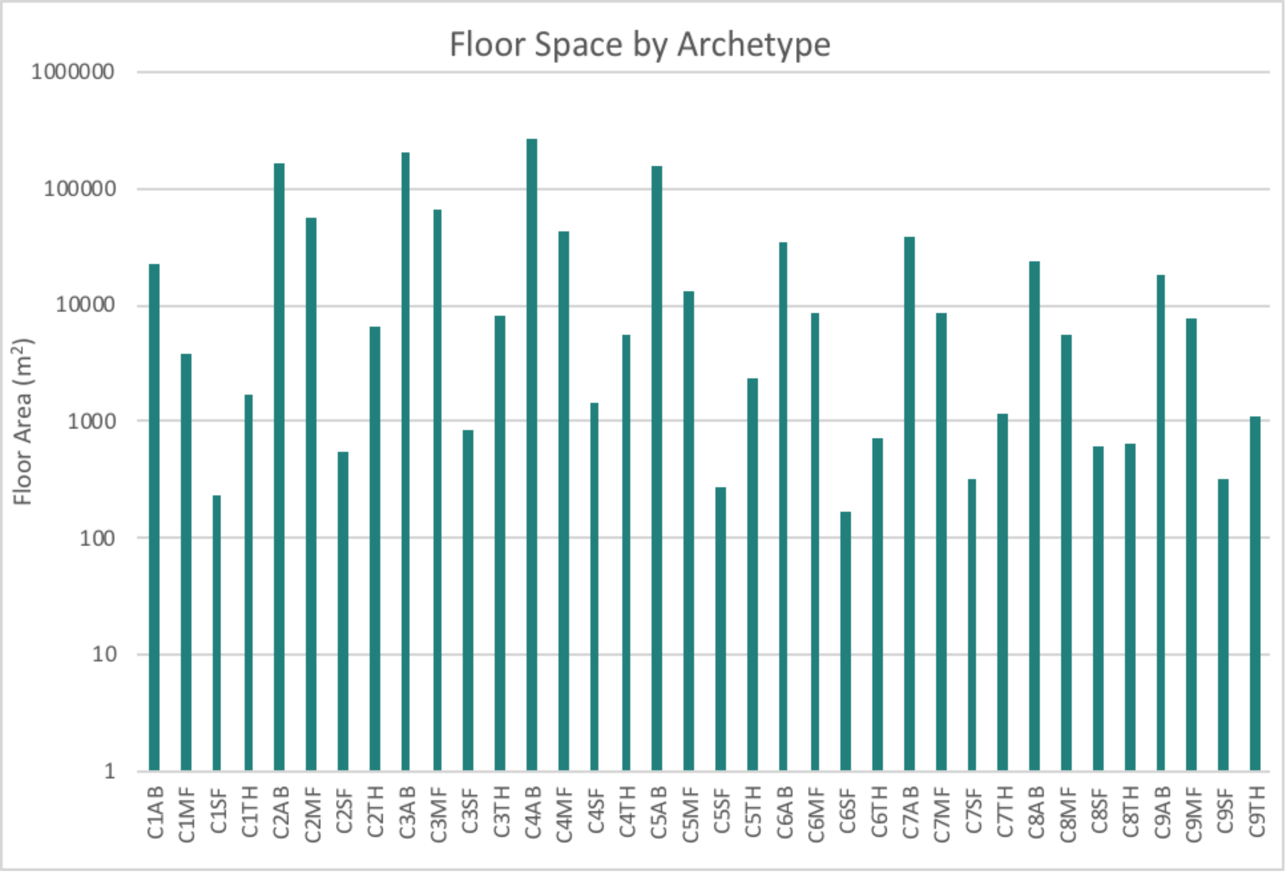

Figure 22: Floor space of district by archetype

3.3.2 Introduction of Appliance Electricity consumption

In order to include the domestic appliance electricity consumption, the results from the socio-techno-economic analysis of the neighborhood must be used. Table 23, with the social group profiles to create the neighborhood demand curve. As can be seen in the table, almost half of the neighborhood is made of two social groups, clerks' families and retired blue-collar worker families with 24% each.

Table 23: Demographic results for district

Group →	0	1	2	3	4	5	6	7	8
Census Section	**Ruling class**	**Silver pensioner**	**Clerks'**	**Young blue-collar**	**Retired blue-collar**	**Young un-employed and seniors living alone**	**Traditional provincial**	**Low-income Italian**	**Low-income foreign**
17	634	819	1565	426	1079	518	236	206	188
31	282	365	697	261	659	317	104	38	84
32	885	1144	2185	76	758	92	1770	393	0
33	1251	1617	3088	531	3971	646	0	0	989
34	645	834	1592	610	1124	742	0	0	118
35	426	551	1052	1475	2521	1793	0	0	372
51	520	672	1284	556	1220	676	0	0	94
52	710	917	1752	630	2106	766	0	0	187
63	1187	1535	2931	1536	2516	1867	160	216	167
%	10%	13%	24%	9%	24%	11%	3%	1%	3%
Total	6540	8454	16146	6103	15953	7416	2270	854	2199

Based on the representation of each social group in the district and the consumption profiles for those households, the monthly appliance electricity consumption can be determined and is presented in Figure 23 by social group. If interested, the breakdown by census section is available in ANNEX 4: Electricity Demand by Census Section. The results of the consumption are proportionate to the social group's representation in the district suggesting that in the case of Turin's 3rd district, any social group whose consumption profile shape varies significantly from that of the group, is only present in the district in a small number, therefore having minimal impact on the shape of the demand curve.

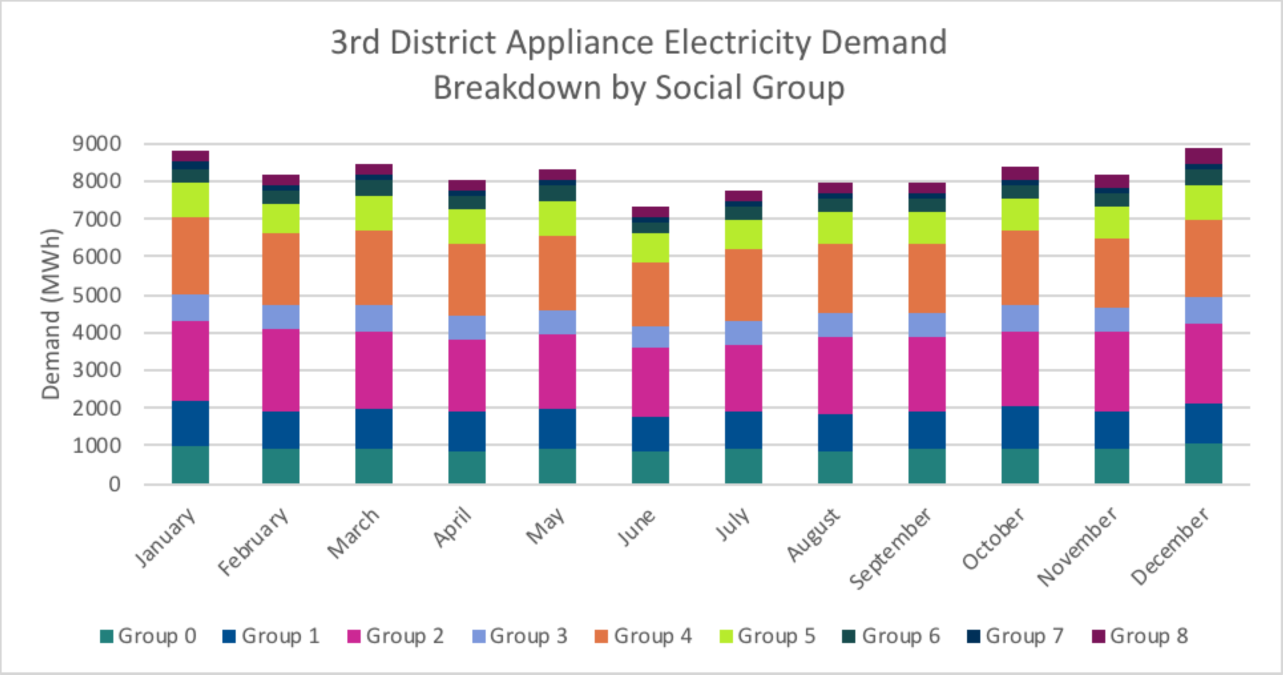

Figure 23: 3rd district monthly appliance electricity demand by social group

From these calculations, the final appliance electricity consumption was found to be 98102.20 MWh/year. This value was used as the starting point in the calculations regarding the evolution of the domestic appliance energy demand.

3.4 Scenario Results

To elaborate the various final scenarios as outlined in Table 13, the rate of interventions as described in Table 10 on the building were applied and maintained constant throughout the projections.

3.4.1 Building Retrofit Results

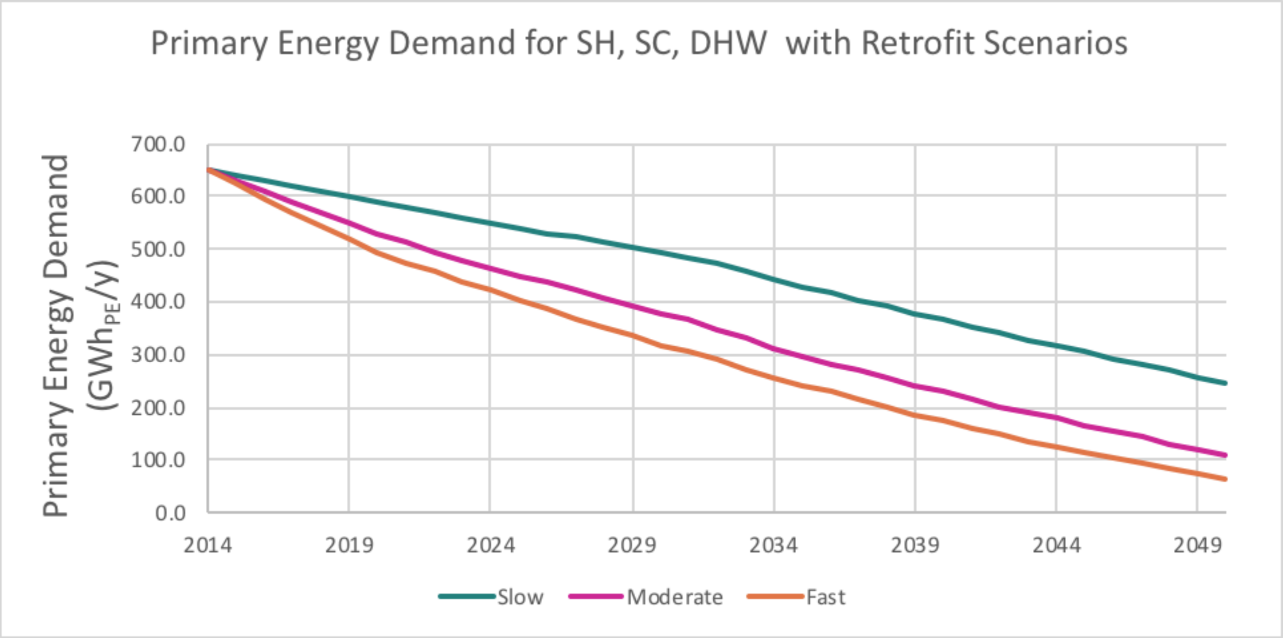

Figure 24:Primary energy demand for SH, SC & DHW with retrofit scenarios

The first set of results pertain to the building retrofit impacts alone. As can be seen in Figure 24, with the slow building retrofit the primary energy demand decreases by approximately 50%. With the moderate and the fast, those decreases are closer to 75% and 90%, respectively. These decreases are due to the building interventions which reduced the final consumptions by reducing the energy need and implementing more efficient technologies for generation systems, and also due to the change in primary energy conversion factor due to the increasing share of renewable energy in the electricity generation mix.

In order to better understand the nature of these changes, the primary energy demands have been broken down by service and by carrier for each of the building retrofit scenarios (see Table 10 for scenario definitions). In Figure 25 and Figure 26, the details regarding the slow energy retrofit are presented. The slow building retrofit proposal comprised of the most conservative intervention proposal, EBSB, with a small portion of EASB with an overall per annum change of 0.6%. Due to these factors and the fact that the PECs for district heat and natural gas are constant while the electricity is decreasing, it can be seen that the contributions to the primary energy demand of heat and DHW in Figure 25 and natural gas and district heat in Figure 26 remain largely unchanged for the period studied. The improvements come mostly from cooling which is the only service that does not change energy carrier as it was considered to be electric from the beginning. The final result is a 62% reduction in primary energy demand.

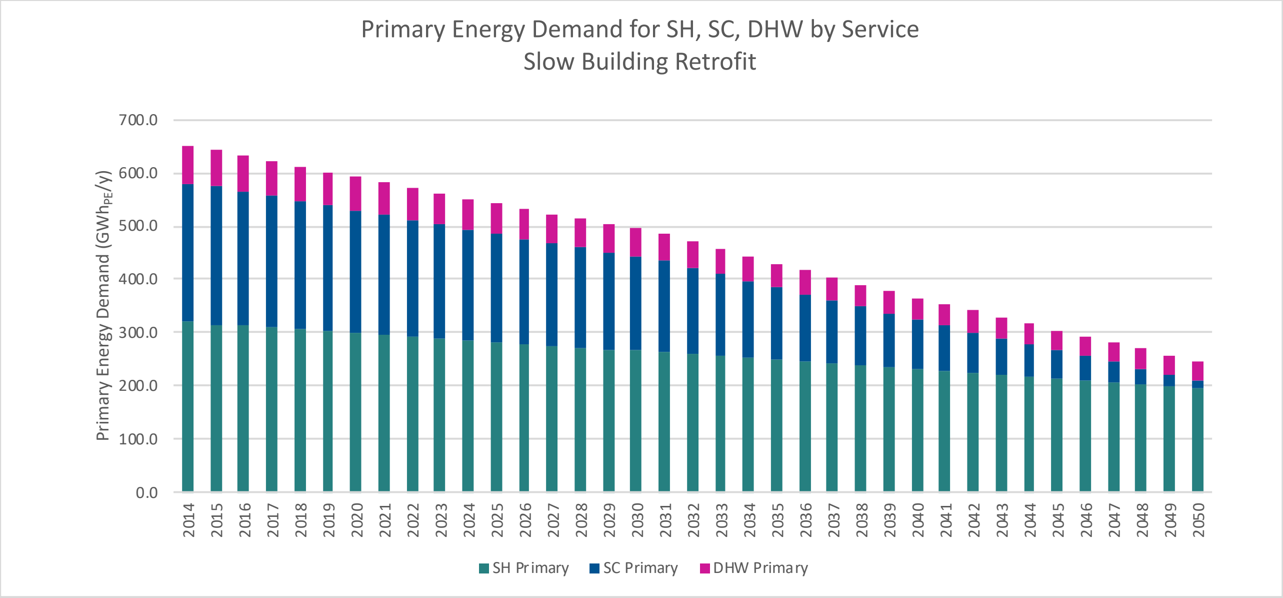

Figure 25: Primary energy demand by service - Slow buildling retrofit

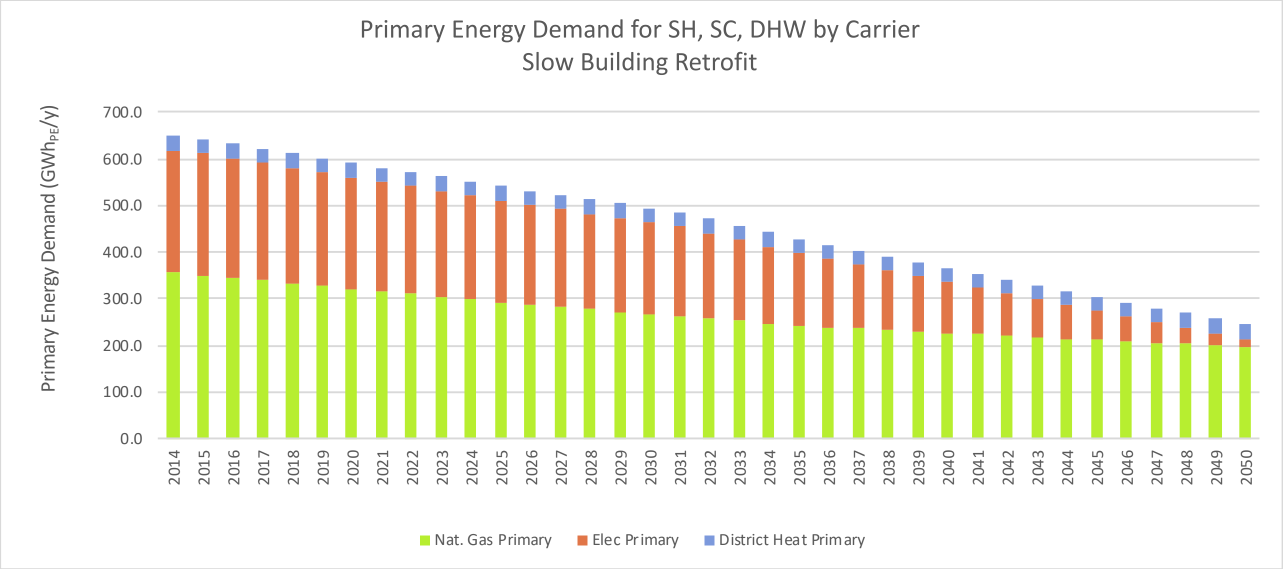

Figure 26: Primary energy demand by carrier - Slow buildling retrofit

When looking at the moderate building retrofit plan, it is clear that there is more improvement in the primary energy intensity of the district compared to the slow scenario. Figure 27 and Figure 28, which represent the priamry energy demand for the moderate building retrofit scenario which introduces some more aggressive rates as well as the EASA intervention combination. The result is therefore visible reductions in primary energy associated to all energy services and for each carrier. As electricity is now used for more energy services than simply cooling, it is starting to become evident in these graphs that the primary energy for cooling is less than the primary energy from electricity, thereby confirming the impact of the electrification of the systems. The final primary energy value is 83% less than the original.

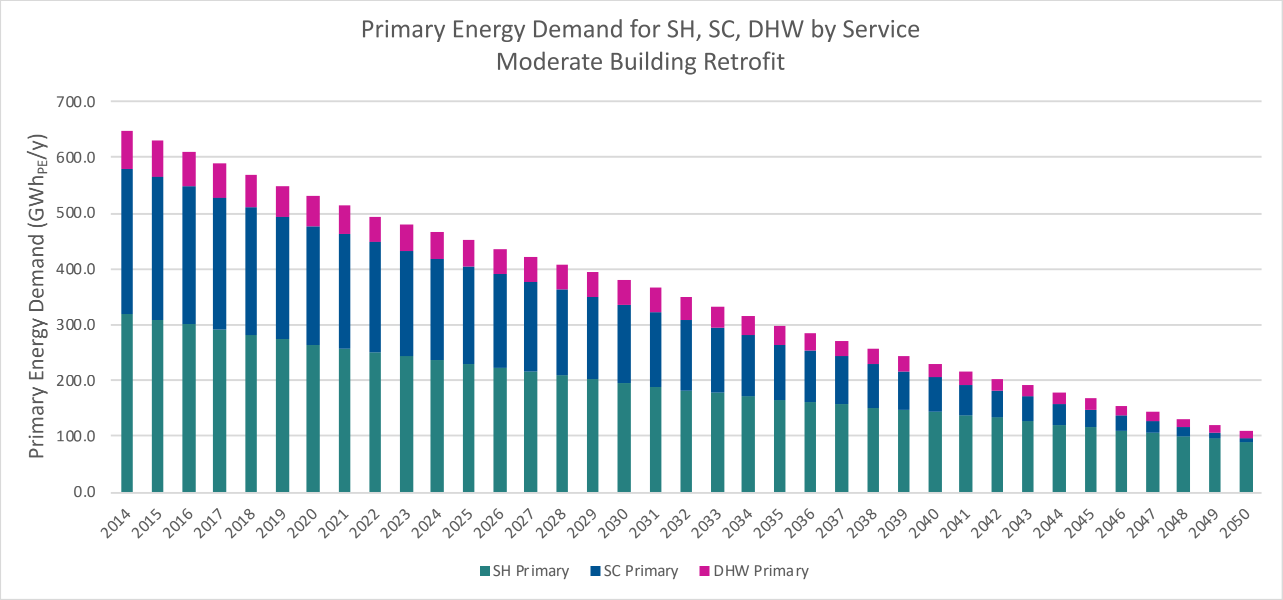

Figure 27: Primary energy demand by service - Moderate building retrofit

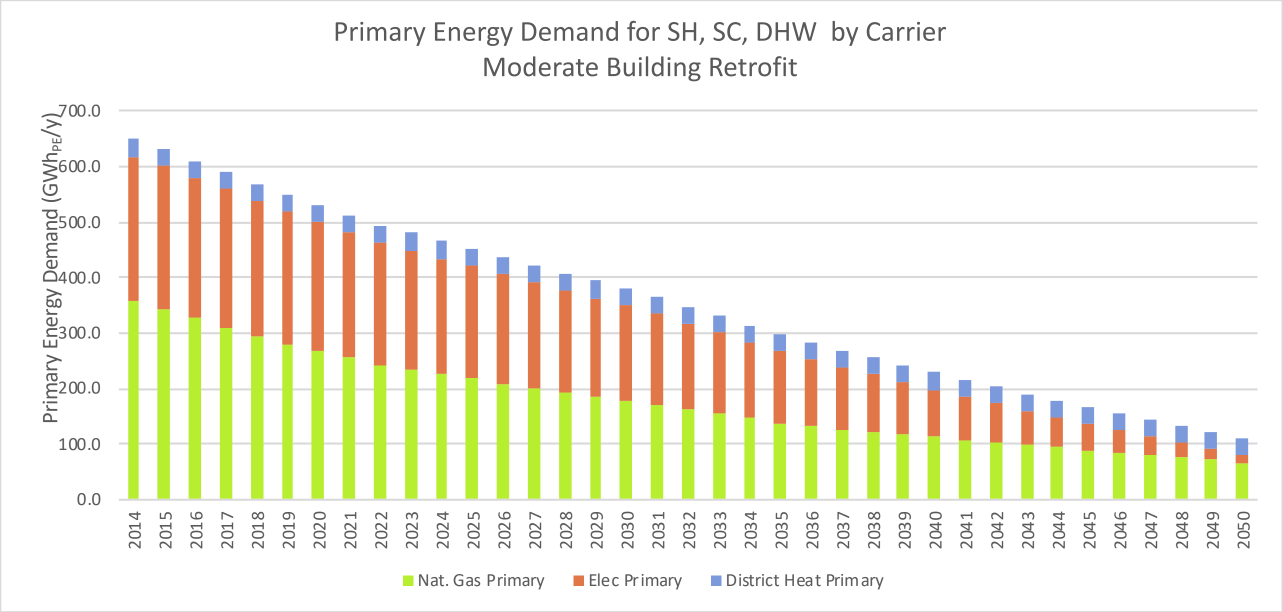

Figure 28: Primary energy demand by carrier - Moderate building retrofit

In Figure 29 and Figure 30, which represent the most aggressive of the building and district interventions, the primary energy demand is reduced by 90% over the period of the study. The previously trend regarding the electrification of the energy systems can be seen in these graphs as well.

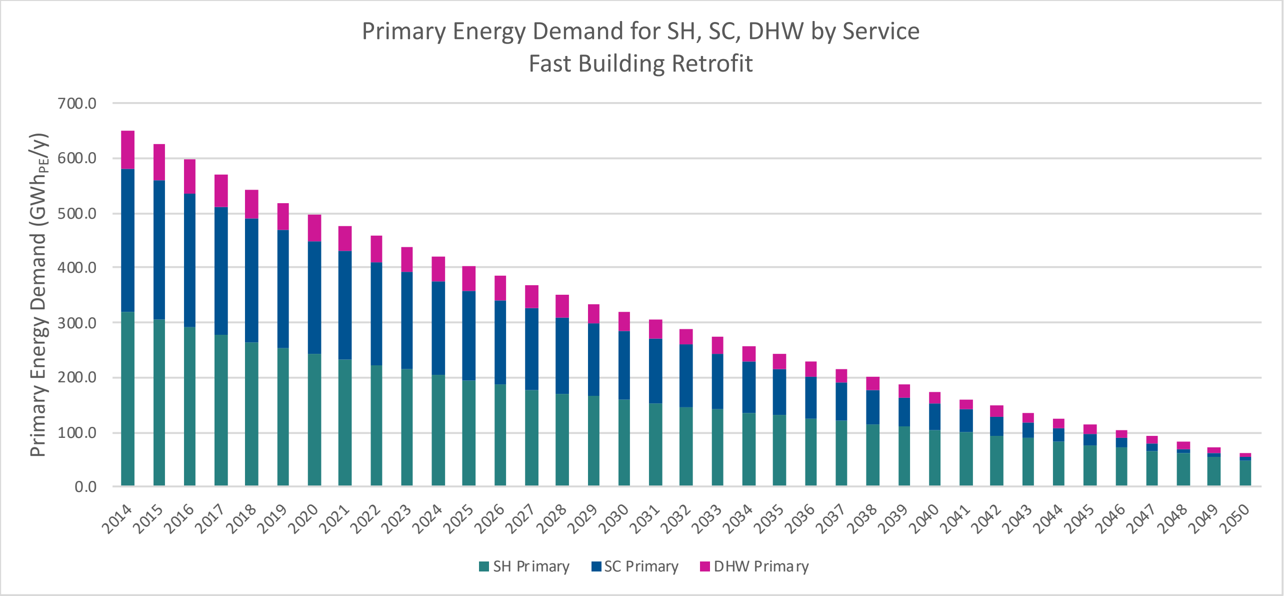

Figure 29: Primary energy demand by service - Fast building retrofit

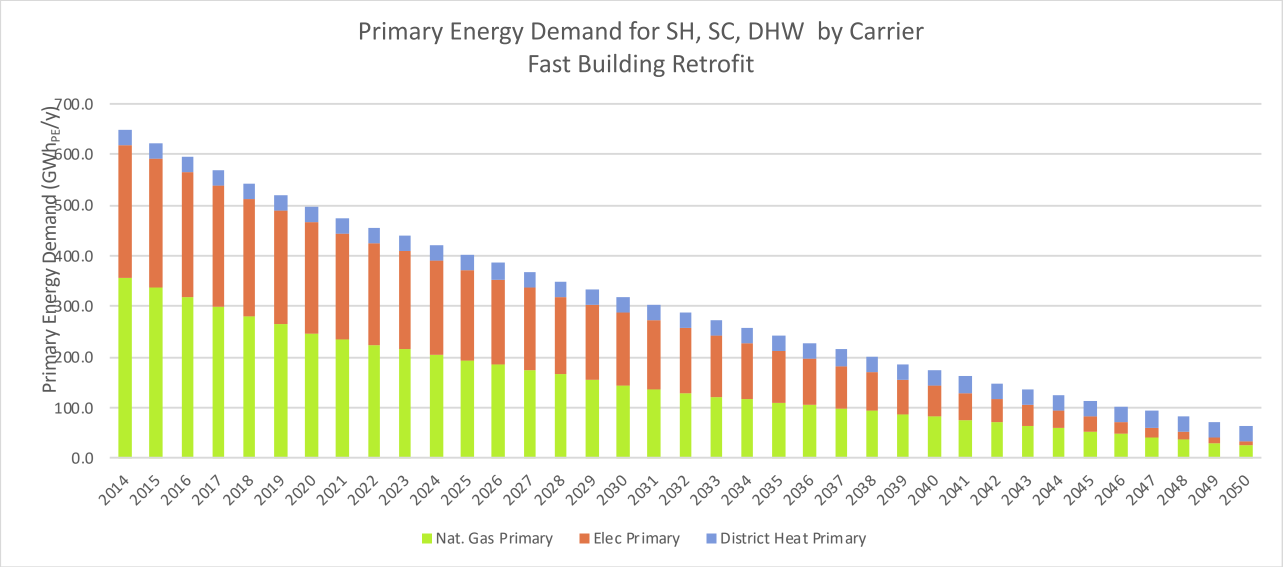

Figure 30: Figure 28: Primary energy demand by carrier - Fast building retrofit

Besides the building consumption due to thermal energy needs, the electrical needs due to appliances were considered as well. In general, as can be seen from Figure 31, owing to the fact that the rates of change are less than 1% different, this should have been expected. Despite the almost negligible impact of the different adoption rates of energy efficient appliances, the contribution of domestic electricity must be considered. As can be seen in Figure 32, Figure 33, and Figure 34, in the year 2014, appliances contribute 30% of the final primary energy consumption.

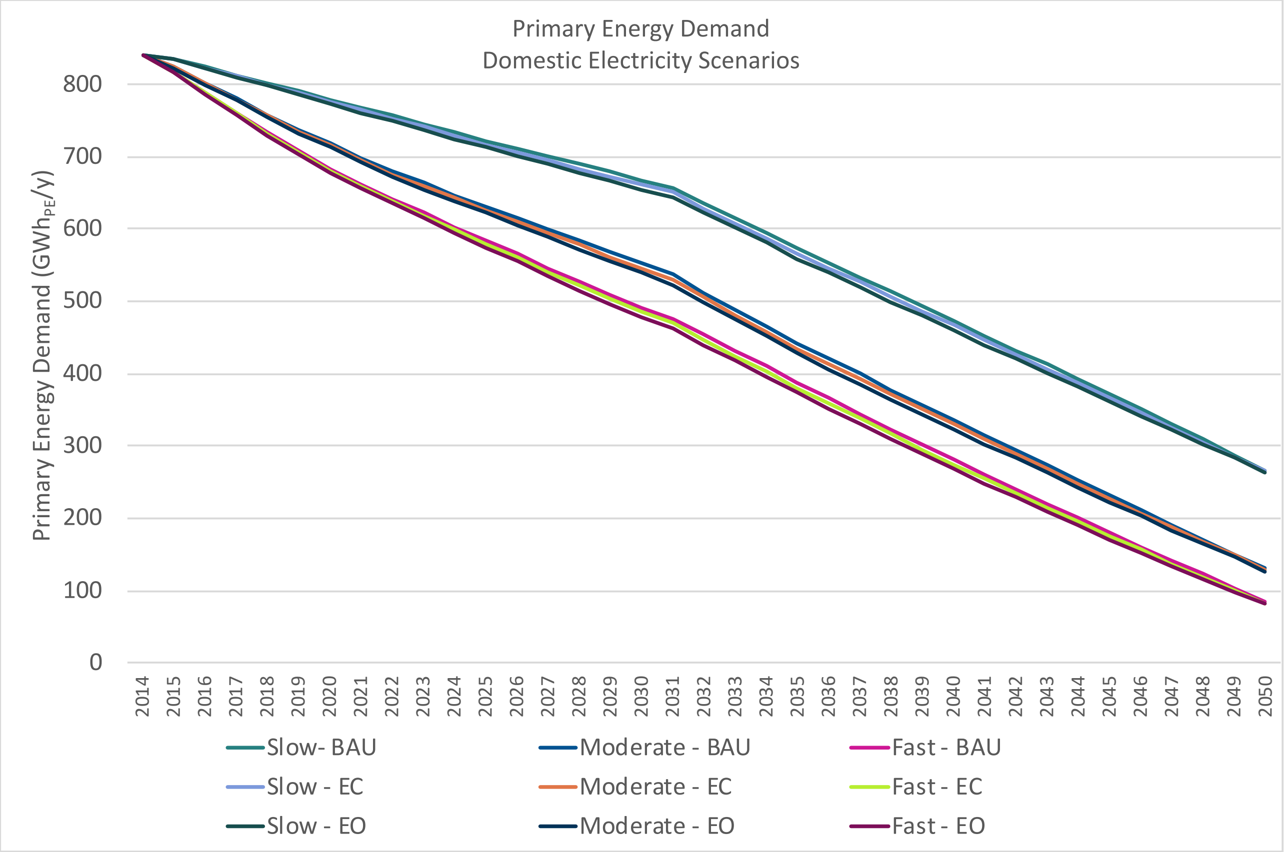

Figure 31: Primary energy demand including variations due to appliance electrical consumption

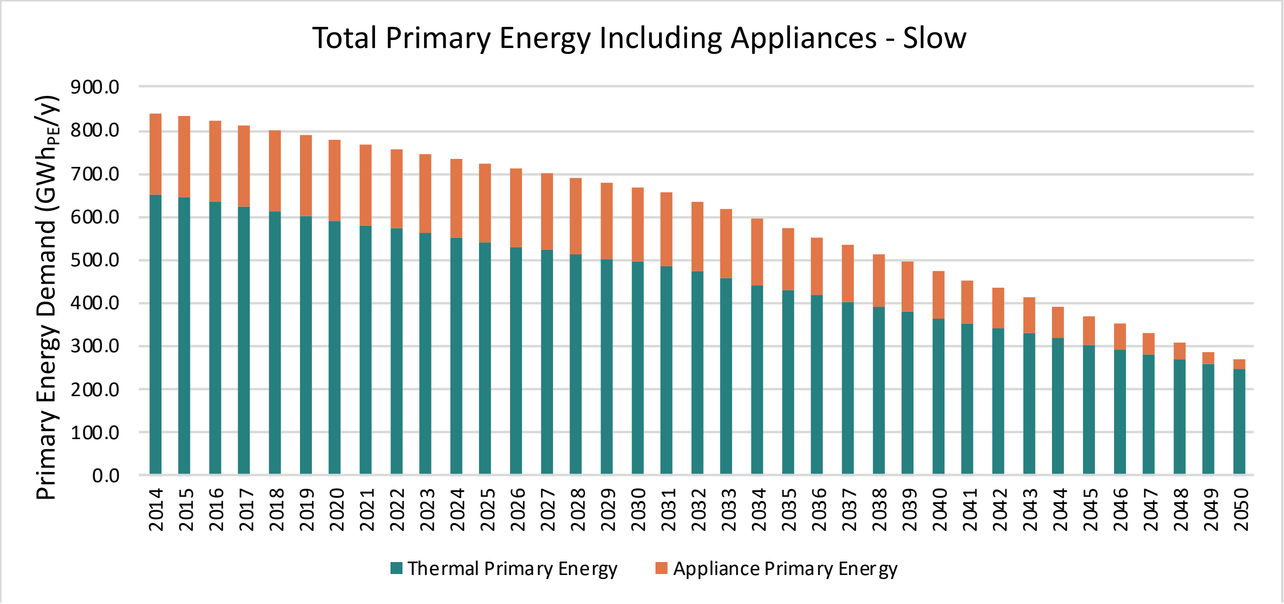

Figure 32: Total primary energy demand including appliances - Slow

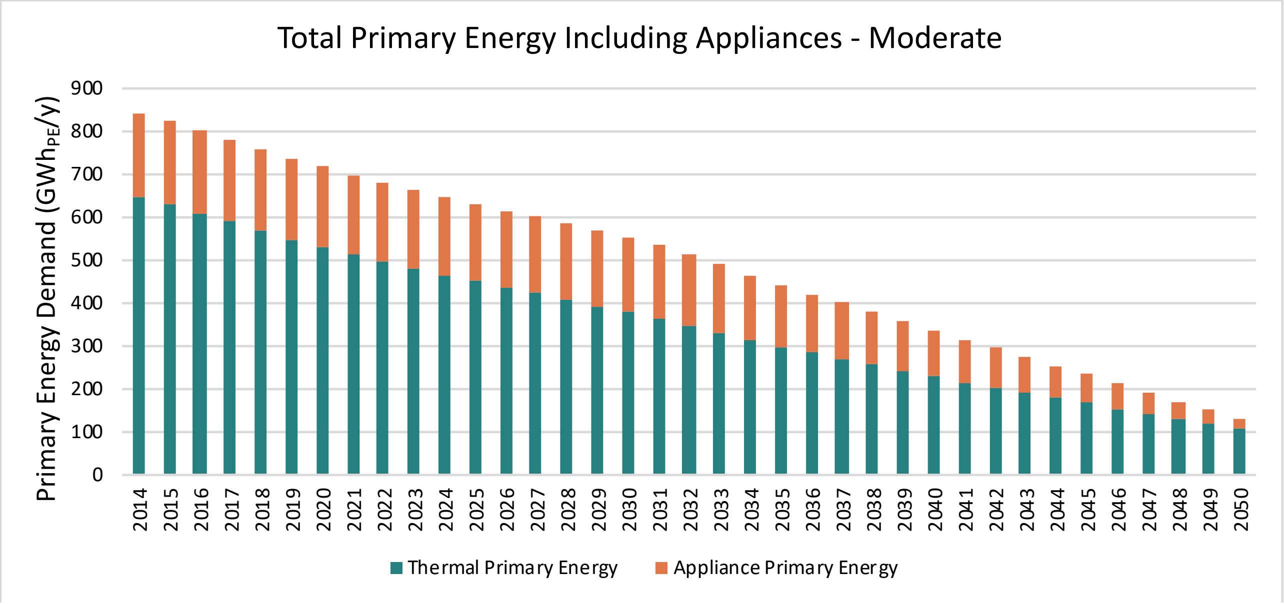

Figure 33: Total primary energy demand including appliances - Moderate

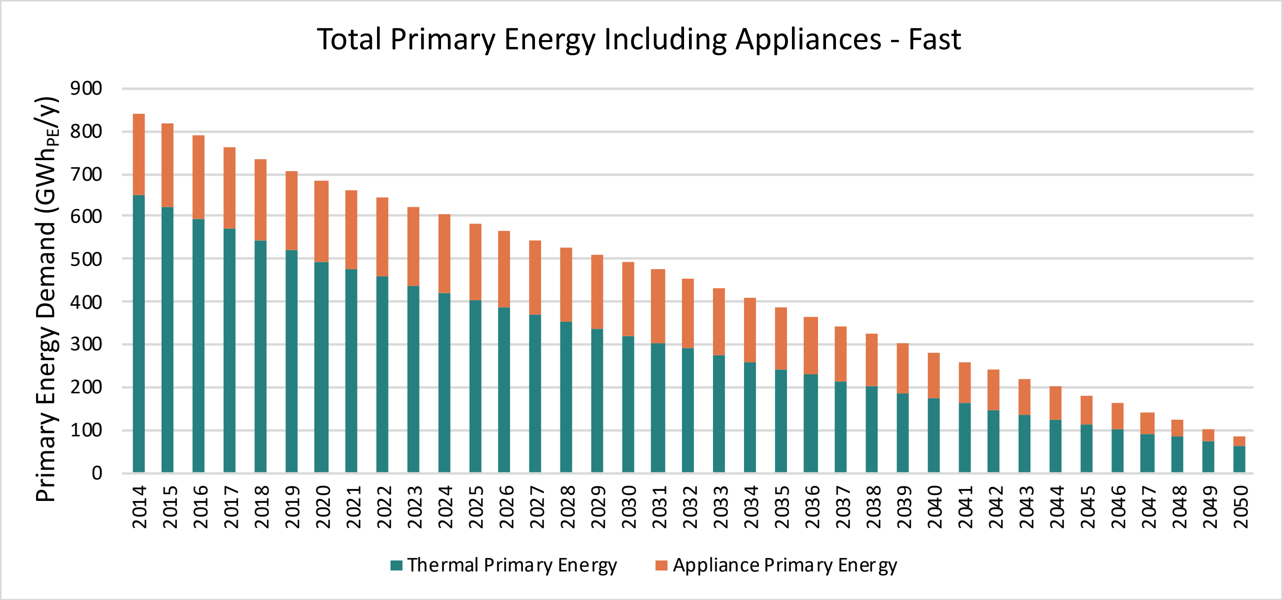

Figure 34: Total primary energy demand including appliances - Fast

As previously mentioned, Turin is one of the cities in Europe with the most frequent violations of WHO air quality standards. Therefore, one of the results of this work was to examine the role that replacement of natural gas boilers, which were assumed to be the source of heat for buildings without district heat, with heat pumps could have on local air pollution levels. There were three main types of pollutants examined, PM, NO_x and SO_2. Figure 35 shows the trends for PM emissions related to the building retrofits.

As is expected, the PM reductions are most evident when more of the building stock experiences a retrofit and therefore more of the boilers are decommissioned.

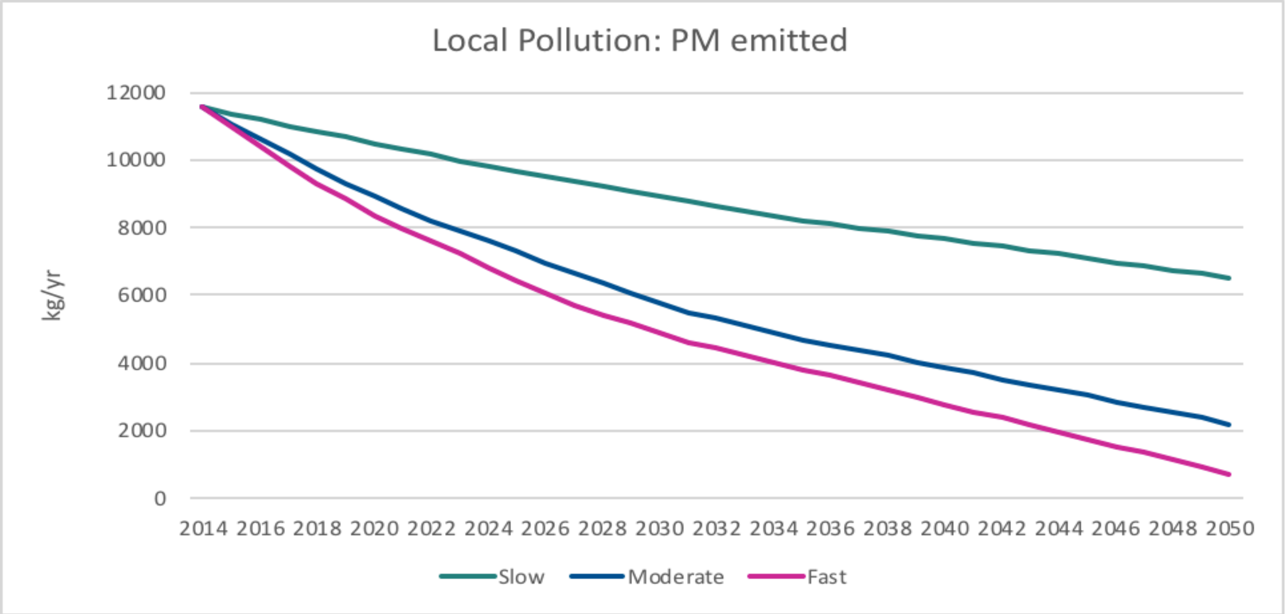

Figure 35: PM emissions vs. building retrofit scenario

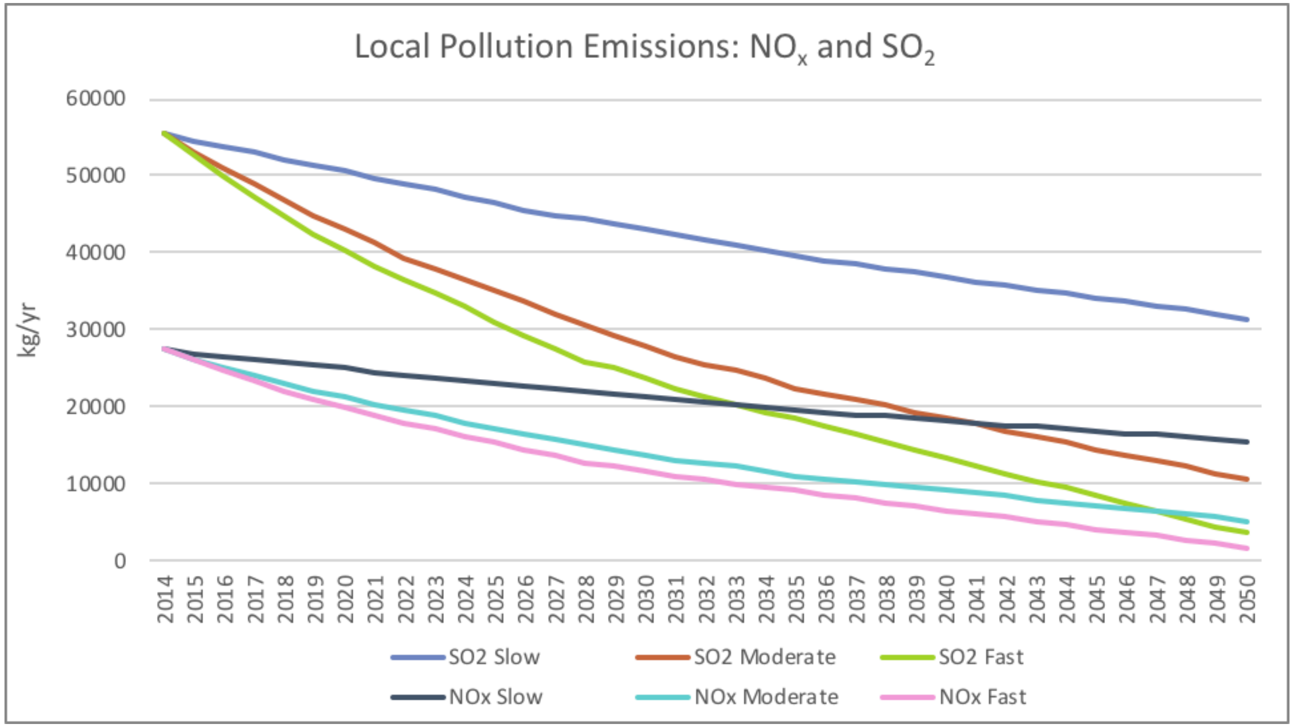

Figure 36: NOx and SO2 emissions vs. building retrofit scenario

The same trend is visible in Figure 36 which pertains to NO$_x$ and SO$_2$ emissions. For each of the emissions, as the equation is based on a coefficient related to the activity (consumption) for which the boiler is used, the curves share the same form.

In regard to GHG emissions, Figure 37, Figure 38, and Figure 39 show the greenhouse gas emissions. From these curves it is evident that the change in electricity generation mix is critical to reducing the GHG emissions. Again, it can be seen that the appliance rates have minimal impact on the value or trend.

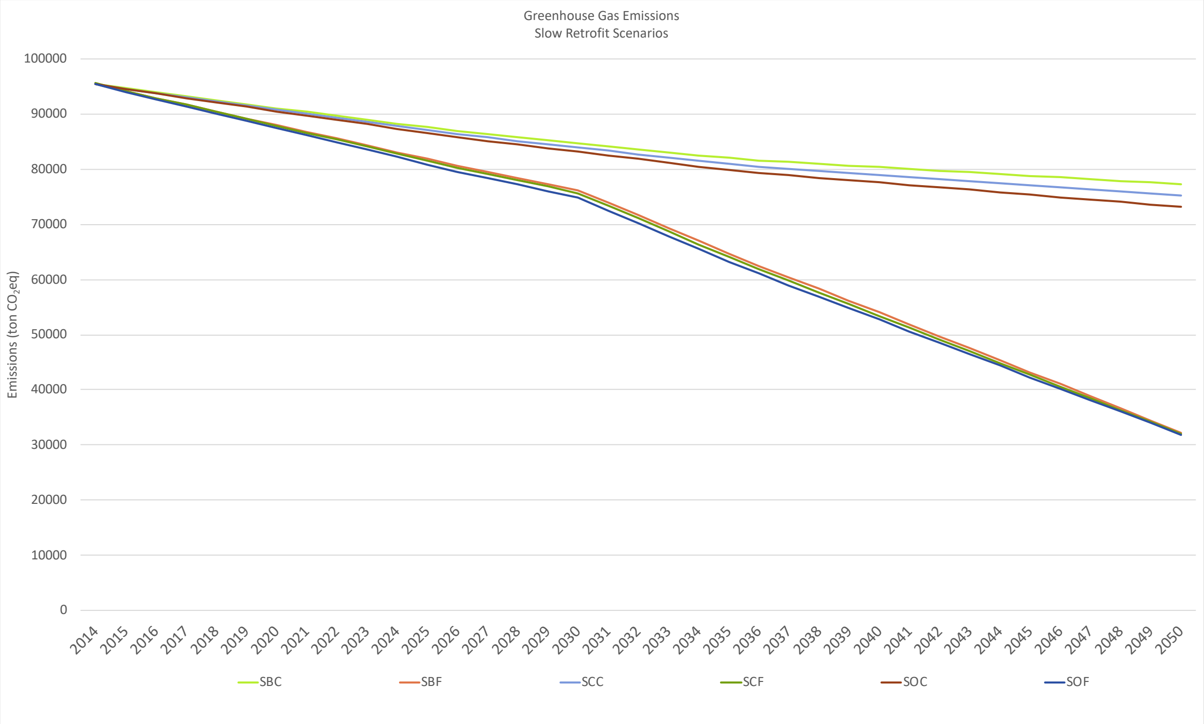

Figure 37: GHG emissions related to slow building retrofit scenarios

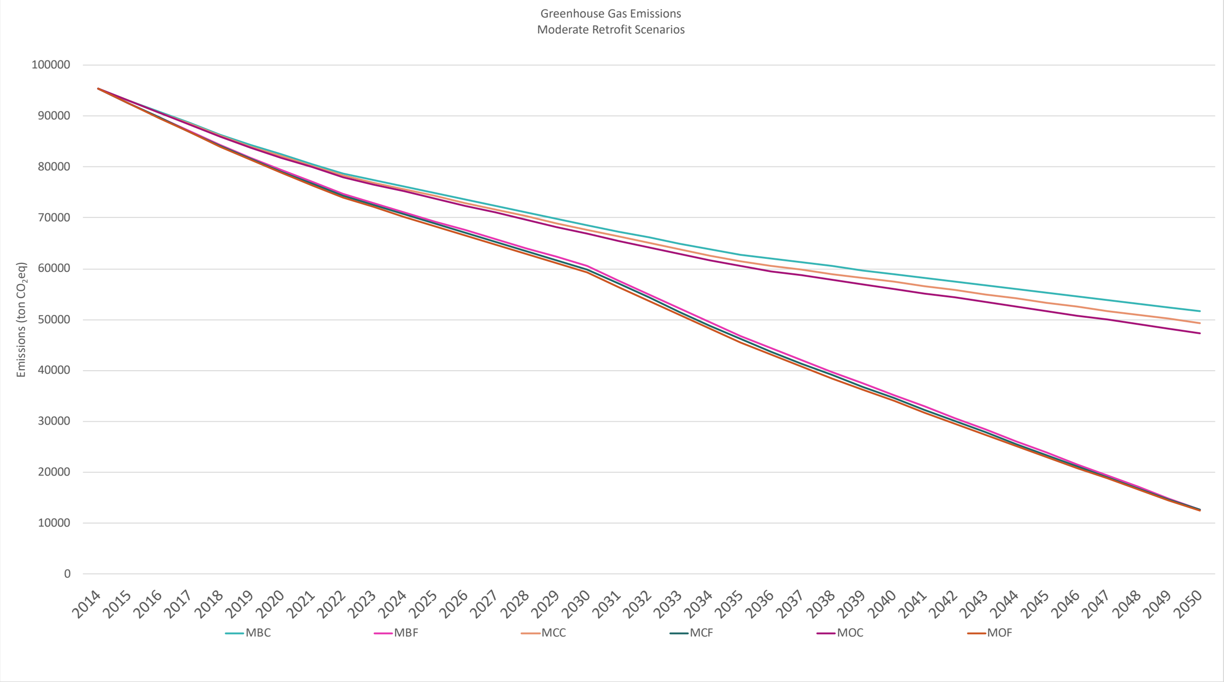

Figure 38: GHG emissions related to moderate building retrofit scenarios

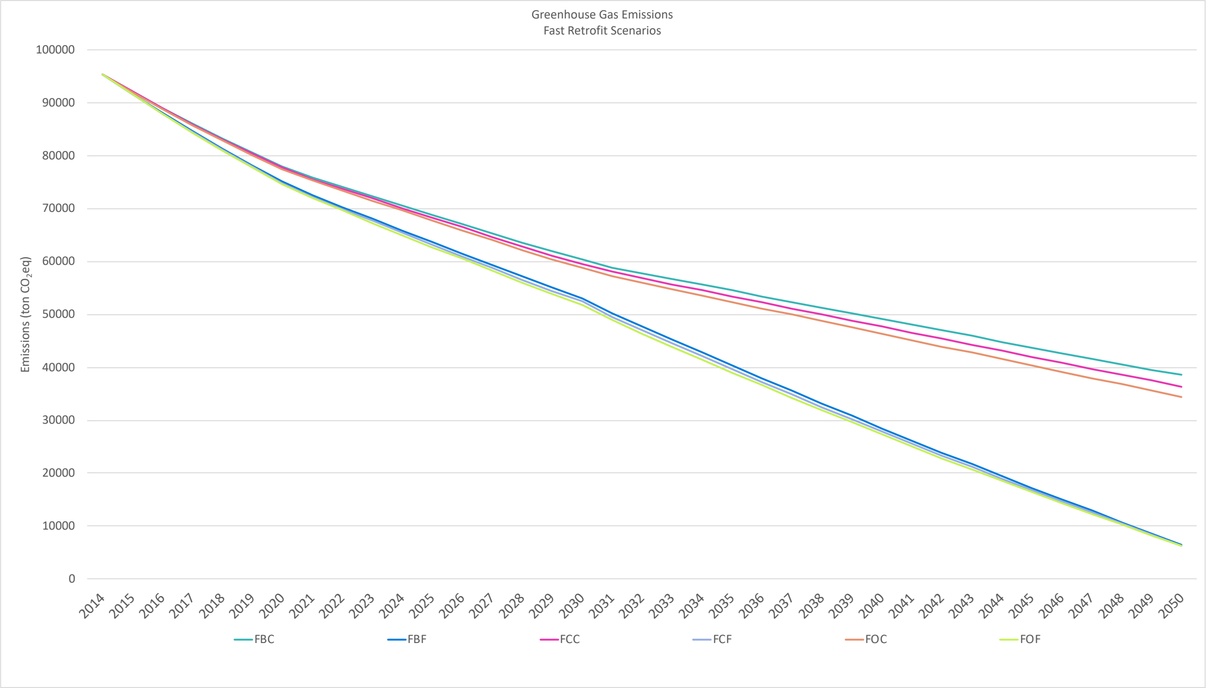

Figure 39: GHG emissions related to fast building retrofit scenarios

3.5 Financial Calculation Results

The global cost methodology was used to determine the costs of the building retrofit interventions (see ANNEX 5: Global Cost Calculation Details) and the results are presented Figure 40.

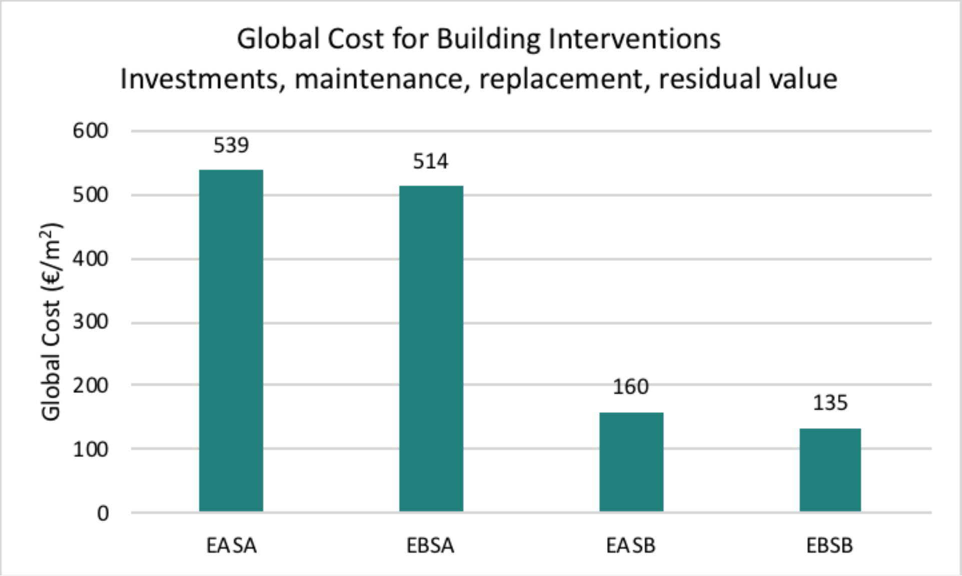

Figure 40: Global costs (excluding energy) for building retrofit measures

The energy costs were determined from the consumption. The total cost breakdowns for each retrofit scenario are presented in Figure 41, Figure 42, and Figure 43. In each case, it is evident that with greater retrofit, the energy costs decrease while the investment costs increase. After prioritizing the building archetypes which were in greatest need of retrofit, the energy saved for each euro invested is declining. The positive point in each of these scenarios is the overall decreasing energy costs.

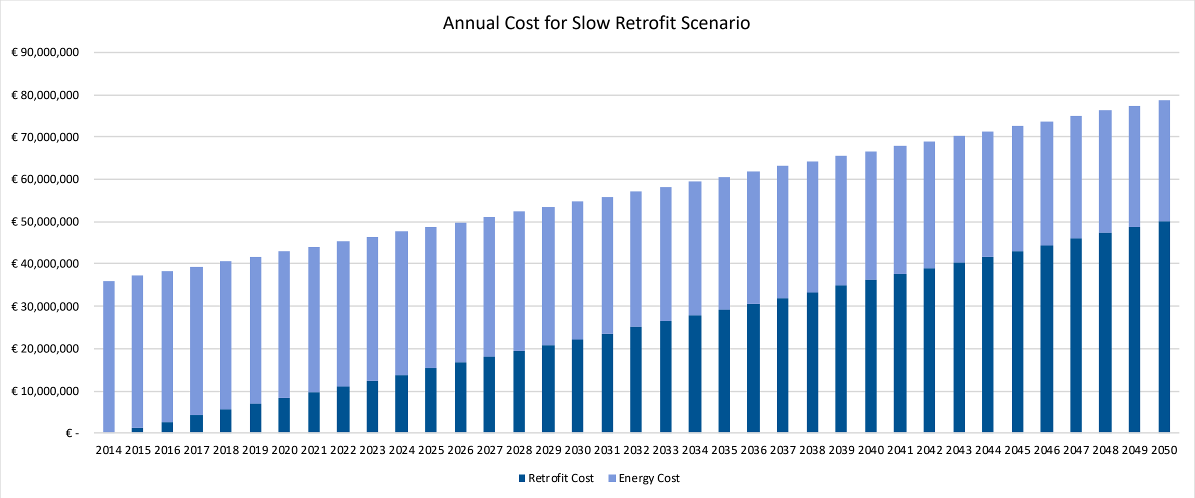

Figure 41: Annual cost breakdown for slow retrofit scenario

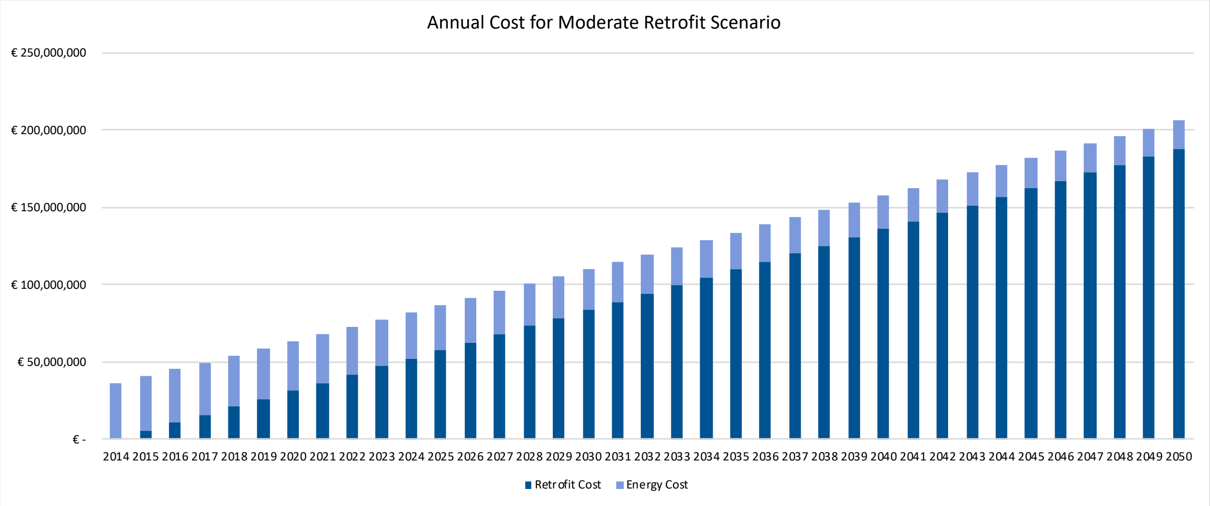

Figure 42: Annual cost breakdown for moderate retrofit scenario

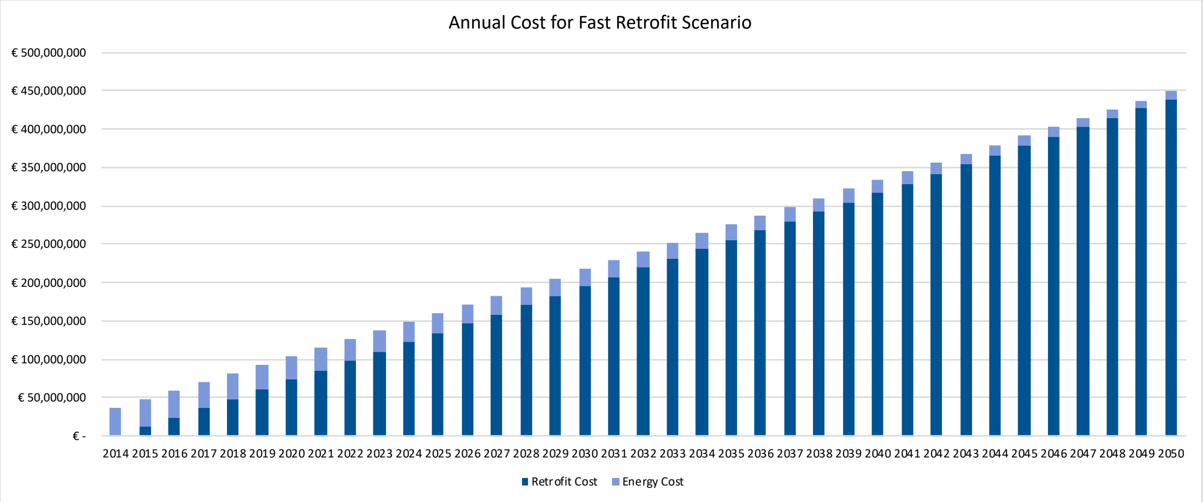

Figure 43: Annual cost breakdown for fast retrofit scenario

When considering other costs associated to energy use, the costs associated to emissions should be considered. Most often, this is discussed in terms of cap and trade systems, but another interesting point for governments to consider is the economic impact associated to the decreased productivity of the workforce caused by health problems linked with poor air quality. Based on the Copenhagen Economics study [43], the savings on healthcare costs were determined. Each retrofit building retrofit scenario is also presented considering the 3 possibilities for appliance electricity consumption. In Figure 44, the slow retrofit scenario, the break-even point occurs approximately 10 years after launching the interventions. With the moderate retrofit scenario, depicted in Figure 45, the break-even point occurs much more quickly, at approximately year 4. The case of the fast retrofit scenario, Figure 46, the high cost of the retrofit is never completely recovered through the interventions proposed.

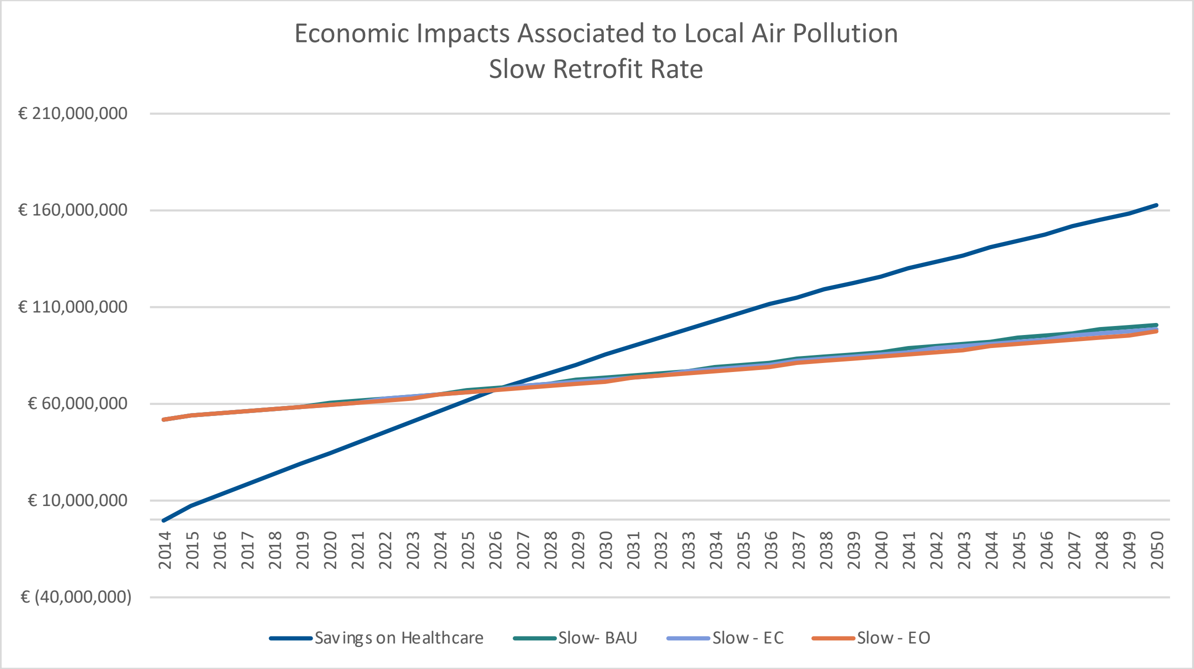

Figure 44: Economic impacts associated to local air pollution - Slow

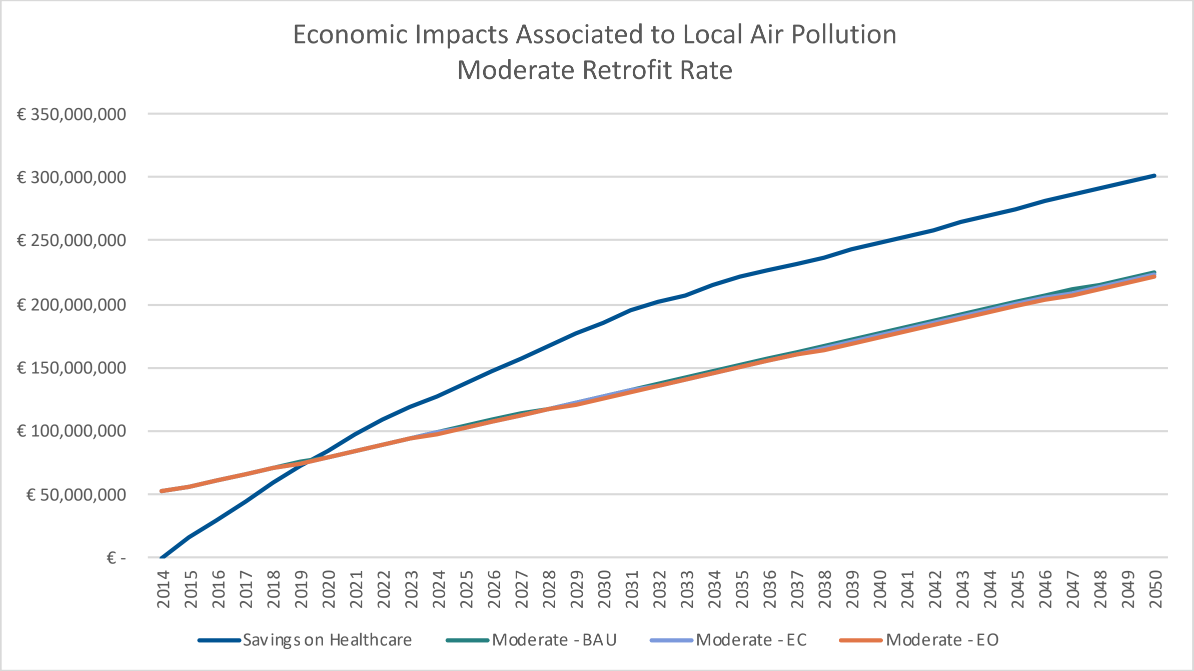

Figure 45: Economic impacts associated to local air pollution - Moderate

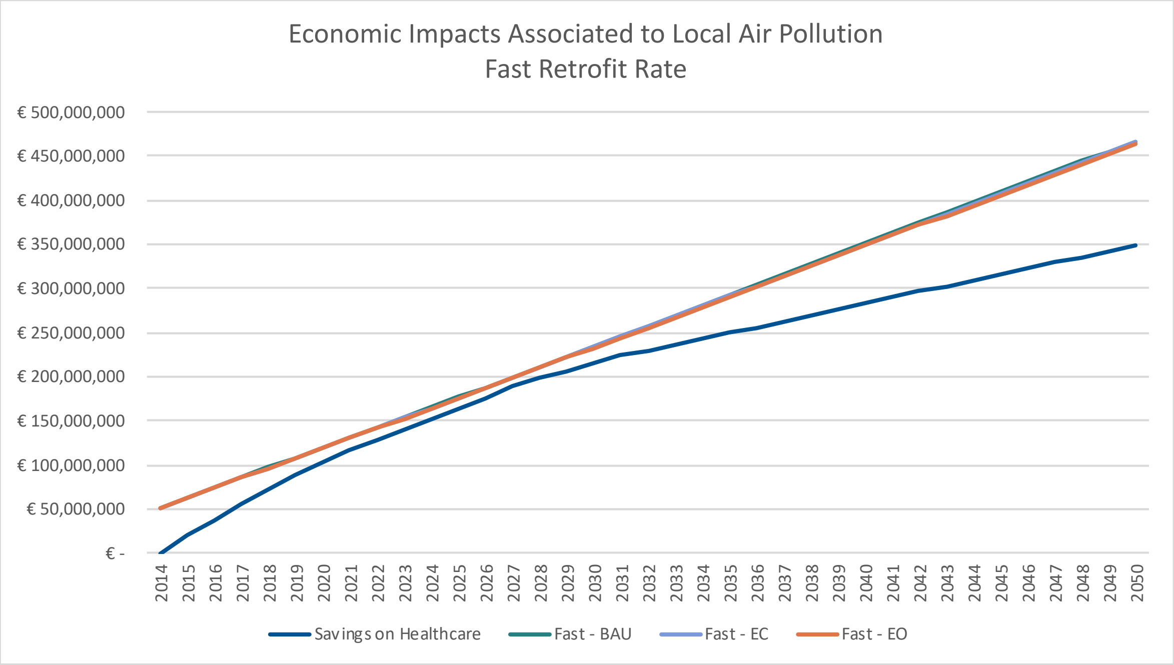

Figure 46: Economic impacts associated to local air pollution - Fast

3.6 QGIS visualization results

The integration of the results above into QGIS in terms of impacts on specific energy consumption provide an opportunity for urban planners to visualize the impacts of different proposals at a district level in order to determine the best course of action for their community.

The following are samples of the types of information which can be obtained from GIS.

Figure 47, Figure 48, and Figure 49 show the visualizations that can be achieved related to the reductions in the specific heating need for the slow, moderate, and fast building retrofit scenarios. The 2DS dictates that approximately 90% of the existing residential building stock will need to be refurbished to a low energy standard (less than 50 kWh/m^{2}y) if the greenhouse gas emission reductions and climate objectives are to be achieved. The QGIS visualizations allow a policy maker to determine from a glance which buildings will meet their targets, and which will fall short. For example, Table 24 shows that with the interventions as planned, only 46% of the building stock will have the desired total final consumptions related to SH, SC, and DHW.

Table 24: Building stock performance compared to 2DS target

	2030		2050	
	Qty Buildings	%	Qty Buildings	%
Slow	0	0%	66	1%
Moderate	229	4%	678	13%
Fast	736	14%	2453	46%

Figure 50, Figure 51, and Figure 52 present the visualization of the results related to SC.

Figure 53, Figure 54, and Figure 55 present the visualization o fthe results related to DHW.

Figure 56, Figure 57, and Figure 58 present the visualization of the specific primary energy reductions related to the building retrofits.

Figure 59, Figure 60, and Figure 61 represent the visualization of the specific total primary energy consumption including appliances. In the interset of brevity, the results presented are only for the EC, or conservative adoption rate, of energy efficient appliances.

Figure 61: GIS visualization, Total Specific Primary Energy Reductions - Fast

.

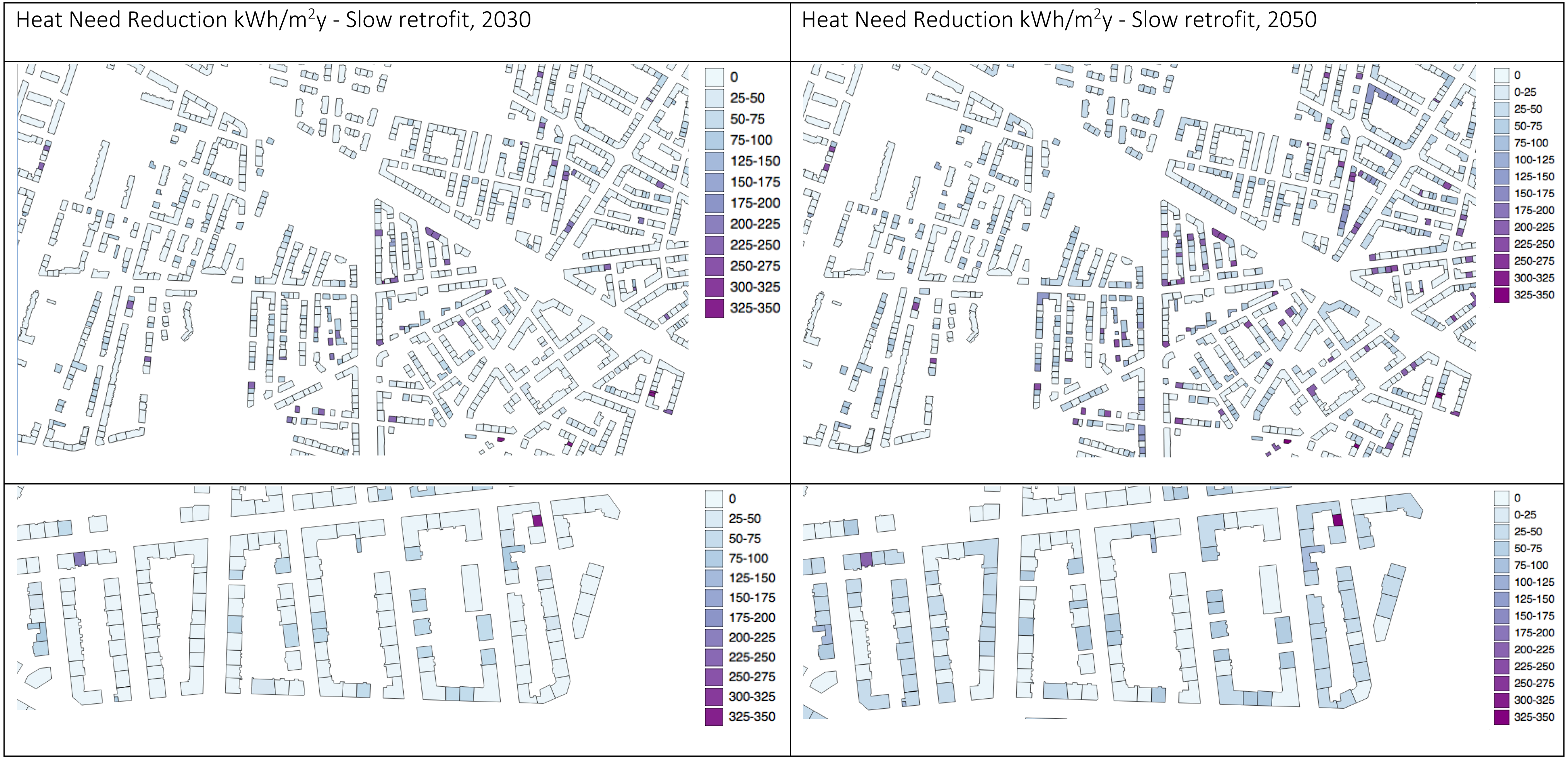
Heat Need Reduction kWh/m^{2}y - Slow retrofit, 2030

Heat Need Reduction kWh/m^{2}y - Slow retrofit, 2050

Figure 47: GIS visualization, Specific Energy Need for Heat Reductions - Slow

Heat Reduction kWh/m^{2}y - Moderate retrofit, 2030

Heat Reduction kWh/m^{2}y - Moderate retrofit, 2050

Figure 48: GIS visualization, Specific Energy Need for Heat Reductions - Moderate

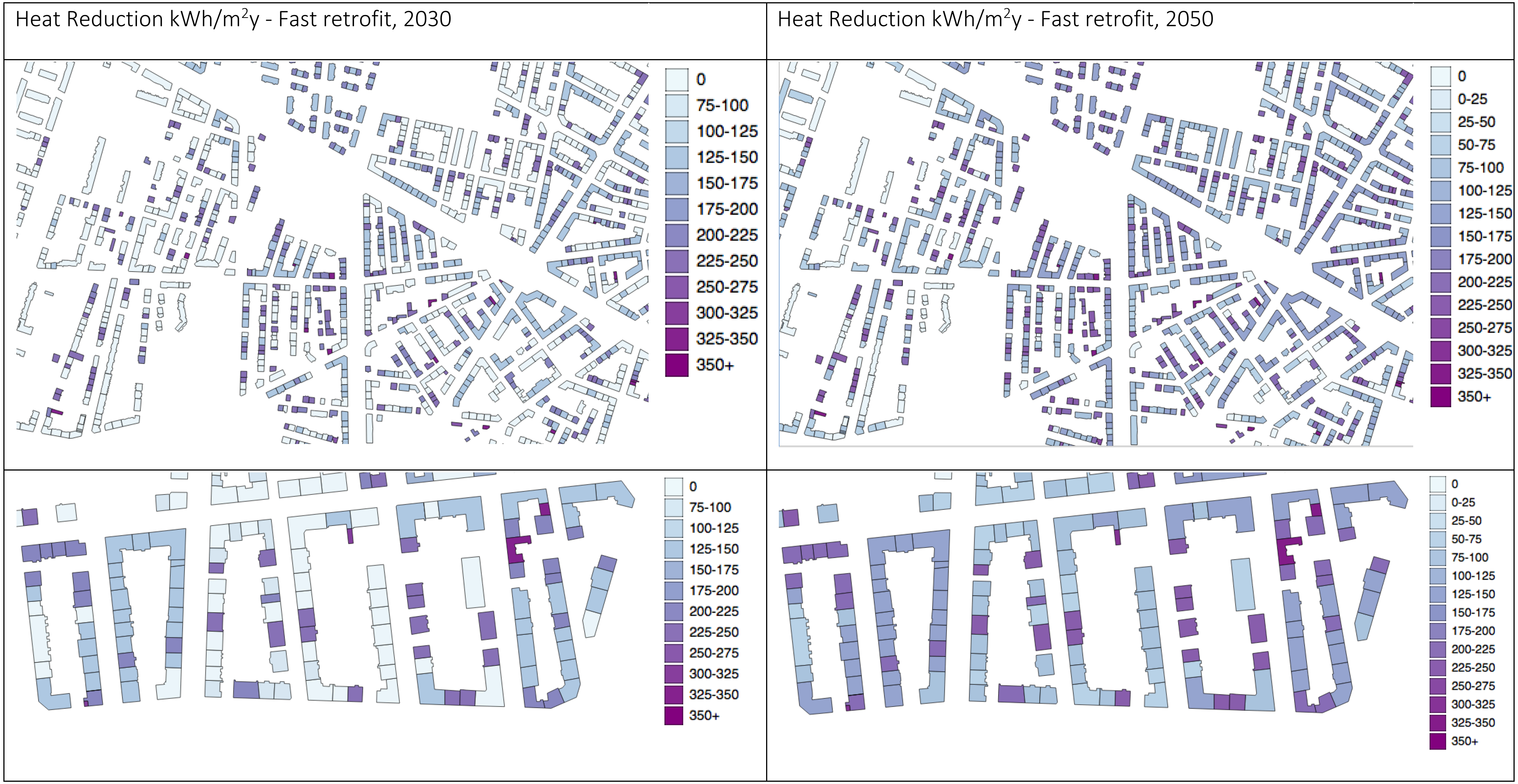
Heat Reduction kWh/m^{2}y - Fast retrofit, 2030

Heat Reduction kWh/m^{2}y - Fast retrofit, 2050

Figure 49: GIS visualization, Specific Energy Need for Heat Reductions - Fast

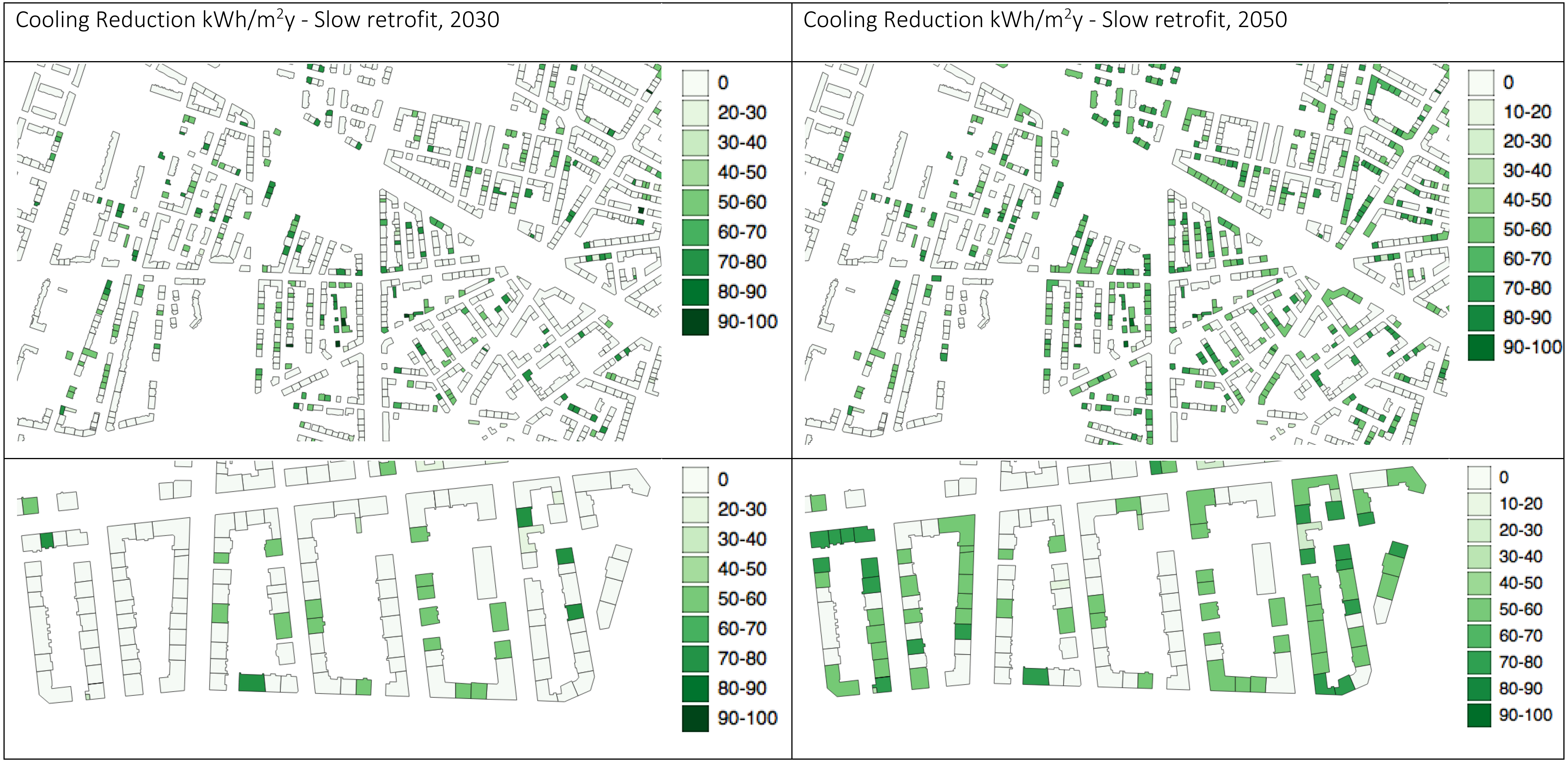

Cooling Reduction kWh/m^{2}y - Slow retrofit, 2030

Cooling Reduction kWh/m^{2}y - Slow retrofit, 2050

Figure 50: GIS visualization, Specific Energy Need for Cooling Reductions - Slow


Cooling Reduction kWh/m^{2}y - Moderate retrofit, 2030

Cooling Reduction kWh/m^{2}y - Moderate retrofit, 2050

Figure 51: GIS visualization, Specific Energy Need for Cooling Reductions - Moderate

Cooling Reduction kWh/m^{2}y - Fast retrofit, 2030

Cooling Reduction kWh/m^{2}y - Fast retrofit, 2050

Figure 52: GIS visualization, Specific Energy Need for Cooling Reductions - Fast

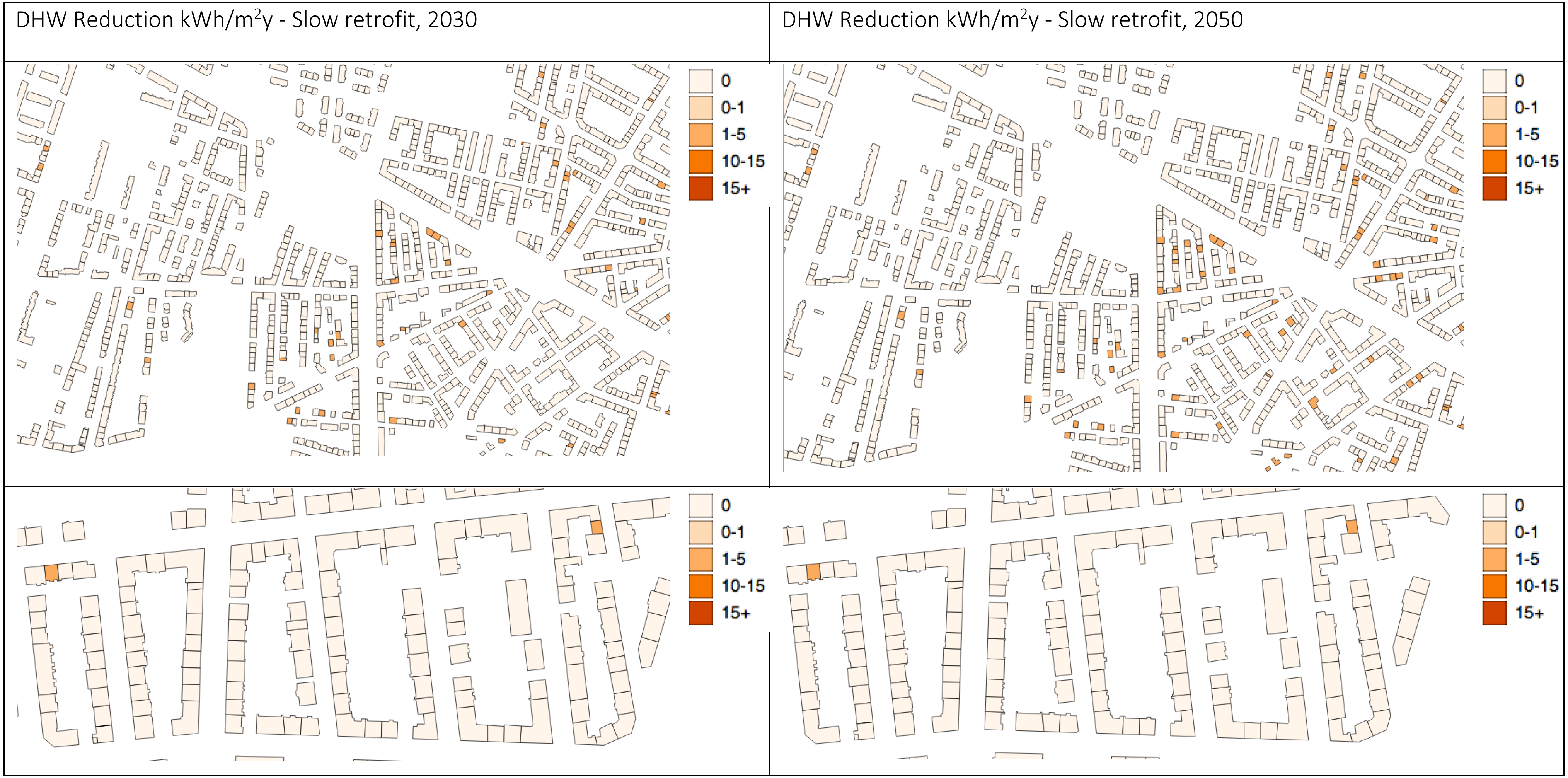
DHW Reduction kWh/m^{2}y - Slow retrofit, 2030

DHW Reduction kWh/m^{2}y - Slow retrofit, 2050

Figure 53: GIS visualization, Specific Energy Need for DHW Reductions - Slow

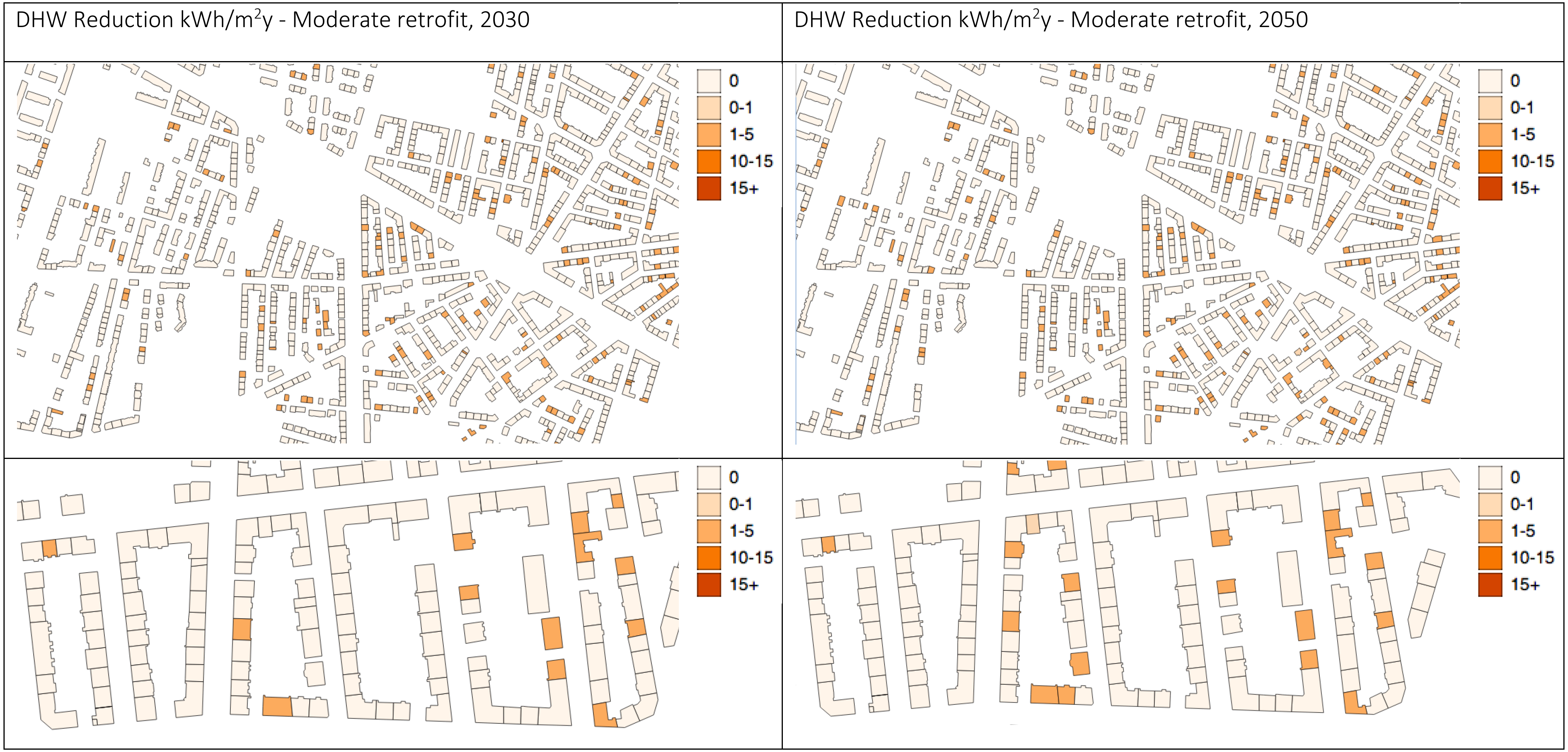

DHW Reduction kWh/m^{2}y - Moderate retrofit, 2030

DHW Reduction kWh/m^{2}y - Moderate retrofit, 2050

Figure 54: GIS visualization, Specific Energy Need for DHW Reductions - Moderate

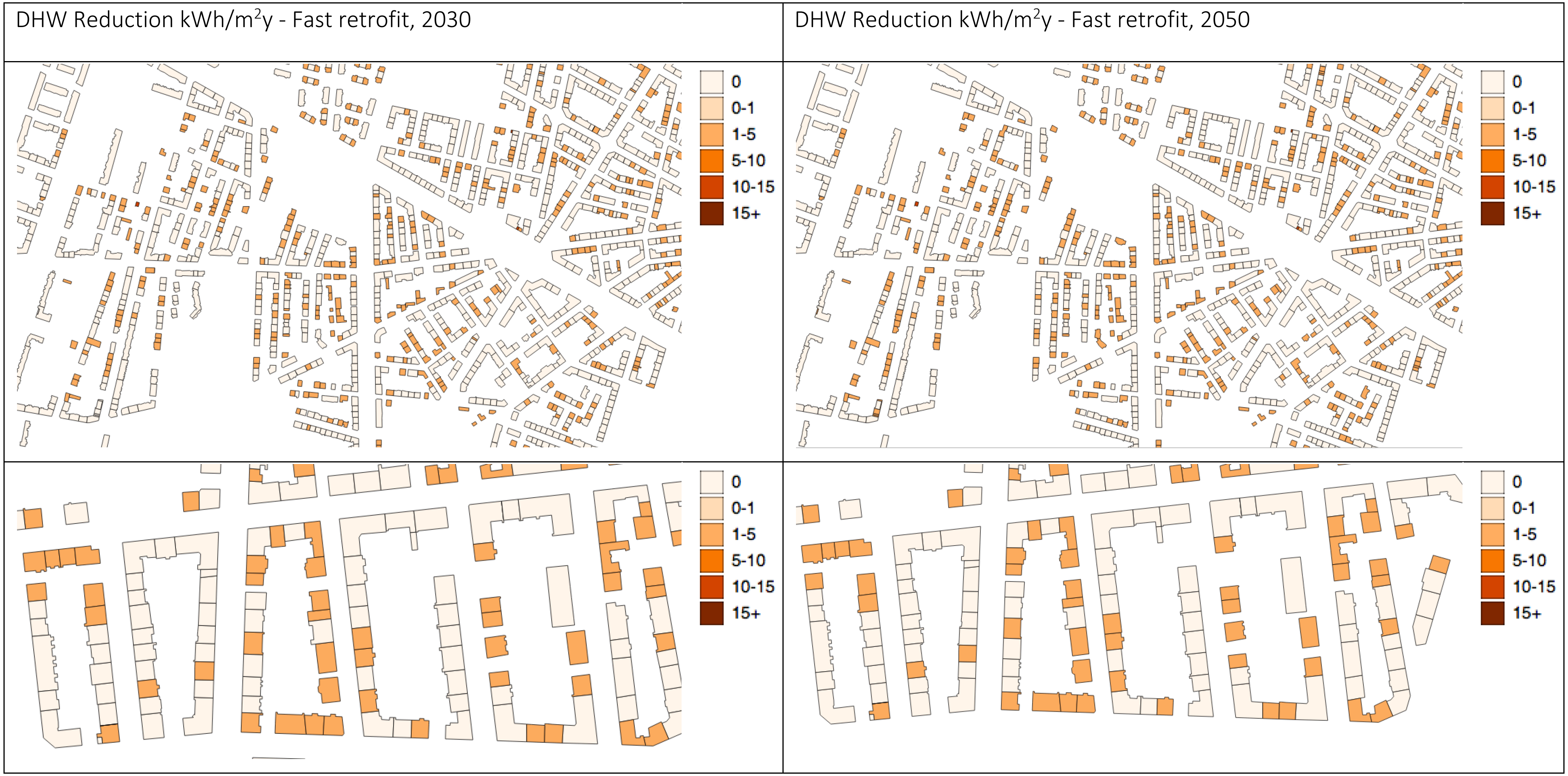

DHW Reduction kWh/m^{2}y - Fast retrofit, 2030

DHW Reduction kWh/m^{2}y - Fast retrofit, 2050

Figure 55: GIS visualization, Specific Energy Need for DHW Reductions - Fast

Primary Energy (excl. appliance) Reduction kWh/m^{2}y - Slow retrofit, 2030

Primary Energy (excl. appliance) Reduction kWh/m^{2}y - Slow retrofit, 2050

Figure 56: GIS visualization, Specific Primary Energy (excl. appliance) Reductions - Slow

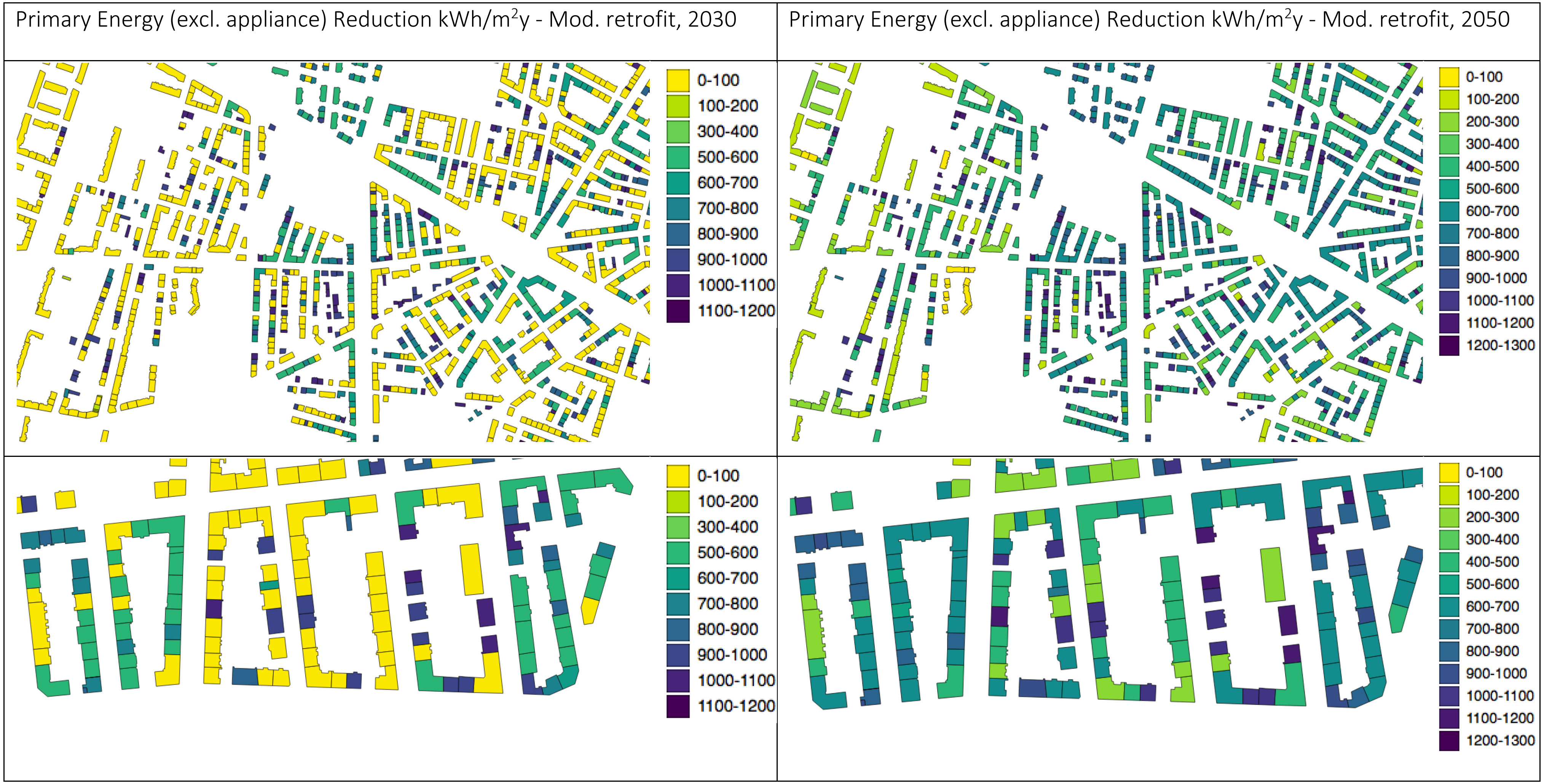

Figure 57: GIS visualization, Specific Primary Energy (excl. appliance) Reductions - Moderate

Primary Energy (excl. appliance) Reduction kWh/m^{2}y - Fast retrofit, 2030	Primary Energy (excl. appliance) Reduction kWh/m^{2}y - Fast retrofit, 2050
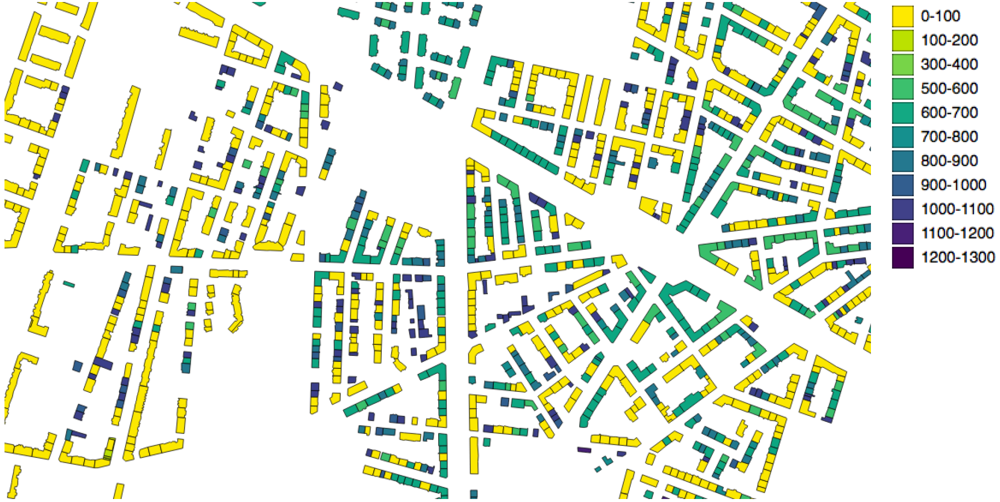	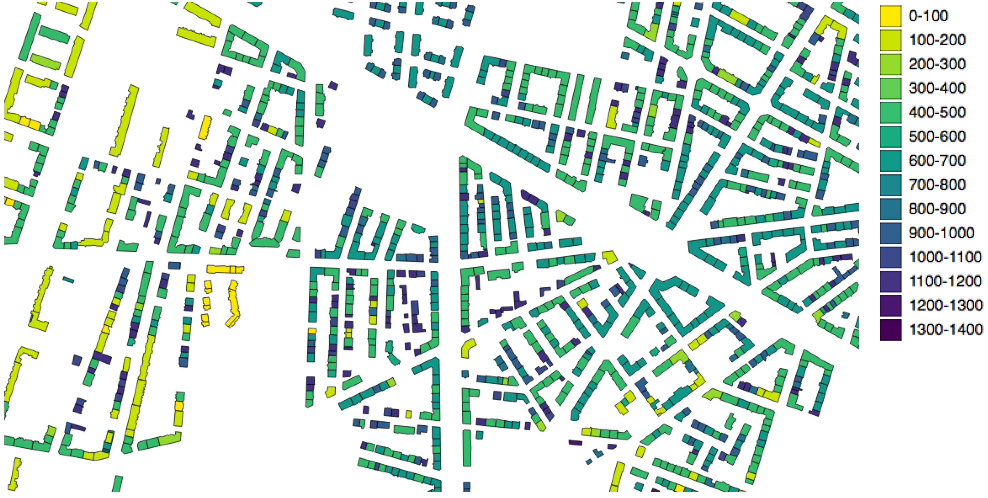
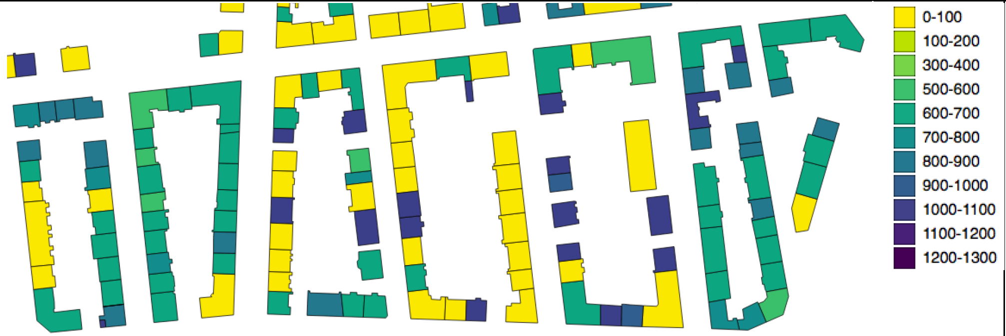	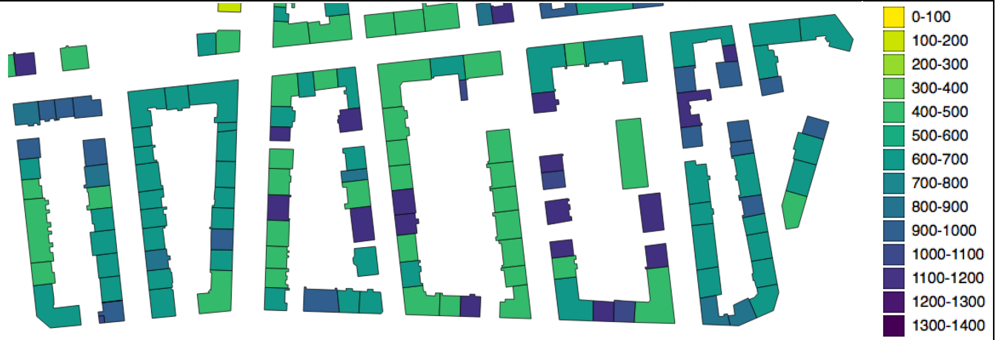

Figure 58: GIS visualization, Specific Primary Energy (excl. appliance) Reductions - Fast

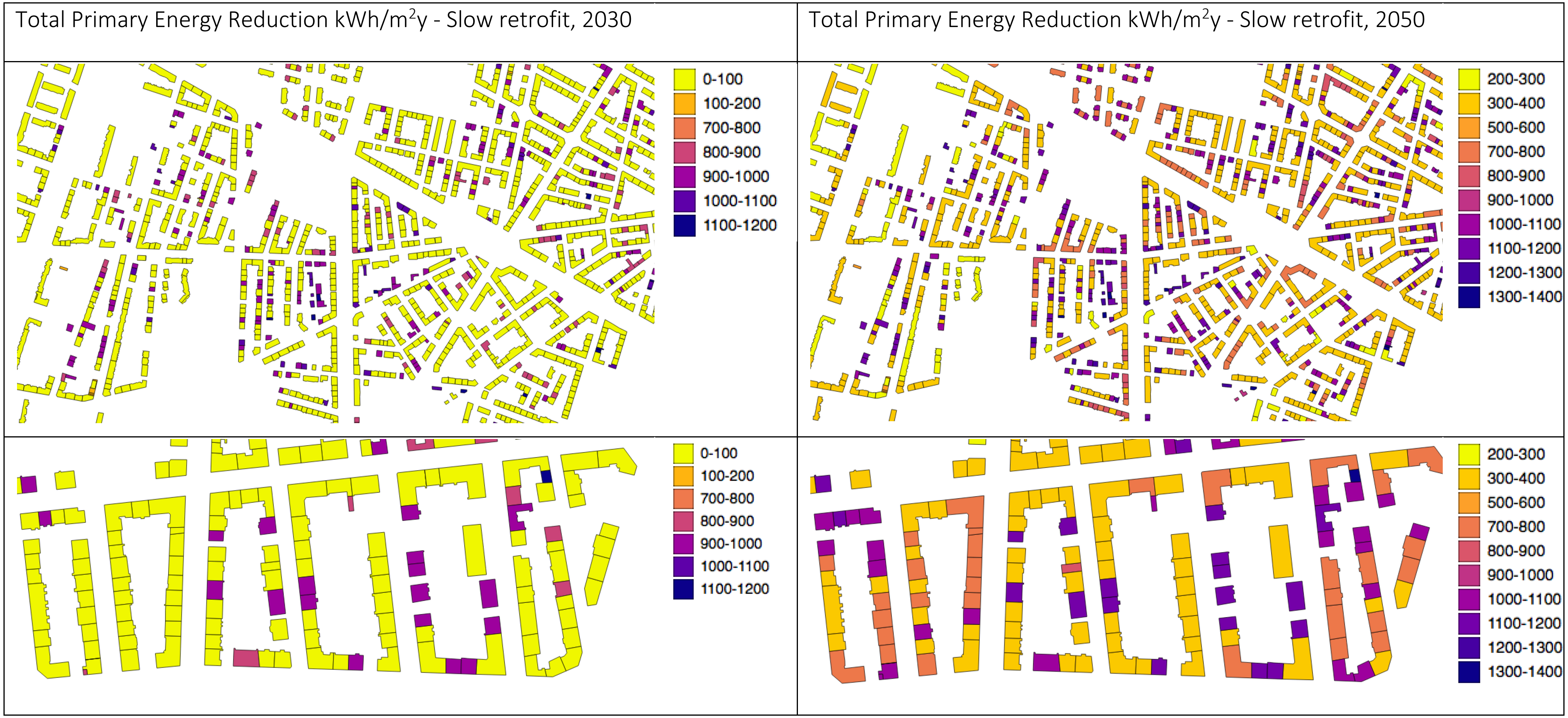

Total Primary Energy Reduction kWh/m^{2}y - Slow retrofit, 2030

Total Primary Energy Reduction kWh/m^{2}y - Slow retrofit, 2050

Figure 59: GIS visualization, Total Specific Primary Energy Reductions - Slow

Total Primary Energy Reduction kWh/m^{2}y - Moderate retrofit, 2030

Total Primary Energy Reduction kWh/m^{2}y - Moderate retrofit, 2050

Figure 60: GIS visualization, Total Specific Primary Energy Reductions - Moderate

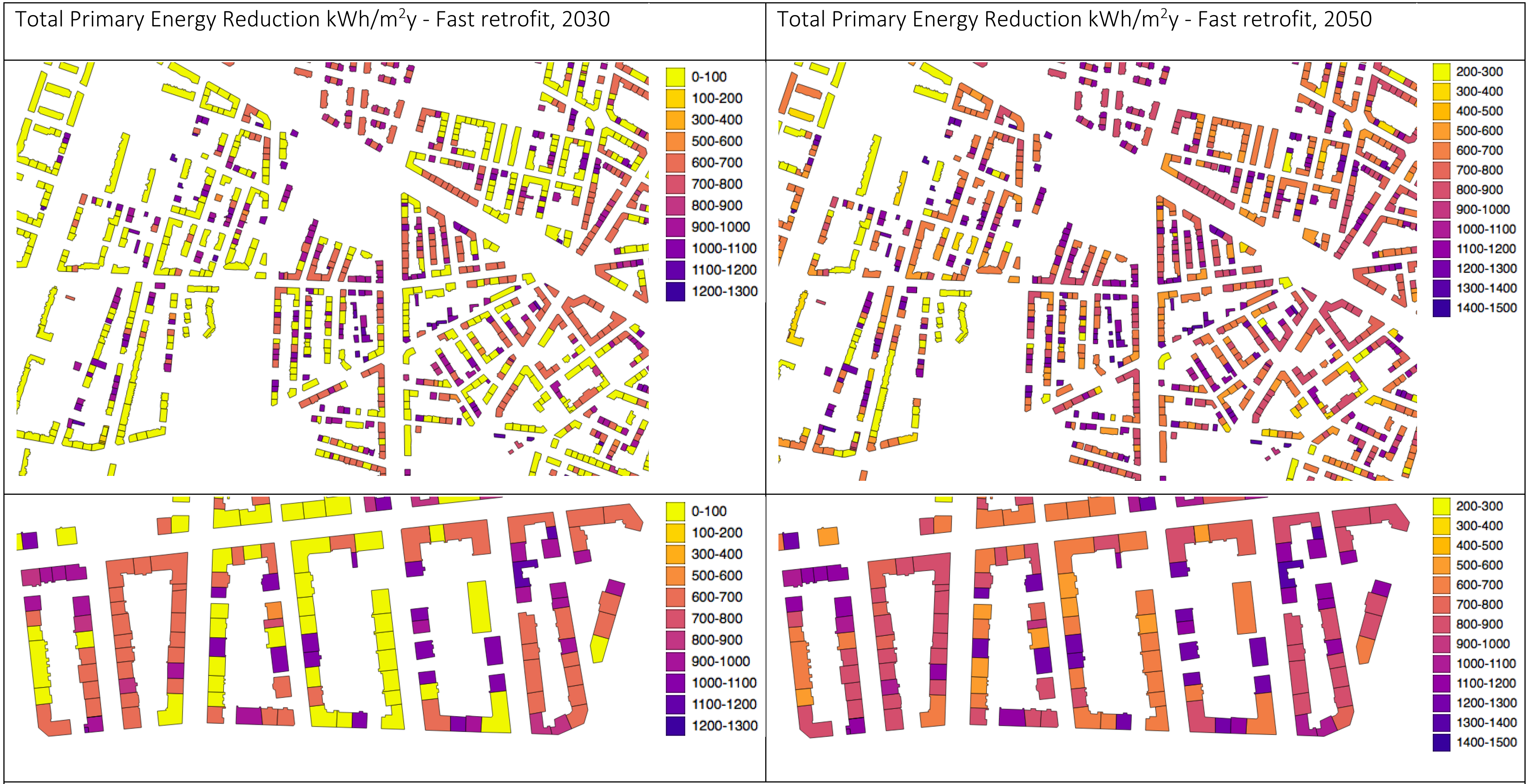

Total Primary Energy Reduction kWh/m^{2}y - Fast retrofit, 2030

Total Primary Energy Reduction kWh/m^{2}y - Fast retrofit, 2050

Figure 61: GIS visualization, Total Specific Primary Energy Reductions - Fast

4 Discussion

The results are summarized in the following tables. There are a few key indicators which are not impacted by the decarbonization of the electricity supply mix. These are related to the local pollution and primary energy demand before considering the contribution to demand of domestic appliances and they are presented in Table 25.

Table 25: Summary results for building retrofit dependent indicators

Building Retrofit Scenario	Slow Retrofit	Moderate Retrofit	Fast Retrofit
2014			
Primary Energy Demand (GWh/yr)	649	649	649
PM Emissions (kg PM/yr)	11546	11546	11546
2030			
Building Stock Retrofit (%)	10%	26%	32%
Building Stock Retrofit (m^2)	112542	300113	375142
Primary Energy Demand Reduction (SH, SC, DHW)	24%	42%	78%
Primary Energy Demand for SH, SC, DHW (GWh/yr)	495	380	143
Pollutant Emission Reduction	23%	50%	58%
PM emissions (kg/yr)	8919	5782	4895
SO_2 Emissions Reduction	23%	50%	58%
NO_x Emissions Reduction	24%	53%	60%
Retrofit ONLY Costs	€ 21,798,933	€ 82,202,710	€ 193,024,215
Savings on Healthcare	€ 84,785,900	€ 186,064,873	€ 214,692,199
Net Savings	€ 62,986,966	€ 103,862,163	€ 21,667,984
2050			
Building Stock Retrofit (%)	22%	58%	72%
Building Stock Retrofit (m^2)	253221	675255	844068
Primary Energy Demand Reduction (SH, SC, DHW)	62%	83%	99%
Primary Energy Demand for SH, SC, DHW (GWh/yr)	245.97	109.62	6.80
Pollutant Emission Reduction	43%	81%	94%
PM emissions (kg/yr)	6530	2196	730
SO_2 Emissions Reduction	43%	81%	94%
NO_x Emissions Reduction	43%	81%	94%
Retrofit ONLY Costs	€ 49,047,600	€ 184,956,096	€ 434,304,484
Savings on Healthcare	€ 161,912,048	€ 301,815,703	€ 349,133,629
Net Savings	€ 112,864,448	€ 116,859,606	(€ 85,170,855)

The slow building retrofit scenario presents a conservative rate of intervention of 0.6% per annum. As shown in Table 25, this scenario presents modest reductions air pollutants with an average of approximately 24% in 2030 and 43% in 2050. The healthcare savings thanks to this reduction offset the cost of the building renovations and from the graph, you can see they also offset the energy costs (Figure 44,). The moderate retrofit, with a per annum building stock renovation rate of 1.6%, shows that air pollutant reductions of approximately 50% are possible while still maintaining a positive net savings, even when including the energy costs (Figure 45), through 2050. The fast retrofit rate, which is 2% per annum, shows impressive reductions in local air pollution emissions, approximately 59% overall in 2030 and 94% in 2050, however the cost of the renovations alone are returned in 2030, but by 2050 the renovation costs are no longer covered by the health savings, and this value excludes energy costs. When considering the energy costs as well, Figure 46 demonstrates that the investment is never completely recovered.

When considering the decarbonization of the electricity supply mix, the changes in total primary energy and GHG emissions can be observed and are presented in the following tables. For a reminder about the codes used, please see Table 13. The most notable result is the clear, if not somewhat obvious, determination that transitioning towards electrification must be paired with decarbonization of the supply. This can be seen in each of the three tables, Table 26, Table 27, and Table 28 which present the final scenario results linked to the slow, moderate, and fast building retrofit scenarios.

Table 26: Summary results for final scenarios linked to slow retrofit

Final Scenario	SBC	SBF	SCC	SCF	SOC	SOF
2014						
Total Primary Energy Demand (GWh/yr)	840	840	840	840	840	840
GHG Emissions (tons CO_2eq.)	95409	95409	95409	95409	95409	95409
2030						
Total Primary Energy Demand (GWh/yr)	668	668	553	553	492	492
Total Primary Energy Demand Reduction	20%	20%	34%	34%	41%	41%
GHG Emissions (tons CO_2eq.)	84713	76234	83908	75680	83133	74821
GHG Emissions Reduction	11%	20%	12%	21%	13%	22%
2050						
Total Primary Energy Demand (GWh/yr)	267	267	130	130	84	84
Total Primary Energy Demand Reduction	68%	68%	84%	84%	90%	90%
GHG Emissions (tons CO_2eq.)	77323	32155	75167	32060	73190	31886
GHG Emissions Reduction	19%	66%	21%	66%	23%	67%

One of the more interesting results in regard to pollution is that the expenditures made in order to achieve reduced emissions have very quick returns, except in the case of the fast building retrofit scenario. In the fast scenario, the most expensive of the retrofit measures are considered and a larger portion of the building stock is impacted. Since the poor performing buildings have the highest priority, the fast scenario eventually starts retrofitting buildings which today are not considered per performers relative to the other buildings in the district. Basically, there are deminisihing returns on the investment from a Euros to energy ratio perspective.

In Table 26, it can be seen that the maximal reduction of GHG emissions is approximately 67% relative to the 2014 values by 2050 when the supply is decarbonized. Without the decarbonization, the maximum reduction of GHG is 23%.

In Table 27, with the increased rate of interventions, better GHG emissions reductions are achieved. The maximum value is 87% reduction by 2050 when compared to the initial levels for this study in 2014. Without decarbonization the greatest reduction is 50%

Table 27: Summary results for final scenarios linked to moderate retrofit

Final Scenario	MBC	MBF	MCC	MCF	MOC	MOF
2014						
Total Primary Energy Demand (GWh/yr)	840	840	840	840	840	840
GHG Emissions (tons CO_2eq.)	95409	95409	95409	95409	95409	95409
2030						
Total Primary Energy Demand (GWh/yr)	662	662	546	546	486	486
Total Primary Energy Demand Reduction	21%	21%	35%	35%	42%	42%
GHG Emissions (tons CO_2eq.)	68566	60538	67633	59888	66857	59261
GHG Emissions Reduction	28%	37%	29%	37%	30%	38%
2050						
Total Primary Energy Demand (GWh/yr)	265	265	129	129	83	83
Total Primary Energy Demand Reduction	68%	68%	85%	85%	90%	90%
GHG Emissions (tons CO_2eq.)	51725	12664	49329	12572	47352	12487
GHG Emissions Reduction	46%	87%	48%	87%	50%	87%

In Table 28, the greatest GHG emissions reduction is 93% relative to 2014 levels in the district. Without decarbonization, the highest value is 64%.

Table 28: Summary results for final scenarios linked to fast retrofit

Final Scenario	FBC	FBF	FCC	FCF	FOC	FOF
2014						
Total Primary Energy Demand (GWh/yr)	840	840	840	840	840	840
GHG Emissions (tons CO_2eq.)	95409	95409	95409	95409	95409	95409
2030						
Total Primary Energy Demand (GWh/yr)	655	655	540	540	479	479
Total Primary Energy Demand Reduction	22%	22%	36%	36%	43%	43%
GHG Emissions (tons CO_2eq.)	60347	53113	59542	52462	58767	51835
GHG Emissions Reduction	37%	44%	38%	45%	38%	46%
2050						
Total Primary Energy Demand (GWh/yr)	263	263	127	127	81	81
Total Primary Energy Demand Reduction	69%	69%	85%	85%	90%	90%
GHG Emissions (tons CO_2eq.)	38538	6459	36382	6366	34405	6281
GHG Emissions Reduction	60%	93%	62%	93%	64%	93%

Without the decarbonization of the grid, the impact of the different adoption rates for energy efficient appliances starts to become more evident. By 2050, there is a 2% and 4% difference in emissions reductions for the conservative and optimistic adoption rates relative to the business as usual case. In regard to the adoption of more energy efficient appliances, unless improvements occur at a more dramatic rate than anticipated by the literature used in this study [63], this factor has little influence on the resulting energy demand. Only in the case that there is no further penetration of renewables into the generation mix does this factor present a noticeable difference in the GHG emissions.

Based on the case study presented, it is critical to mention that even with most aggressive interventions, higher rate of application, and optimistic outlooks in regard to decarbonization of electricity supply and adoption of energy efficiency technologies, only 46% of the buildings, 72% of which were modified, will meet the 2DS objective of global consumption less than 50 kWh/m^{2}y. This suggest that the best-case scenario presented in this study - fast building retrofit rate, optimistic adoption of energy efficient appliances, and the decarbonized future electricity supply (FOF) - is insufficient. Therefore, the building retrofit rate should be increased, and the types of interventions should likely be more aggressive (more of the advanced envelope and systems). This study did not consider endogenous sources of energy, but their application along with these measures could ensure that the 2DS targets are met.

4.1 Future Work

There are few areas of this study that warrant further investigation. The first area is the consideration of the future energy prices on the cost-benefit analysis which was performed relative to the health care costs. This value had been fixed due to uncertainty, but it could be interesting to perform a sensitivity analysis on the topic.

In regard to the analytical model, with additional measured data regarding the space heating consumption, further calibrations could be performed on the model and the RB definitions could be refined to improve the accuracy beyond what it is today.

Additionally, exploitation of endogenous energy sources and the expansion of the district heating network are 2 possible uses for this model which were not explored over the course of this study.

5 Conclusion

As part of the 2050 Energy Roadmap [78], the European Union has committed to 80-95 % GHG reduction by 2050. Buildings represent 40% of final energy consumption [64] and therefore it is critical that we create the tools and methodologies necessary in order to support the research and policy decisions which will be made in the future.

With the elaboration of this work, an innovative approach to district level energy modelling was carried out. The model integrated dynamic building energy analysis, spatial analysis, statistical analysis, and socio-techno-economic analysis methods to create a district level characterization of the energy balance starting in 2014 as the reference year and calculated through 2050. Measures focused on efficiency and electrification were introduced and beyond the building performance, the resident's domestic appliance use and evolution were also considered. Several scenarios were created based on the building interventions, resident social groups, and decarbonization scenarios of the electricity supply. RBs were created for each archetype present in the district, as opposed to focusing on a few of the most predominant, in order to have a result which more closely resembles the energy consumption patterns of the district.

For the 13 archetypes used in calibration, the percentage of error in the model was found to be less than 10%. There were 2 outliers, for which the error was unsatisfactory, but this is likely due to insufficient sample size to create an appropriate mean value, error in the measurement in the case of C9AB, and possible conscientious consumption on the part of the consumers in C4MF and C6AB.

While this model was used for analysis related to electrification and decentralized solutions for space heating, the same model could be used by an engineer to assess the impacts of greater district heat penetration.

These capabilities along with the ability to visualize the precise location of energy consumption and create district level patterns provide a useful tool for urban energy planning.

6 Works Cited

[1] International Energy Agency (IEA), *Transition to sustainable buildings: Strategies and opportunities to 2050*, vol. 9789264202. 2013.

[2] Ministero dello Sviluppo Economico, “Italy’s National Energy Strategy 2017,” p. 4, 2017.

[3] International Energy Agency (IEA), “Energy and Air Pollution,” 2016.

[4] J. Gabbatiss, “Milan and Turin ban cars to combat smog and air pollution,” *The Independent*, 28-Dec-2017.

[5] “Torino - OpenStreetMap Wiki.” [Online]. Available: https://wiki.openstreetmap.org/wiki/Torino. [Accessed: 24-Aug-2018].

[6] V. Corrado, I. Ballarini, S. P. Corgnati, and N. Talà, “Typology Approach for Building Stock Energy Assessment (TABULA): Building Typology Brochure – Italy,” 2011.

[7] SERVIZIO STATISTICA E TOPONOMASTICA UFFICIO PUBBLICAZIONI STATISTICHE, “Annuario Statistico della Città di Torino- Capitolo 3: Demografia,” 2012.

[8] C. Delmastro, G. Mutani, and S. P. Corgnati, “A supporting method for selecting cost-optimal energy retrofit policies for residential buildings at the urban scale,” *Energy Policy*, vol. 99, pp. 42–56, 2016.

[9] United Nations, “World Urbanization Prospects, 2014.,” 2014.

[10] Z. Shi, J. A. Fonseca, and A. Schlueter, “A review of simulation-based urban form generation and optimization for energy-driven urban design,” *Build. Environ.*, vol. 121, pp. 119–129, 2017.

[11] European Commission, “A strategy for smart, sustainable and inclusive growth,” 2010.

[12] European Parliament and the Council of the European Union, *Directive 2010/31/EU of the European Parliament and of the Council of 19 May 2010 on the energy performance of buildings*. 2010.

[13] European Commission, “Roadmap 2050,” *Policy*, no. April, pp. 1–9, 2012.

[14] V. Oliveira, *Urban Morphology: An Introduction to the Study of the Physical Form of Cities*. Switzerland: Springer,Cham, 2016.

[15] L. G. Swan and V. I. Ugursal, “Modeling of end-use energy consumption in the residential sector: A review of modeling techniques,” *Renew. Sustain. Energy Rev.*, vol. 13, no. 8, pp. 1819–1835, 2009.

[16] J. Mikkola and P. D. Lund, “Models for generating place and time dependent urban energy demand profiles,” *Appl. Energy*, vol. 130, pp. 256–264, 2014.

[17] B. Howard, L. Parshall, J. Thompson, S. Hammer, J. Dickinson, and V. Modi, “Spatial distribution of urban building energy consumption by end use,” *Energy Build.*, vol. 45, pp. 141–151, 2012.

[18] P. Caputo, G. Costa, and S. Ferrari, “A supporting method for defining energy strategies in the building sector at urban scale,” *Energy Policy*, vol. 55, pp. 261–270, 2013.

[19] P. Wate and V. Coors, “3D data models for urban energy simulation,” *Energy Procedia*, vol. 78, no. 0, pp. 3372–3377, 2015.

[20] D. Robinson *et al.*, “CITYSIM: Comprehensive Micro-Simulation Of Resource Flows For Sustainable Urban Planning,” *Int. IBPSA Conf.*, pp. 1083–1090, 2009.

[21] F. Chingcuanco and E. J. Miller, “A microsimulation model of urban energy use: Modelling residential space heating demand in ILUTE,” *Comput. Environ. Urban Syst.*, vol. 36, no. 2, pp. 186–194, 2012.

[22] A. J. Firth, S.K.; Lomas, K.J.; Wright, “Targeting household energy efficiency measures using sensitivity analysis,” *Build. Res. Inf.*, vol. 38, no. 1, pp. 25–41, 2010.

[23] Y. Yamaguchi, Y. Shimoda, and M. Mizuno, “Proposal of a modeling approach considering urban form for evaluation of city level energy management,” *Energy Build.*, vol. 39, no. 5, pp. 580–592, 2007.

[24] L. Girardin, F. Marechal, M. Dubuis, N. Calame-Darbellay, and D. Favrat, “EnerGis: A geographical information based system for the evaluation of integrated energy conversion systems in urban areas,” *Energy*, vol. 35, no. 2, pp. 830–840, 2010.

[25] J. A. Fonseca and A. Schlueter, “Integrated model for characterization of spatiotemporal building energy consumption patterns in neighborhoods and city districts,” *Appl. Energy*, vol. 142, pp. 247–265, 2015.

[26] R. Madlener and Y. Sunak, “Impacts of urbanization on urban structures and energy demand: What can we learn for urban energy planning and urbanization management?,” *Sustain. Cities Soc.*, vol. 1, no. 1, pp. 45–53, 2011.

[27] P. H. G. Berkhout, J. C. Muskens, and J. W. Velthuijsen, “Defining the rebound effect,” *Energy Policy*, vol. 28, no. 6–7, pp. 425–432, Jun. 2000.

[28] I. Ballarini and V. Corrado, “Application of energy rating methods to the existing building stock: Analysis of some residential buildings in Turin,” *Energy Build.*, vol. 41, no. 7, pp. 790–800, 2009.

[29] C. Delmastro, F. Martinsson, G. Mutani, and S. P. Corgnati, “Modeling Building Energy Demand Profiles and District Heating Networks for Low Carbon Urban Areas,” *Procedia Eng.*, vol. 198, no. September 2016, pp. 386–397, 2017.

[30] A. Senor, D. Panepinto, and G. Genon, “A case study: an environmental and economic analysis of Turin District’s heating system combined with a cogeneration plant,” vol. 168, pp. 651–662, 2015.

[31] I. Ballarini, S. P. Corgnati, V. Corrado, and N. Talà, “Improving energy modeling of large building stock through the development of archetype buildings,” *Build. Simul.*, pp. 2874–2881, 2011.

[32] I. Ballarini, S. P. Corgnati, V. Corrado, and N. Talà, “Definition of building typologies for energy investigations on residential sector by Tabula Iee-Project: Application to Italian case studies,” *Roomvent*, no. November 2014, pp. 19–22, 2011.

[33] F. Report, “Financing Urban District Energy Systems,” 2013.

[34] International Energy Agency (IEA), “ECBCS Annual Report 2011,” 2011.

[35] Energiesprong UK, “What is Energiesprong?” [Online]. Available: https://www.energiesprong.uk/about. [Accessed: 13-Jul-2018].

[36] R. Roy and N. A. Braathen, “The Rising Cost of Ambient Air Pollution thus far in the 21st Century,” *OECD Environ. Work. Pap.*, vol. 124, no. 124, 2017.

[37] T. Gayer, “Pricing Pollution,” *Brookings*, pp. 1–12, 2011.

[38] World Bank, “Air Pollution Deaths Cost Global Economy US$225 Billion,” *Press Release*, no. 202, p. 1, 2016.

[39] B. Chelsea and H. January, “The staggering economic cost of air pollution,” 2011.

[40] Y. J. Lee, Y. W. Lim, J. Y. Yang, C. S. Kim, Y. C. Shin, and D. C. Shin, “Evaluating the PM damage cost due to urban air pollution and vehicle emissions in Seoul, Korea,” *J. Environ. Manage.*, vol. 92, no. 3, pp. 603–609, 2011.

[41] A. Cohen *et al.*, “Chapter 17: Urban Air Pollution,” *Comp. Quantif. Heal. Risks; Glob. Reg. Burd. Dis. Attrib. to Sel. Major Risk Factors*, vol. 1, 2004.

[42] J. Gulliver, K. de Hoogh, D. Fecht, D. Vienneau, and D. Briggs, “Comparative assessment of GIS-based methods and metrics for estimating long-term exposures to air pollution,” *Atmos. Environ.*, vol. 45, no. 39, pp. 7072–7080, 2011.

[43] Copenhagen Economics, “Multiple benefits of investing in energy efficient renovation of buildings: Impact on Public Finances,” no. October, pp. 1–80, 2012.

[44] D. S. Schiera, “A preliminary study of an Agent-Based Model of a Candidate :,” 2018.

[45] ISTAT, “Energia - Consumo per uso domestico,” 2018. [Online]. Available: http://dati.istat.it/Index.aspx?DataSetCode=DCCV_CNSENRG. [Accessed: 23-Jul-2018].

[46] ARPA, “Accesso ai dati - Gradi giorno,” 2018. [Online]. Available: http://www.arpa.piemonte.it/rischinaturali/accesso-ai-dati/selezione-gradi-giorno/selezione-gradi-giorno.html. [Accessed: 25-Jun-2018].

[47] UNI Ente italiano di normalizione, *UNI/TS 10349-1, Riscaldamento e raffrescamento degli edifici - Dati climatici - Parte 1: Medie mensili per la valutazione della prestazione termo-energetica dell’edificio e metodi per ripartire l’irradianza solare nella frazione diretta e diffusa e per ca*. 2016.

[48] UNI Ente italiano di normalizione, “UNI/TS 11300-2, Energy performance of buildings Part 2: Evaluation of primary energy need and of system efficiencies for space heating, domestic hot water production, ventilation and lighting for non-residential buildings,” 2014.

[49] European Committee for Standardization, *EN ISO 13790: Energy performance of buildings - Calculation of energy use for space heating and cooling (ISO 13790:2008)*. 2008.

[50] European Committee for Standardization, *EN 15316-1: Energy performance of buildings - Method for calculation of system energy requirements and system efficiencies - Part 1: General and Energy performance expression, Module M3-1, M3-4, M3-9, M8-1, M8-4 Performance*. 2017.

[51] European Committee for Standardization, *16798-5-1: Energy performance of buildings - Ventilation for buildings -Part 5-1: Calculation methods for energy requirements of ventilation and air conditioning systems (Modules M5-6, M5-8, M6-5, M6-8, M7-5, M7-8) - Method 1: Distribution and generation*. 2017.

[52] European Committee for Standardization, *EN ISO 14683: Linear thermal transmittance - Simplified methods and default values (ISO 14683:2007)*. 2007.

[53] European Committee for Standardization, *EN 15241: Ventilation for buildings - Calculation methods for energy losses due to ventilation and infiltration in buildings (EN 15241:2007/AC)*. 2011.

[54] European Committee for Standardization, *EN 16798-5-2: Energy performance of buildings - Ventilation for buildings - Part 5-2: Calculation methods for energy requirements of ventilation systems (Modules M5-6, M5-8, M6-5, M6-8, M7-5, M7-8) - Method 2: Distribution and generation*. 2017.

[55] UNI Ente italiano di normalizione, “UNI/TS 11300-1, Energy Performance of Buildings - Part 1: Evaluation of Energy Need for Space Heating and Cooling,” 2014.

[56] UNI Ente italiano di normalizione, “UNI/TS 11300-4, Energy performance of buildings Part 4: Renewable energy and other generation systems for space heating and domestic hot water production.” 2012.

[57] UNI Ente italiano di normalizione, “UNI 10339: Impianti aeraulici a fini di benessere. Generalità, classificazione e requisiti.,” 2007.

[58] J. H. Eto, “On using degree-days to account for the effects of weather on annual energy use in office buildings,” *Energy Build.*, vol. 12, no. 2, pp. 113–127, 1988.

[59] International Energy Agency (IEA), “Energy Statistics Manual,” paris, 2005.

[60] ENEA, “Energy Efficiency Trends and Policies in ITALY,” Rome, 2015.

[61] H. Bülow-hübe, “Energy-Efficient Window Systems in Buildings,” Lund Institute of Technology (LTH), 2001.

[62] ISTAT, “Rapporto Annuale 2017: La situazione del Paese,” Rome, 2017.

[63] J. L. Reyna and M. V. Chester, “Energy efficiency to reduce residential electricity and natural gas use under climate change,” *Nat. Commun.*, vol. 8, no. May, pp. 1–12, 2017.

[64] Buildings Performance Institute Europe (BPIE), “EUROPE’S BUILDINGS UNDER THE MICROSCOPE: A country-by-country review of the energy performance of buildings,” 2011.

[65] International Energy Agency (IEA), “Energy Policies of IEA Countries: Italy 2016 Review,” 2016.

[66] U.S. Environmental Protection Agency, “Emission Factors for Greenhouse Gas Inventories,” vol. 2017, no. 9 March, p. 5, 2018.

[67] U.S. Environmental Protection Agency, “AP 42 - Chapter 1: External Combustion Sources,” *Compil. Air Pollut. Emiss. Factors, Vol. 1 Station. Point Area Sources*, 1995.

[68] Green House Protocol, “Global Warming Potential Values (AR5),” *Greenh. Gas Protoc.*, vol. 2014, no. 1995, pp. 2–5, 2015.

[69] M. Molenbroek, E. Stricker, and T. Boermans, “Primary energy factors for electricity in buildings Toward a flexible electricity supply,” pp. 1–52, 2011.

[70] E. Della Tutela and D. E. L. Territorio, “Decreto del Ministero dello sviluppo economico 26 giugno 2015,” 2015.

[71] Intergovernmental Panel on Climate Change (IPCC), “Non-CO2 Emissions From Stationary Combustion,” in *Good Practice Guidance and Uncertainty Management in National Greenhouse Gas Inventories*, pp. 41–54.

[72] European Committee for Standardization, *EN 15459: Energy performance of buildings - Economic evaluation procedure for energy systems in buildings*. 2007.

[73] European Union, “Guidelines accompanying Commission Delegated Regulation (EU) No 244/2012 of 16 January 2012 supplementing Directive 2010/31/EU of the European Parliament and of the Council on the energy performance of buildings by establishing a comparative methodology f,” *Off. J. Eur. Union*, vol. C 115/1, pp. 1–28, 2012.

[74] European Commission, “COMMISSION DELEGATED REGULATION (EU) No 244/2012 of 16 January 2012 supplementing DirectiveDirective 2010/31/EU of the European Parliament and of the Council on the energy performance of buildings by establishing a comparative methodology framework for ca,” *Off. J. Eur. Union*, p. 28, 2012.

[75] Piemonte Regione, “Prezzi di riferimento per opere e lavori pubblici nella Regione Piemonte – SEZIONE 3 Bioedilizia,” 2016.

[76] Piemonte Regione, “Prezzi di riferimento per opere e lavori pubblici nella Regione Piemonte – SEZIONE 01: Opere edili,” vol. 2015, pp. 29–675, 2016.

[77] V. Corrado, I. Ballarini, S. P. Corgnati, and N. Talà, “TABULA WebTool.” [Online]. Available: http://webtool.building-typology.eu/#bm. [Accessed: 20-Aug-2007].

[78] European Commission, “Roadmap 2050,” *Policy*, no. April, pp. 1–9, 2012.

ANNEX 1: Supplementary QGIS Initialization Results

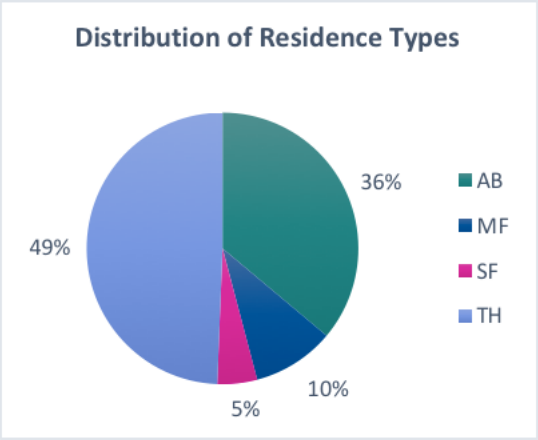

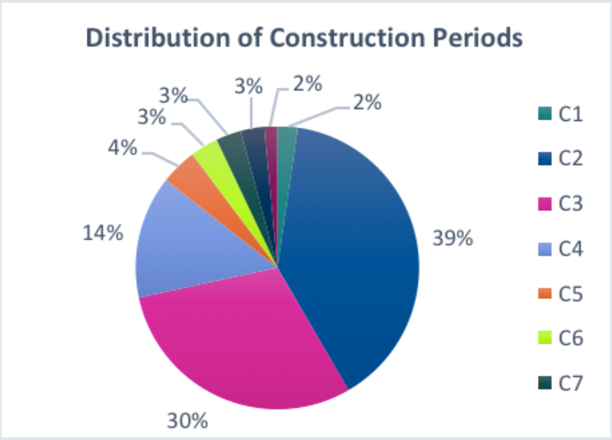

ANNEX 2: QGIS Visualization of Building Archetype Distribution

Figure 62: QGIS Representation zoom breakout map

Figure 63: QGIS representation - zoom 1

Figure 64: QGIS representation - zoom 2

3.

Figure 65: QGIS representation - zoom 3

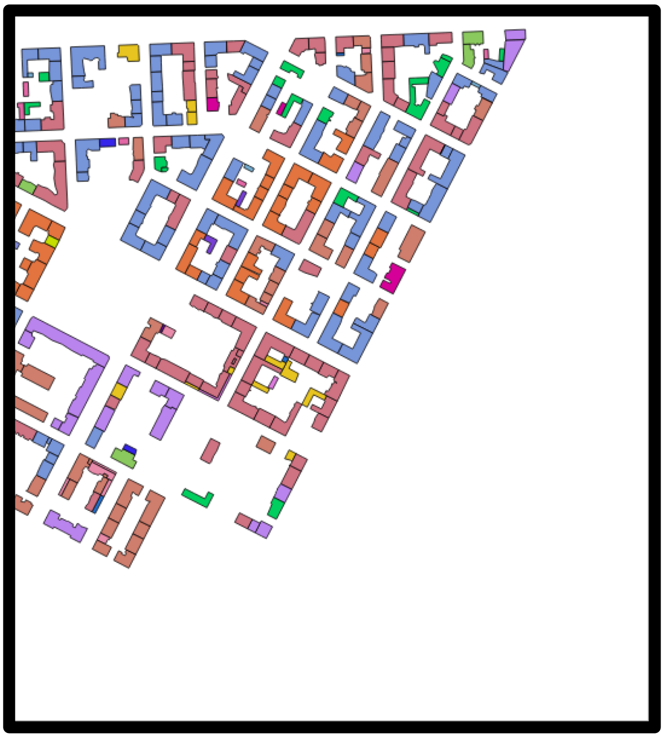

Figure 66: QGIS representation - zoom 4

Figure 67: QGIS representation - zoom 5

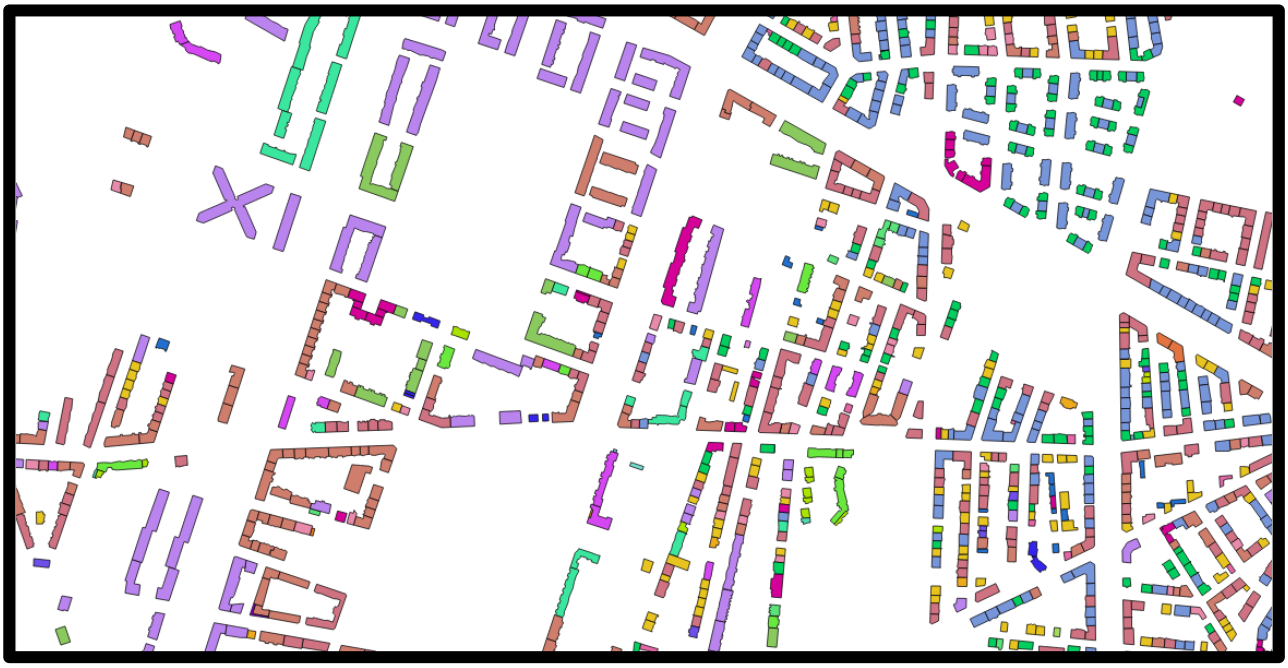

Figure 68: QGIS representation - zoom 6

Figure 69: QGIS representation - zoom 7

Figure 70: QGIS representation - zoom 8

9.

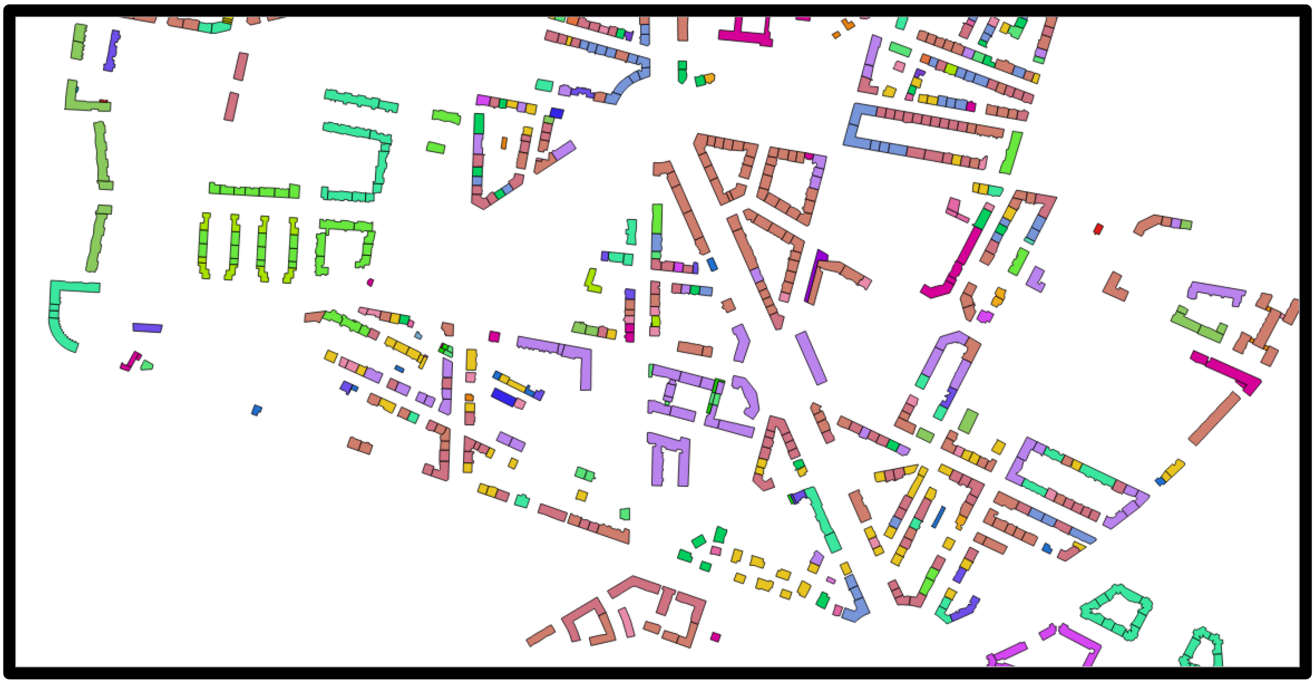

Figure 71: QGIS representation - zoom 9

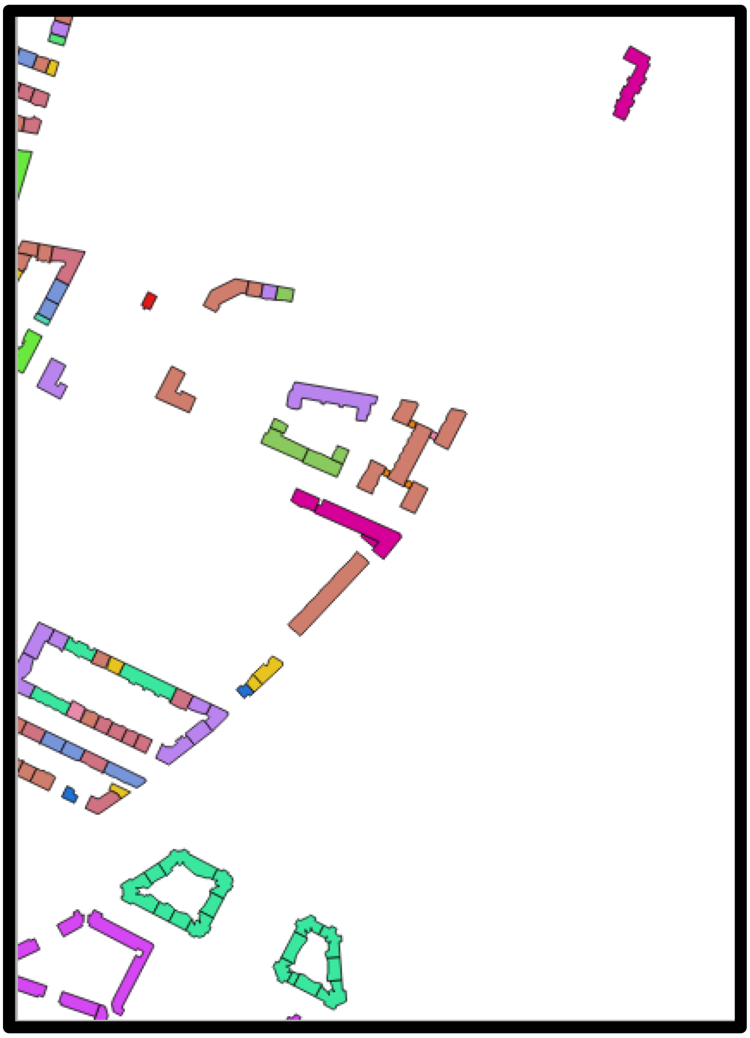

Figure 72: QGIS representation - zoom 10

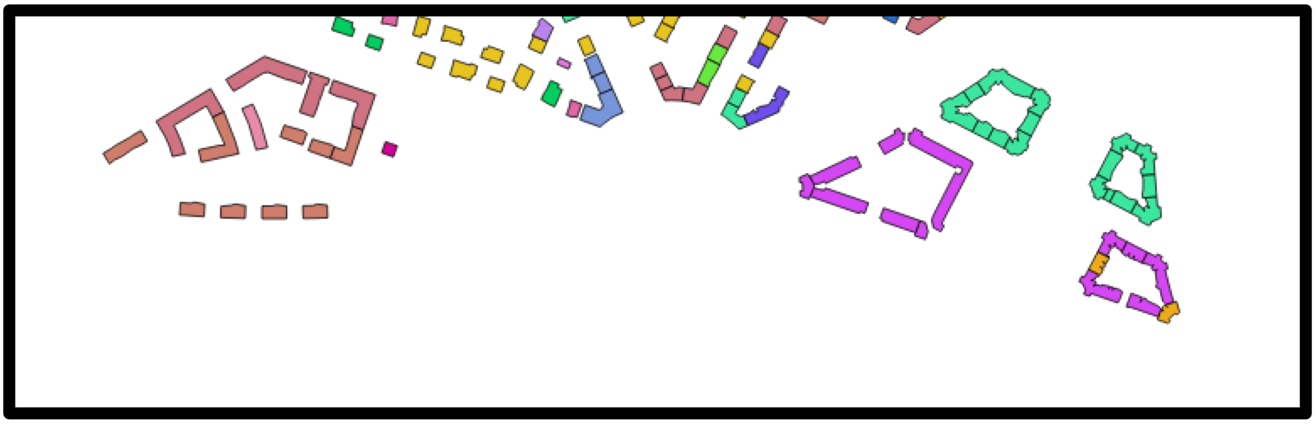

Figure 73: QGIS representation - zoom 11

ANNEX 3: Results from Analytical Model for Original and Modified Buildings

Table 29: Results from analytical model calculations for original buildling, and retrofits EASA and EBSA

	Original						EASA						EBSA					
RB	Heating (kWh/m^2y)		Cooling (kWh/m^2y)		DHW (kWh/m^2y)		Heating (kWh/m^2y)		Cooling (kWh/m^2y)		DHW (kWh/m^2y)		Heating (kWh/m^2y)		Cooling (kWh/m^2y)		DHW (kWh/m^2y)	
	Need	Used	Need	Used	Need	Used	Need	Used	Need	Used	Need	Used	Need	Used	Need	Used	Need	Used
C1AB	156.13	284.08	58.55	106.54	10.39	14.23	29.46	8.07	17.27	4.73	10.39	2.60	104.16	29.43	28.62	8.09	10.39	2.60
C1MF	197.00	371.72	61.12	115.33	115.28	149.71	26.60	7.36	22.23	6.15	112.44	28.11	137.29	38.80	31.91	9.02	115.28	28.82
C1SF	251.58	378.35	39.39	59.24	119.04	148.80	11.19	3.16	22.46	6.35	115.80	28.95	166.84	47.15	24.72	6.99	119.04	29.76
C1TH	288.23	528.97	71.37	130.97	118.87	158.50	22.24	6.16	31.35	8.68	115.25	28.81	217.60	61.50	38.28	10.82	118.87	29.72
C2AB	156.45	284.67	73.12	133.06	12.80	17.53	24.90	6.82	11.72	0.00	12.80	3.20	115.77	32.72	20.24	5.72	12.80	3.20
C2MF	228.92	352.12	94.57	145.47	122.41	142.34	21.52	5.90	17.88	4.90	119.43	29.86	199.55	56.39	23.97	6.77	122.41	30.60
C2SF	340.48	536.65	86.56	136.43	15.02	19.51	22.50	6.23	40.71	11.27	15.02	3.75	252.87	71.46	48.20	13.62	15.02	3.75
C2TH	367.92	553.29	57.72	86.81	122.71	159.37	23.59	6.53	28.18	7.80	119.15	29.79	282.20	79.75	32.33	9.14	122.71	30.68
C3AB	103.88	159.79	77.95	119.91	12.53	16.71	23.61	6.47	11.19	0.00	12.53	3.13	88.25	24.94	21.41	6.05	12.53	3.13
C3MF	275.42	428.81	98.32	153.07	122.42	163.22	28.81	7.97	34.22	9.47	119.41	29.85	215.27	60.83	46.13	13.04	122.42	30.60
C3SF	289.50	456.29	74.44	117.33	119.57	144.06	19.86	5.50	35.18	9.74	18.04	4.51	225.10	63.61	41.15	11.63	119.57	29.89
C3TH	248.40	391.52	145.01	228.56	121.57	146.47	28.77	7.96	49.55	13.71	117.72	29.43	166.03	46.92	73.53	20.78	121.57	30.39
C4AB	87.17	154.92	70.09	124.56	10.90	14.94	22.11	6.06	9.14	0.00	10.90	2.73	78.55	22.20	18.41	5.20	10.90	2.73
C4MF	113.02	154.85	103.03	141.17	121.35	144.47	19.02	5.21	16.56	4.54	118.45	29.61	104.51	29.54	28.48	8.05	121.35	30.34
C4SF	243.16	361.58	88.33	131.34	118.84	148.54	19.71	5.45	36.43	10.08	115.06	28.76	166.32	47.00	47.71	13.48	118.84	29.71
C4TH	233.17	346.72	41.92	62.33	118.88	148.60	19.89	5.45	22.34	6.12	115.28	28.82	167.69	47.39	25.84	7.30	118.88	29.72
C5AB	66.96	94.07	48.74	68.48	6.90	8.62	25.09	6.87	7.51	0.00	6.90	1.72	59.08	16.35	19.14	5.30	6.90	1.72
C5MF	105.82	140.31	49.70	65.90	122.40	139.09	21.63	5.93	21.03	5.76	119.45	29.86	81.25	22.96	31.59	8.93	122.40	30.60
C5SF	145.20	250.98	106.19	183.55	16.11	21.48	21.95	6.08	46.02	12.74	14.81	3.70	119.58	33.79	66.50	18.79	16.11	4.03
C5TH	200.22	297.72	73.86	109.82	118.87	148.59	24.84	6.80	33.82	9.27	115.23	28.81	169.80	47.99	45.46	12.85	118.87	29.72
C6AB	66.56	93.51	51.23	71.98	7.78	9.72	24.22	6.63	8.26	0.00	7.78	1.94	59.28	16.41	20.33	5.63	7.78	1.94
C6MF	109.42	145.09	62.53	82.91	122.36	139.04	23.41	6.41	23.98	6.57	119.61	29.90	81.12	22.92	38.65	10.92	122.36	30.59
C6SF	159.92	276.43	133.81	231.29	24.36	32.48	27.52	7.62	54.80	15.17	24.36	6.09	148.12	41.86	80.56	22.77	24.36	6.09
C6TH	109.11	160.09	33.67	49.41	118.86	158.49	13.86	3.80	20.70	5.67	115.21	28.80	77.90	22.01	25.10	7.09	118.86	29.72
C7AB	73.89	95.91	60.65	78.72	7.85	9.35	27.69	7.59	17.95	4.92	7.85	1.96	57.96	16.04	34.87	9.65	7.85	1.96
C7MF	48.13	73.82	61.75	94.70	121.37	151.72	18.07	4.95	15.82	4.33	118.61	29.65	48.74	13.49	33.23	9.20	121.37	30.34
C7SF	113.06	156.66	171.99	238.31	16.61	20.76	28.85	7.98	62.05	17.17	15.33	3.83	95.19	26.90	103.44	29.23	16.61	4.15
C7TH	109.98	171.68	58.94	92.00	118.82	152.34	19.64	5.38	28.22	7.73	114.96	28.74	81.71	23.09	39.66	11.21	118.82	29.71
C8AB	80.35	104.30	79.40	103.06	9.47	11.27	28.64	7.93	23.86	6.60	9.47	2.37	60.99	16.88	46.04	12.74	9.47	2.37
C8MF	48.56	74.48	66.76	102.39	121.35	151.68	17.98	4.93	18.04	4.94	118.35	29.59	49.73	13.76	36.49	10.10	121.35	30.34
C8SF	98.71	136.77	100.19	138.82	16.90	21.12	14.81	4.10	44.65	12.36	16.90	4.22	79.31	22.41	64.45	18.21	16.90	4.22
C8TH	121.15	189.11	151.52	236.51	17.09	21.92	25.74	7.12	57.40	15.89	15.84	3.96	90.92	25.69	93.75	26.49	17.09	4.27
C9AB	57.08	83.65	30.36	44.49	11.38	12.65	22.08	6.05	12.01	0.00	11.38	2.85	53.41	14.78	20.54	5.68	11.38	2.85
C9MF	64.65	73.03	50.43	56.97	121.35	134.83	20.25	5.55	22.03	6.03	118.38	29.60	60.36	16.71	34.99	9.68	121.35	30.34
C9SF	75.80	90.25	76.57	91.17	16.39	16.56	13.01	3.56	39.81	10.91	16.39	4.10	67.06	18.95	56.16	15.87	16.39	4.10
C9TH	74.06	88.18	48.39	57.62	118.81	120.01	14.64	4.01	26.58	7.28	114.88	28.72	66.56	18.81	35.94	10.16	118.81	29.70

Table 30: Results from analytical model calculations for original buildling, and retrofits EASB and EBSB

RB	EASB						EBSB					
	Heating (kWh/m^{2}y)		Cooling (kWh/m^{2}y)		DHW (kWh/m^{2}y)		Heating (kWh/m^{2}y)		Cooling (kWh/m^{2}y)		DHW (kWh/m^{2}y)	
	Need	Used	Need	Used	Need	Used	Need	Used	Need	Used	Need	Used
C1AB	29.46	11.13	17.27	6.52	10.39	3.58	104.16	40.60	28.62	11.16	10.39	3.58
C1MF	26.60	10.16	22.23	8.49	112.44	38.77	137.29	53.51	31.91	12.44	115.28	39.75
C1SF	11.19	4.36	22.46	8.76	115.80	39.93	166.84	65.03	24.72	9.64	119.04	41.05
C1TH	22.24	8.49	31.35	11.97	115.25	39.74	217.60	84.82	38.28	14.92	118.87	40.99
C2AB	24.90	9.41	11.72	0.00	12.80	4.41	115.77	45.13	20.24	7.89	12.80	4.41
C2MF	21.52	8.13	17.88	6.76	119.43	41.18	199.55	77.78	23.97	9.34	122.41	42.21
C2SF	22.50	8.59	40.71	15.54	15.02	5.18	252.87	98.57	48.20	18.79	15.02	5.18
C2TH	23.59	9.01	28.18	10.76	119.15	41.09	282.20	110.00	32.33	12.60	122.71	42.31
C3AB	23.61	8.92	11.19	0.00	12.53	4.32	88.25	34.40	21.41	8.35	12.53	4.32
C3MF	28.81	11.00	34.22	13.06	119.41	41.18	215.27	83.91	46.13	17.98	122.42	42.21
C3SF	19.86	7.58	35.18	13.43	18.04	6.22	225.10	87.74	41.15	16.04	119.57	41.23
C3TH	28.77	10.98	49.55	18.91	117.72	40.59	166.03	64.72	73.53	28.66	121.57	41.92
C4AB	22.11	8.35	9.14	0.00	10.90	3.76	78.55	30.62	18.41	7.18	10.90	3.76
C4MF	19.02	7.19	16.56	6.26	118.45	40.84	104.51	40.74	28.48	11.10	121.35	41.85
C4SF	19.71	7.52	36.43	13.91	115.06	39.67	166.32	64.83	47.71	18.60	118.84	40.98
C4TH	19.89	7.52	22.34	8.44	115.28	39.75	167.69	65.36	25.84	10.07	118.88	40.99
C5AB	25.09	9.48	7.51	0.00	6.90	2.38	59.08	22.56	19.14	7.31	6.90	2.38
C5MF	81.25	31.67	31.59	12.31	122.40	42.21	81.25	31.67	31.59	12.31	122.40	42.21
C5SF	21.95	8.38	46.02	17.57	14.81	5.11	119.58	46.61	66.50	25.92	16.11	5.56
C5TH	24.84	9.38	33.82	12.78	115.23	39.74	169.80	66.19	45.46	17.72	118.87	40.99
C6AB	24.22	9.15	8.26	0.00	7.78	2.68	59.28	22.63	20.33	7.76	7.78	2.68
C6MF	23.41	8.84	23.98	9.06	119.61	41.24	81.12	31.62	38.65	15.06	122.36	42.19
C6SF	27.52	10.51	54.80	20.92	24.36	8.40	148.12	57.74	80.56	31.40	24.36	8.40
C6TH	13.86	5.24	20.70	7.82	115.21	39.73	77.90	30.36	25.10	9.78	118.86	40.99
C7AB	27.69	10.46	17.95	6.78	7.85	2.71	57.96	22.13	34.87	13.31	7.85	2.71
C7MF	18.07	6.83	15.82	5.98	118.61	40.90	48.74	18.61	33.23	12.69	121.37	41.85
C7SF	28.85	11.01	62.05	23.69	15.33	5.29	95.19	37.10	103.44	40.32	16.61	5.73
C7TH	19.64	7.42	28.22	10.66	114.96	39.64	81.71	31.85	39.66	15.46	118.82	40.97
C8AB	28.64	10.93	23.86	9.11	9.47	3.27	60.99	23.28	46.04	17.58	9.47	3.27
C8MF	17.98	6.80	18.04	6.82	118.35	40.81	49.73	18.99	36.49	13.93	121.35	41.84
C8SF	14.81	5.65	44.65	17.05	16.90	5.83	79.31	30.91	64.45	25.12	16.90	5.83
C8TH	25.74	9.83	57.40	21.91	15.84	5.46	90.92	35.44	93.75	36.54	17.09	5.89
C9AB	22.08	8.34	12.01	0.00	11.38	3.92	53.41	20.39	20.54	7.84	11.38	3.92
C9MF	20.25	7.65	22.03	8.32	118.38	40.82	60.36	23.04	34.99	13.36	121.35	41.84
C9SF	13.01	4.92	39.81	15.04	16.39	5.65	67.06	26.14	56.16	21.89	16.39	5.65
C9TH	14.64	5.53	26.58	10.04	114.88	39.61	66.56	25.94	35.94	14.01	118.81	40.97

ANNEX 4: Electricity Demand by Census Section

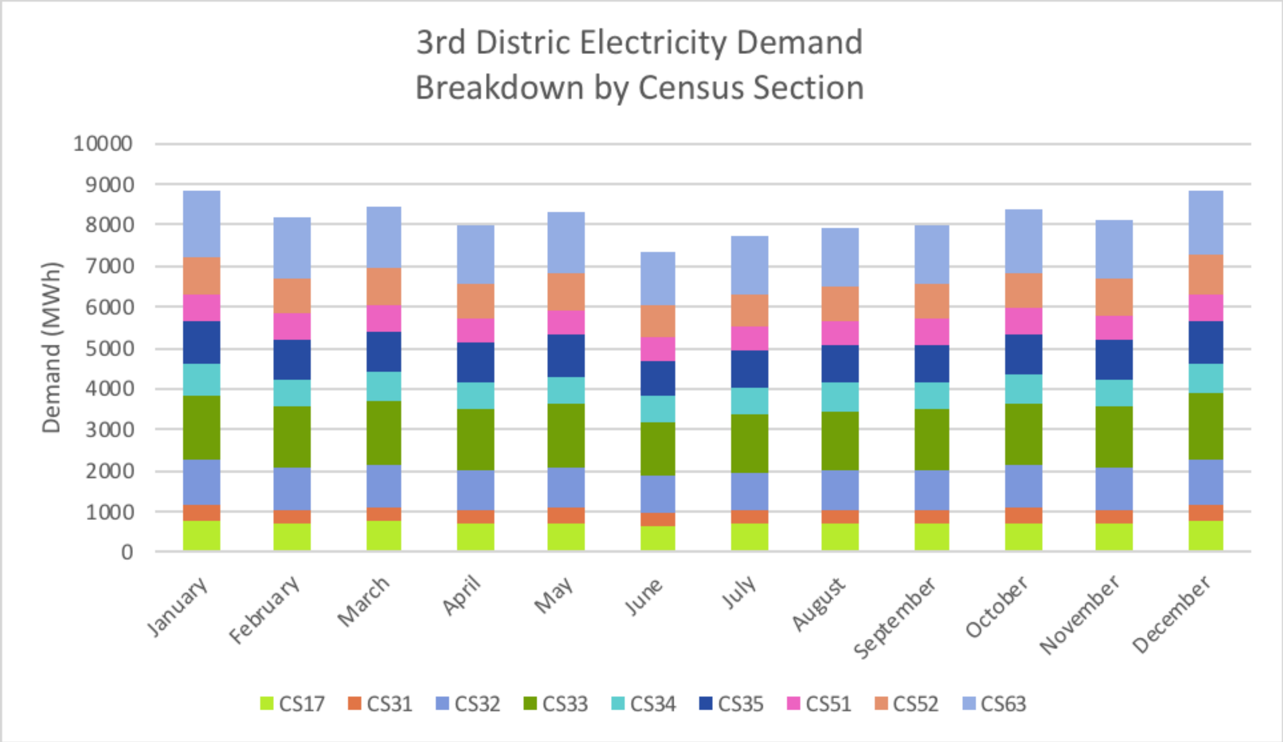

Figure 74:3rd district monthly appliance electricity demand by census section

ANNEX 5: Global Cost Calculation Details

	EASA	EBSA	EASB	EBSB
INVESTMENT COSTS				
Retrofit Investmet. Insulation, heat pumps, labor.	€ 620,881,683.60	€ 591,188,919.65	€ 184,931,318.79	€ 155,238,357.09
REPLACEMENT COSTS				
Heat Pumps				
Cost of Replacement of HP	€ 23,536,705	€ 23,536,705	€ 4,496,308	€ 4,496,308
Life of the HP (Years)	€ 25	€ 25	€ 20	€ 25
Discounted Cost of Replacement	€ 2,722,150	€ 2,722,150	€ 520,023	€ 520,023
Total Cost of Replacement	€ 2,722,150	€ 2,722,150	€ 520,023	€ 520,023
MAINTENANCE COSTS				
Heat Pumps				
Maintenance Cost (% CAPEX)	1%	1%	1%	1%
Annual Maintenance Cost	€ 235,367.05	€ 235,367.05	€ 44,963.08	€ 44,963.08
Discounted Maintenance Cost	€ 4,206,845	€ 4,206,845	€ 803,650	€ 803,650
Net Annual Maintenance	€ 4,206,845	€ 4,206,845	€ 803,650	€ 803,650
Quantity	5301	5301	5301	100
Value after ammortization each(Salvage Cost)	€ 1,434	€ 1,434	€ 37	€ 37
Total Salvage value	€ 7,604,166	€ 7,604,166	€ 197,788	€ 3,730
Actualized Salvage Cost	€ 2,344,506	€ 2,344,506	€ 60,982	€ 1,150
GLOBAL COST				
Total Global Cost	€ 625,466,171.98	€ 595,773,408.03	€ 186,194,009.89	€ 156,560,879.79
Global Cost (per m2)	€ 533.53	€ 508.20	€ 158.83	€ 133.55

Measure #	Components	Type	Price per unit (Euros)	No. of Units in 3D				Unit	Total Price (Euros)				Name in Price List	Source
				EASA	EBSA	EASB	EBSB		EASA	EBSA	EASB	EBSB		
1	Window Double Glaze	Envelope	257.80		149394		149394	m^2	0	38513850	0	38513850	01.P20.M00.020 - finestra a battente; di superficie oltre 2,0 m²	http://www.regione.piemonte.it/oopp/prezzario/dwd/sez01.pdf
2	Window Triple Glaze	Envelope	320.13	149394		149394	0	m2	47825596	0	47825596	0	portafinestra ad anta battente; di superficie fino a 3,5 m²	http://www.regione.piemonte.it/oopp/prezzario/dwd/sez01.pdf
3	New Windows - Structural modifiction & Installation	Envelope	10.31	149394	149394	149394	149394	m2	1540554	1540554	1540554	1540554	01.A17.N00.055 Maggiori riparazioni di serramenti in legno consistenti nella sostituzione dei montanti o traverse,cambio di serratura e maniglie,sostituzione di pannelli,riapplicazione della ferramenta con rappezzi ai montanti,ripiazzamento del serramento: 40% del prezzo del serramento nuovo	http://www.regione.piemonte.it/oopp/prezzario/dwd/sez01.pdf
5	Insulation Advanced Walls	Envelope	30.09	7976201		7976201		m2	240003888	0	240003888	0	03.P09.H06- Cellulose fiber panels; produced from pure newspaper, with a dry process, free from toxic and harmful substances. Density 75 Kg / m³ approx. Lambda <= 0.039	http://www.regione.piemonte.it/oopp/prezzario/dwd/sez03.pdf
7	Insulation Advanced Attic (U = 0.13, 15cm)	Envelope	34.12	1172317		1172317			39998296	0	39998296	0	03.P09.H06- Cellulose fiber panels; produced from pure newspaper, with a dry process, free from toxic and harmful substances. Density 75 Kg / m³ approx. Lambda <= 0.039	http://www.regione.piemonte.it/oopp/prezzario/dwd/sez03.pdf
8	Insulation Advanced Floor to Bsement (U = 0.23, 15cm)	Envelope	34.12	1172317		1172317			39998296	0	39998296	0	03.P09.H06- Cellulose fiber panels; produced from pure newspaper, with a dry process, free from toxic and harmful substances. Density 75 Kg / m³ approx. Lambda <= 0.039	http://www.regione.piemonte.it/oopp/prezzario/dwd/sez03.pdf
9	Insulation Basic Attic (U = 0.27, 11cm)	Envelope	25.90		1172317		1172317		0	30365364	0	30365364	03.P09.H06- Cellulose fiber panels; produced from pure newspaper, with a dry process, free from toxic and harmful substances. Density 75 Kg / m³ approx. Lambda <= 0.039	http://www.regione.piemonte.it/oopp/prezzario/dwd/sez03.pdf
10	Insulation Basic Floor to Bsement (U = 0.3, 10cm)	Envelope	27.31		1172317		1172317		0	32015987	0	32015987		
11	Realization of Internal Insulation	Envelope	21.19	7976201		7976201			169019687	0	169019687	0	03.A07.A02.005	http://www.regione.piemonte.it/oopp/prezzario/dwd/sez03.pdf
12	Realization of Roof and Floor Insulation	Envelope	41.13	1172317	1172317	1172317	1172317		48217413	48217413	48217413	48217413	03.A07.A02.010	http://www.regione.piemonte.it/oopp/prezzario/dwd/sez03.pdf
13	Heat Pump COP 4.0 (greater than 2000m^2) - 31kW	Systems	7769.45	649	649			each	5042373	5042373	0	0	03.P13.L05.005	http://www.regione.piemonte.it/oopp/prezzario/dwd/sez03.pdf
14	Heat Pump COP 4.0 (1000-2000m^2) -25kW	Systems	7116.50	2731	2731			each	19435162	19435162	0	0	03.P13.L05.010	http://www.regione.piemonte.it/oopp/prezzario/dwd/sez03.pdf
15	Heat Pump COP 4.0 (less than 1000m^2) - 18kW	Systems	4440.05	1921	1921			each	8529336	8529336	0	0	03.P13.L05.015	http://www.regione.piemonte.it/oopp/prezzario/dwd/sez03.pdf
16	Heat Pump COP 2.9 (greater than 2000m2) -20kW	Systems	978.79			649	649	each	0	0	635235	635235	03.P13.L06.005	http://www.regione.piemonte.it/oopp/prezzario/dwd/sez03.pdf
17	Heat Pump COP 2.9 (1000-2000m2) -15kW	Systems	848.20			2731	2731	each	0	0	2316434	2316434	03.P13.L06.010	http://www.regione.piemonte.it/oopp/prezzario/dwd/sez03.pdf
18	Heat Pump COP 2.9 (less than 1000m2) -10kW	Systems	783.54			1921	1921	each	0	0	1505180	1505180	03.P13.L06.015	http://www.regione.piemonte.it/oopp/prezzario/dwd/sez03.pdf
19	Installation HP Advanced 2000+	Systems	263.67	649	649			each	171122	171122	0	0	03.A12.F02.005	http://www.regione.piemonte.it/oopp/prezzario/dwd/sez03.pdf
20	Installation HP Advanced 1000-2000	Systems	263.67	2731	2731			each	720083	720083	0	0	03.A12.F02.010	http://www.regione.piemonte.it/oopp/prezzario/dwd/sez03.pdf
21	Installation HP Advanced 0-1000	Systems	197.75	1921	1921			each	379878	379878	0	0	03.A12.F02.015	http://www.regione.piemonte.it/oopp/prezzario/dwd/sez03.pdf
22	Installation HP basic	Systems	197.75			649	649	each	0	198	128340	128340	03.A12.F03.005	http://www.regione.piemonte.it/oopp/prezzario/dwd/sez03.pdf

ANNEX 6: Full District GIS Maps of Results

Heat Reduction kWh/m^{2}y - Slow retrofit, 2030	

Heat Reduction kWh/m^{2}y - Slow retrofit, 2050


0
0-25
25-50
50-75
75-100
100-125
125-150
150-175
175-200
200-225
225-250
250-275
300-325
325-350

Heat Reduction kWh/m^{2}y - Moderate retrofit, 2030

Heat Reduction kWh/m^{2}y - Moderate retrofit, 2050

Heat Reduction kWh/m^{2}y - Fast retrofit, 2030


0
75-100
100-125
125-150
150-175
175-200
200-225
225-250
250-275
300-325
325-350
350+

Heat Reduction kWh/m^{2}y - Fast retrofit, 2050

Cooling Reduction kWh/m^{2}y - Slow retrofit, 2030

Cooling Reduction kWh/m^{2}y - Slow retrofit, 2050

Cooling Reduction kWh/m^{2}y - Moderate retrofit, 2030

Cooling Reduction kWh/m^{2}y - Moderate retrofit, 2050

Cooling Reduction kWh/m^{2}y - Fast retrofit, 2030

Cooling Reduction kWh/m^{2}y - Fast retrofit, 2050

DHW Reduction kWh/m^{2}y - Slow retrofit, 2030

DHW Reduction kWh/m^{2}y - Slow retrofit, 2050

DHW Reduction kWh/m^{2}y - Moderate retrofit, 2030

DHW Reduction kWh/m^{2}y - Moderate retrofit, 2050

DHW Reduction kWh/m^2y - Fast retrofit, 2030

DHW Reduction kWh/m²y - Fast retrofit, 2050

Primary Energy (excl. appliances) Reduction kWh/m^{2}y - Slow retrofit, 2030

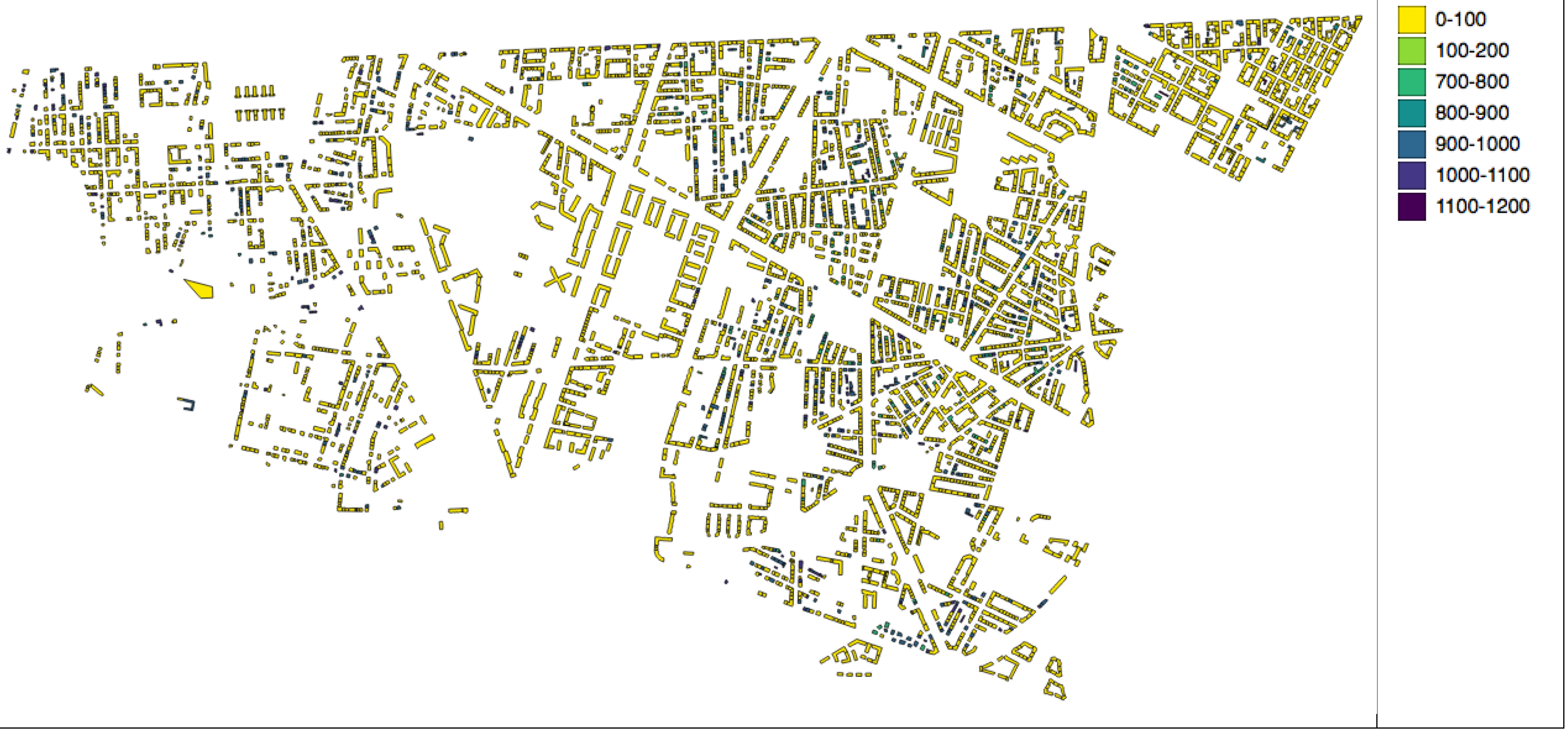

Primary Energy (excl. appliances) Reduction kWh/m^{2}y - Slow retrofit, 2050

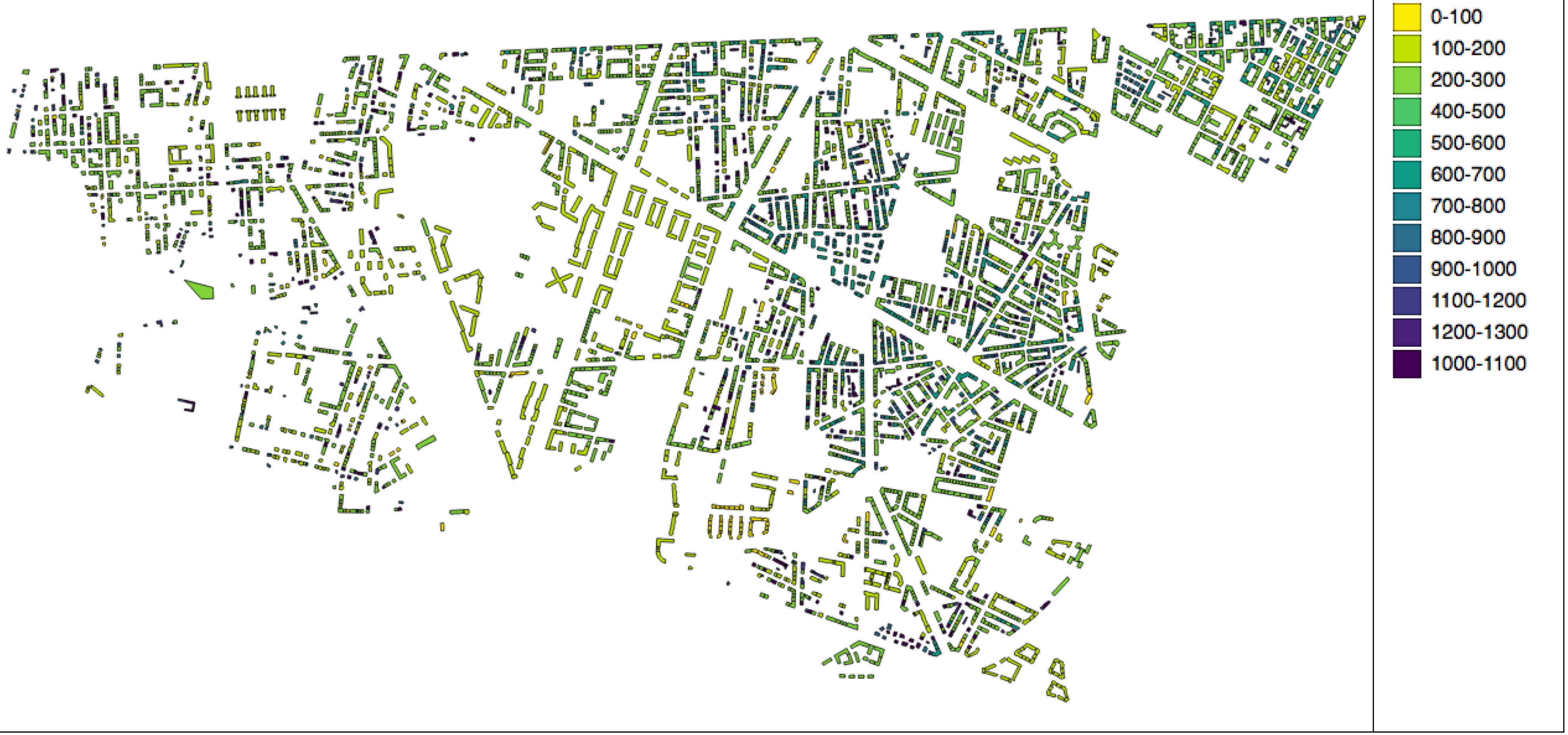

Primary Energy (excl. appliances) Reduction kWh/m^{2}y - Moderate retrofit, 2030

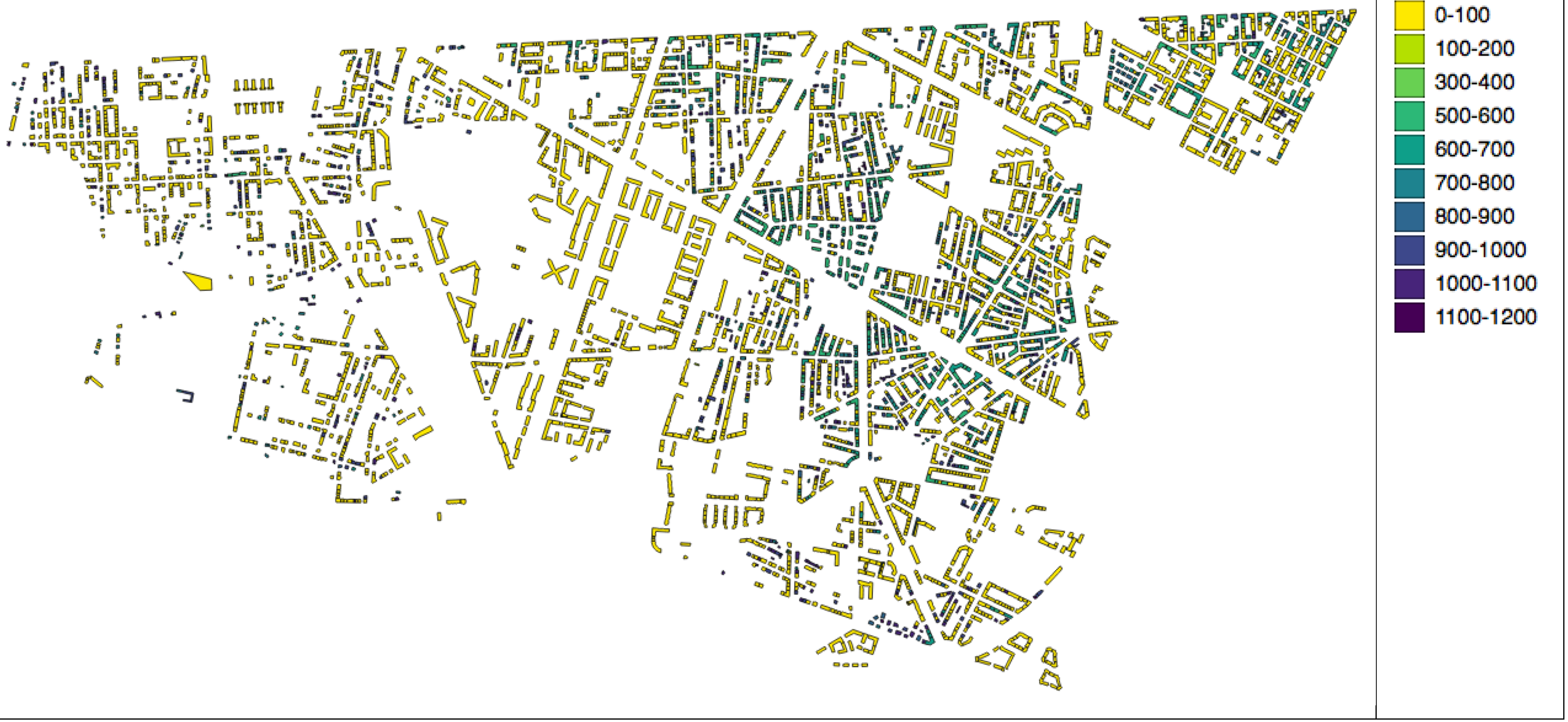

Primary Energy (excl. appliances) Reduction kWh/m^{2}y - Moderate retrofit, 2050

Primary Energy (excl. appliances) Reduction kWh/m^2y - Fast retrofit, 2030

Primary Energy (excl. appliances) Reduction kWh/m^{2}y - Fast retrofit, 2050

🟨	0-100
🟨	100-200
🟩	200-300
🟩	300-400
🟩	400-500
🟩	500-600
🟩	600-700
🟦	700-800
🟦	800-900
🟦	900-1000
🟦	1000-1100
🟪	1100-1200
🟪	1200-1300
🟪	1300-1400

Total Primary Energy Reduction kWh/m^{2}y - Slow retrofit, 2030

Total Primary Energy Reduction kWh/m^{2}y - Slow retrofit, 2050

Total Primary Energy Reduction kWh/m^2y - Moderate retrofit, 2030

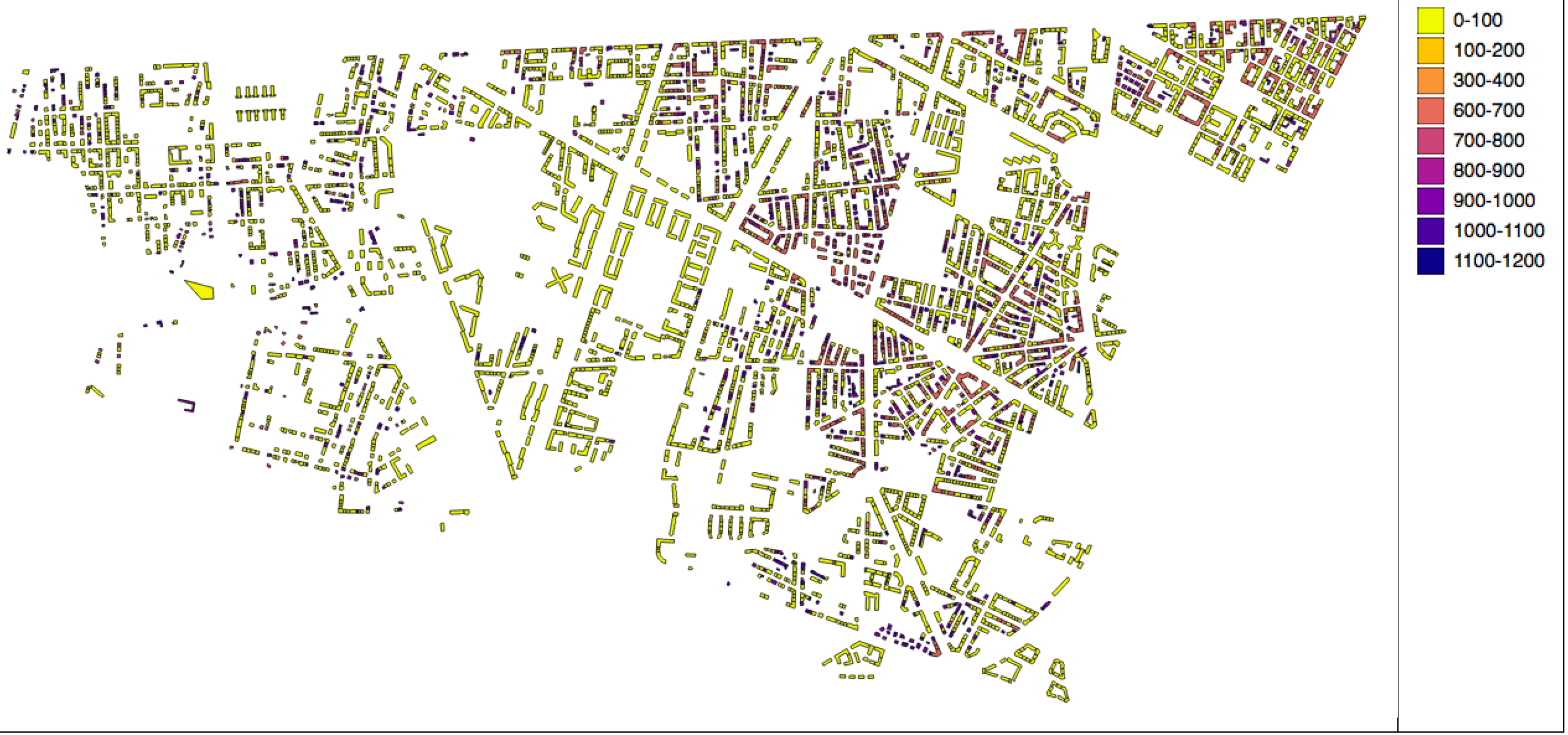

Total Primary Energy Reduction kWh/m²y - Moderate retrofit, 2050

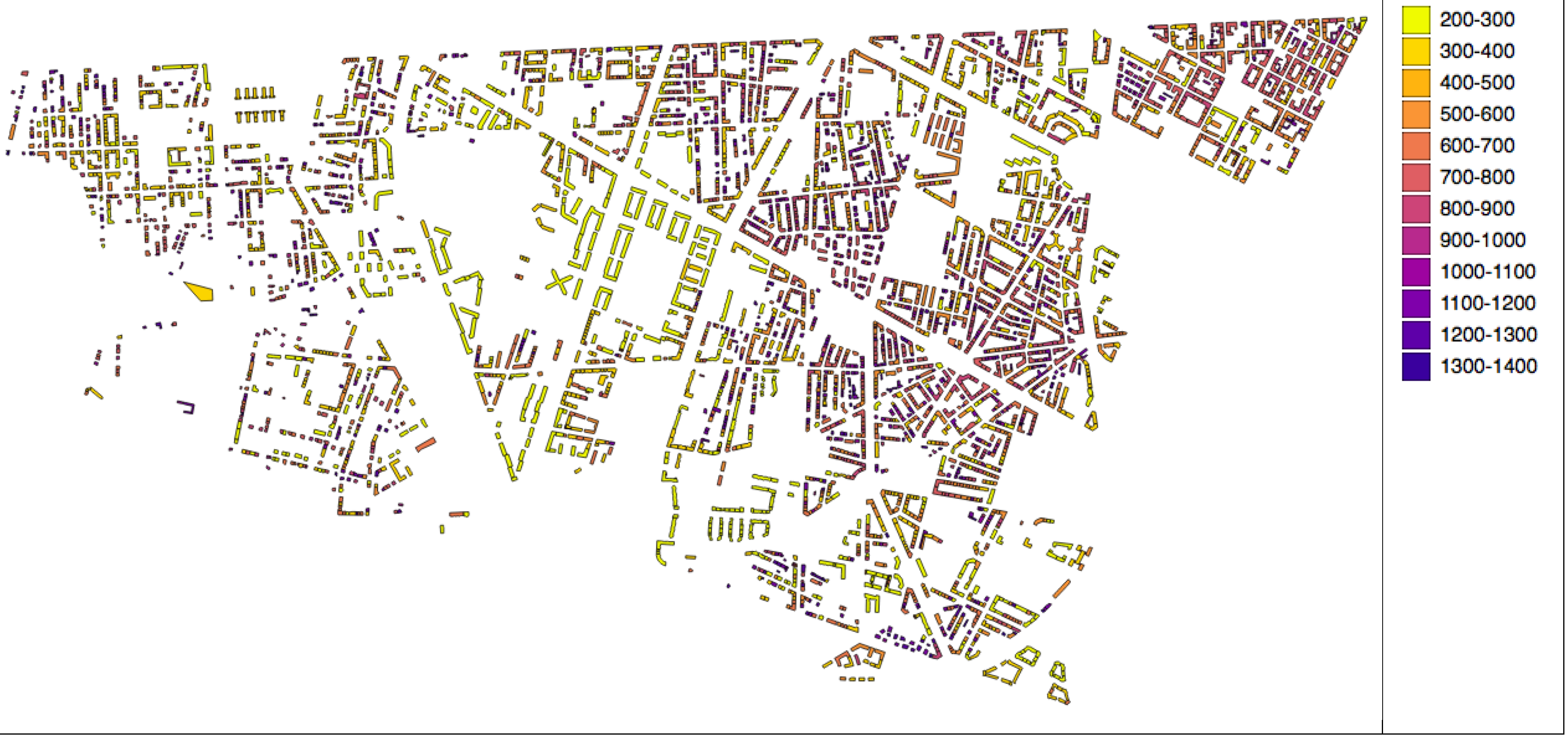

Total Primary Energy Reduction kWh/m^2y - Fast retrofit, 2030

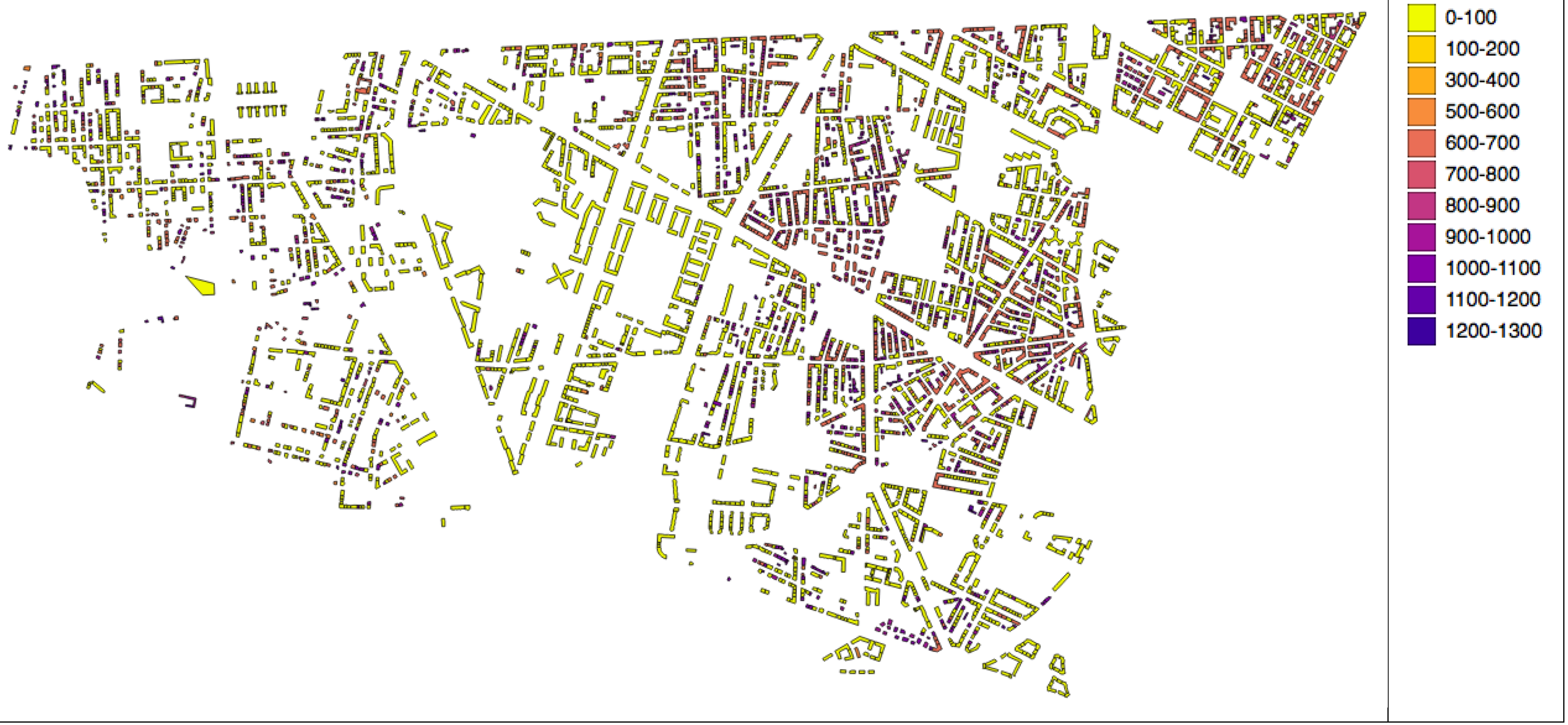

Total Primary Energy Reduction kWh/m^{2}y - Fast retrofit, 2050

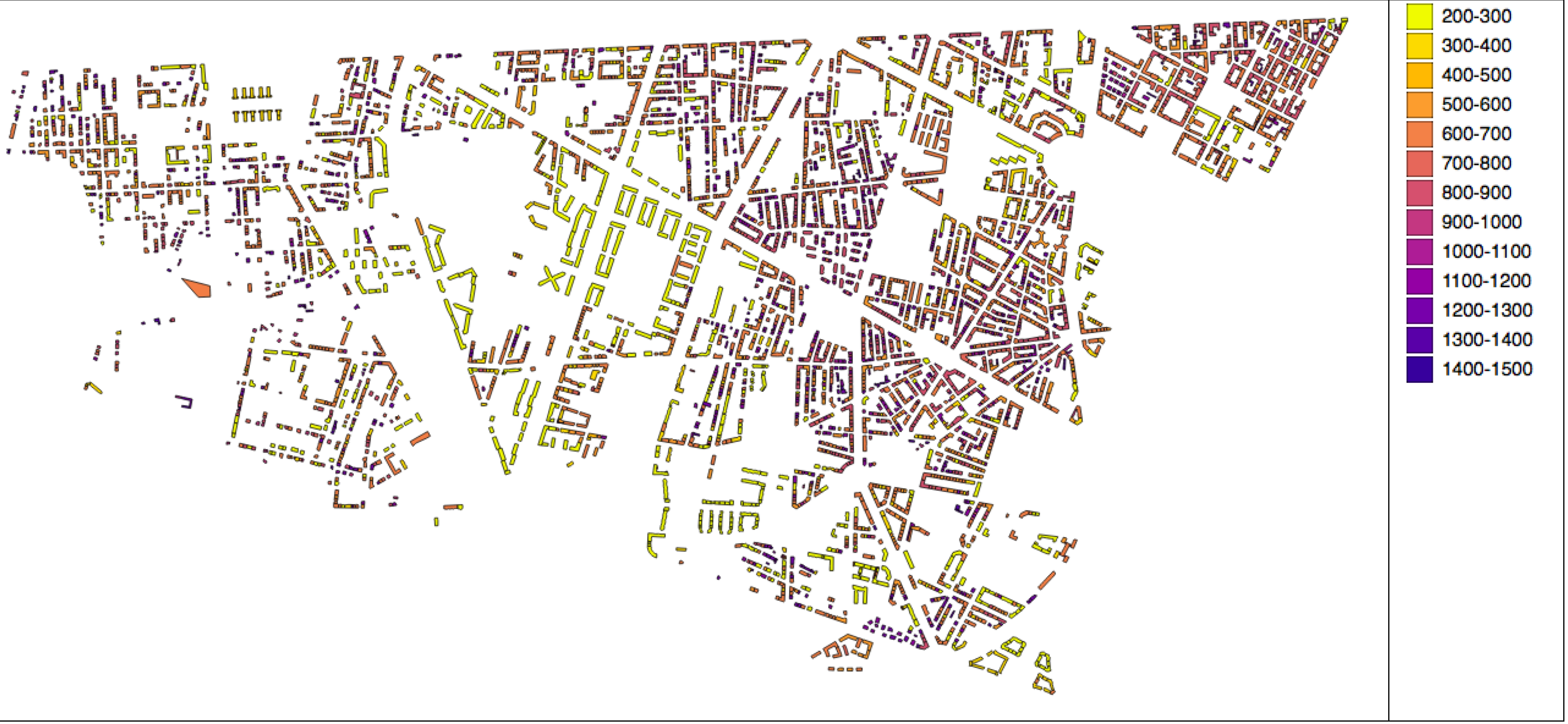

Acknowledgements

I would like to start by thanking Professor Corgnati and Professor Becchio for the opportunity to work on this project.

I would especially like to thank Chiara Delmastro and Giulia Vergerio for their continued support and encouragement during this process.

Thank you to the very understanding researchers in LAME and the Energy Center for allowing me to come work with you day to day.